Istituto di Fisica del Plasma "Piero Caldirola"
Consiglio Nazionale delle Ricerche

Neutron measurements in fusion research

M.Tardocchi

Istituto di Fisica del Plasma, CNR, Milan, Italy

Istituto di Fisica del Plasma "Piero Caldirola"
Consiglio Nazionale delle Ricerche

Outline

Thermonuclear Fusion power

Neutron emission in fusion plasmas

History of neutron measurements on fusion plasmas

Neutron detectors used in fusion

Principles and state of the art of neutron spectrometers

Some examples of results

Latest developments

Milestones in history of nuclear fusion power

- 1938 Fusion theory presented as sun's energy as source ($E=mc^2$).
- 1950's Fusion reactor and ignition (with atom bombs from 1945) experiments.
- 1951 Argentina reports fusion reactor success, but was found to be a hoax
- 1952 First thermonuclear (TN) ignition experiment (the hydrogen bomb)
- 1954 Success beyond belief with H-bomb (15 Mton TNT, 1000x that of the A-bomb). Super bombs of 100-Mton tested but abandon for military and civil uses.
- 1955 TN fusion neutron production reported from Los Alamos. Claim retracted.
- 1959 TN neutrons seen in ZETA machine in UK. Claim retracted.
- 1960 TN neutrons reported from Los Alamos. The experiments were done 1958!
- 1960's Various fusion reactor experiments with no real progress.
- 1968 Surprising and dramatic progress with 'tokamak' reactor in SU.
- 1997 The JET tokamak with DT fuel produces 16 MW power at gain of $Q=P_f/P_{in}\approx 0.6$.
- 2000 Renewed interest in fusion-fission hybrid reactors with high Q.
- >2020 ITER tokamak (under construction) is expected to reach $P_f=500$ MW at $Q\approx 10$
- >>2050 DEMO and PROTO: Two steps to commercial fusion energy reactor:

JET

- World's largest tokamak, outside of Oxford in England; major radius 3 m, plasma volume 85 m^3
- Heating systems:
  - NBI: 2 injector boxes each with 8 PINIs capable of providing about 1.5 MW (at 80 or 130 keV). Total capacity ~23 MW
  - ICRH: old antennae A-D and new (ITER like) antennae E, total capacity ~10 MW + 4 MW
  - LHCD: a few MW
- World record in produced fusion power, 16.7 MW

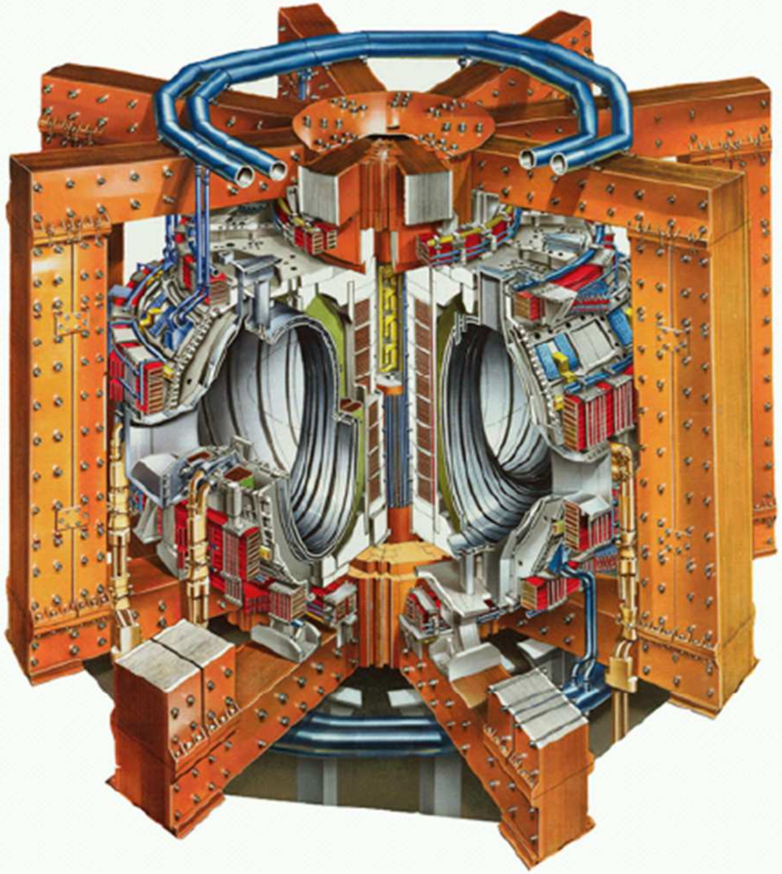

Istituto
di Fisica del Plasma
"Piero Caldirola"
Consiglio Nazionale delle Ricerche

JET plasma

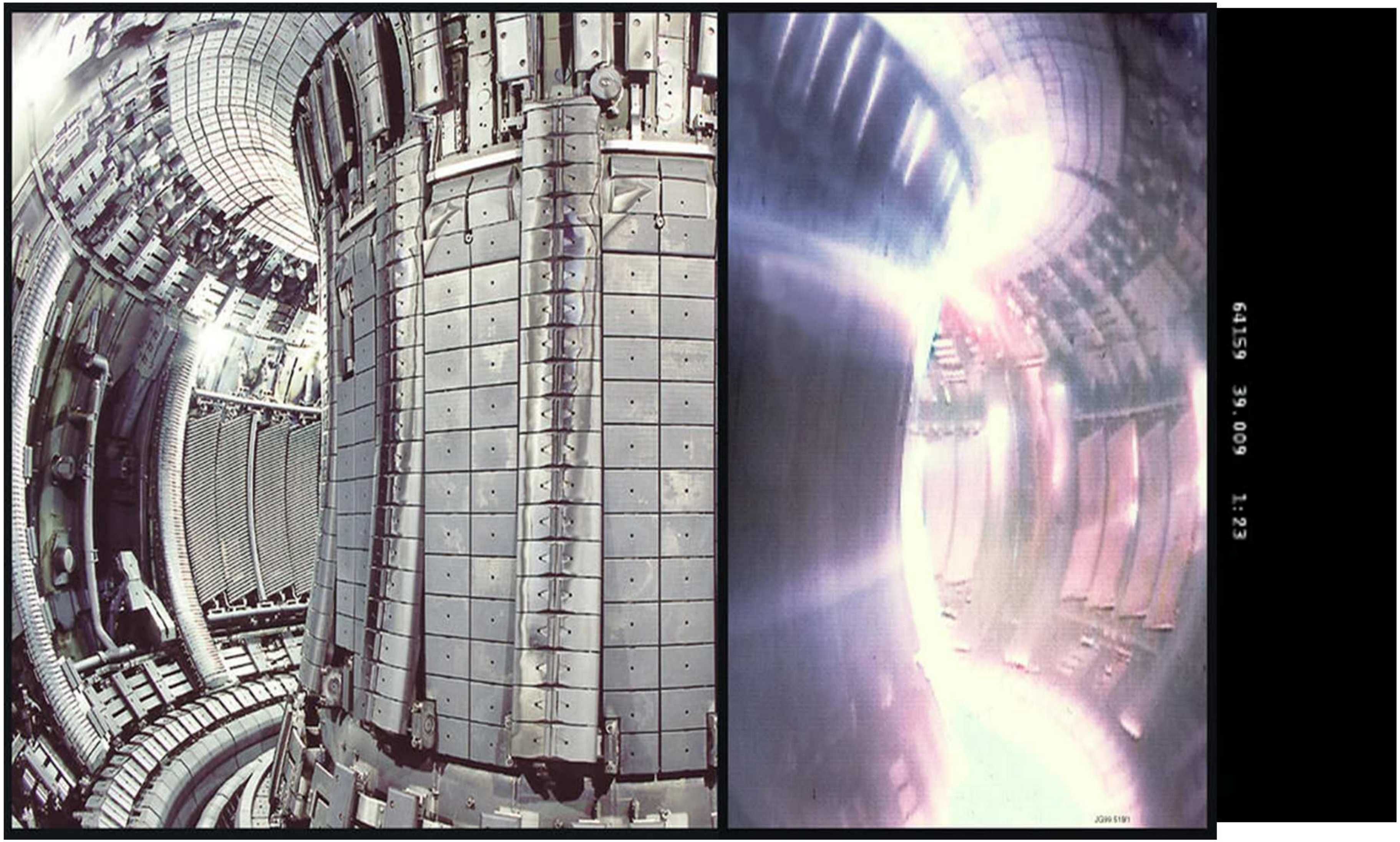

Istituto di Fisica del Plasma "Piero Caldirola"
Consiglio Nazionale delle Ricerche

Progress in fusion

Fusion power

$Q = P_{fus}/P_{aux}$

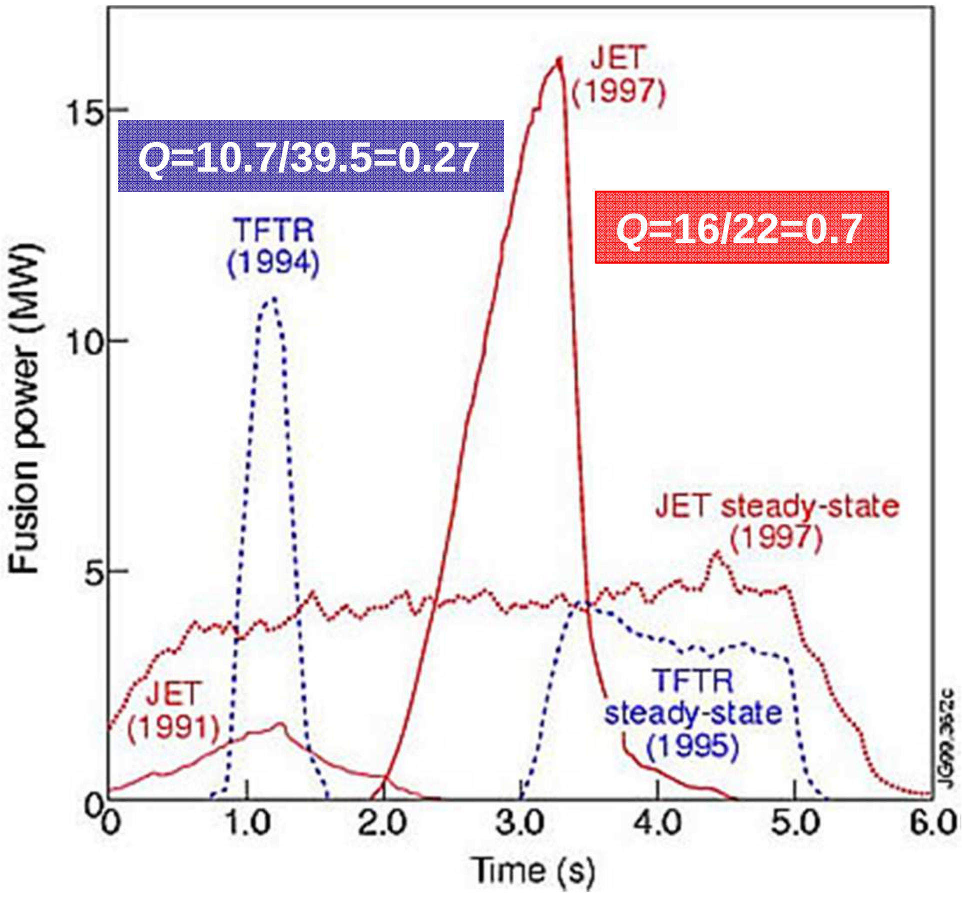

Q = 10 (ITER)

Next steps

Q = 30-50 (DEMO, reattore)

Triple product

$n_i T_i \tau_E$ (x10^{20}m^{-3} sec keV

P τ_E

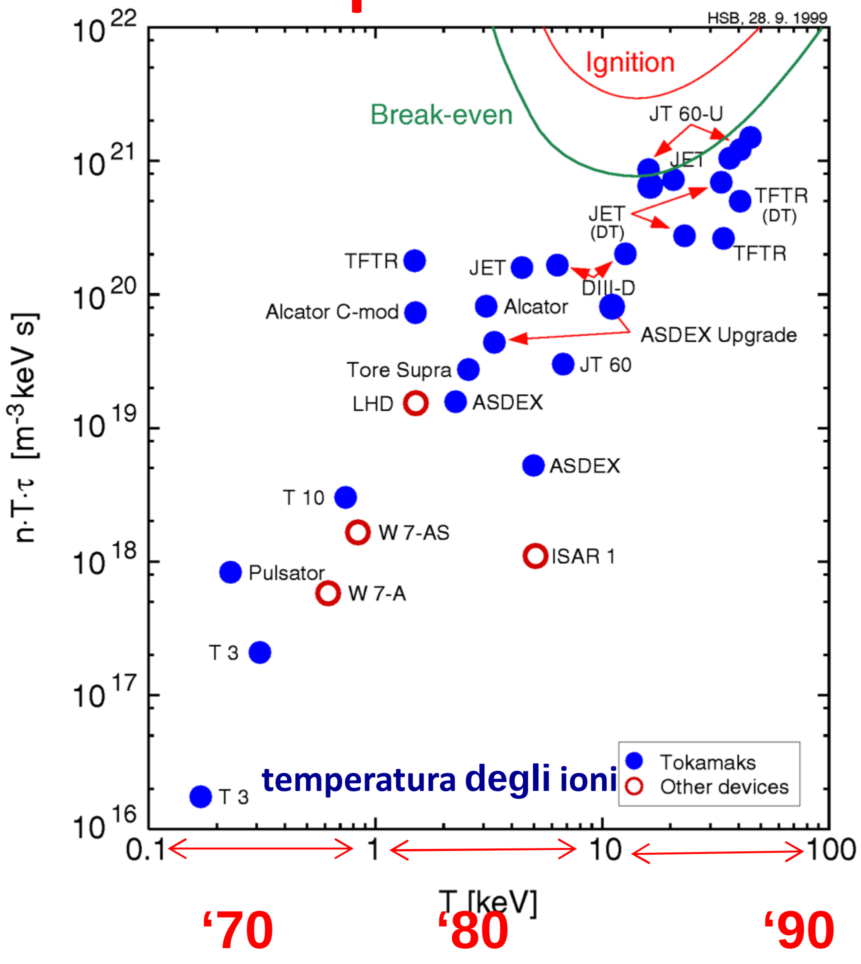

Scaling law

$$\tau_E \propto I\ R^2\ P^{-2/3}$$

Istituto
di Fisica del Plasma
"Piero Caldirola"
Consiglio Nazionale delle Ricerche

ITER project

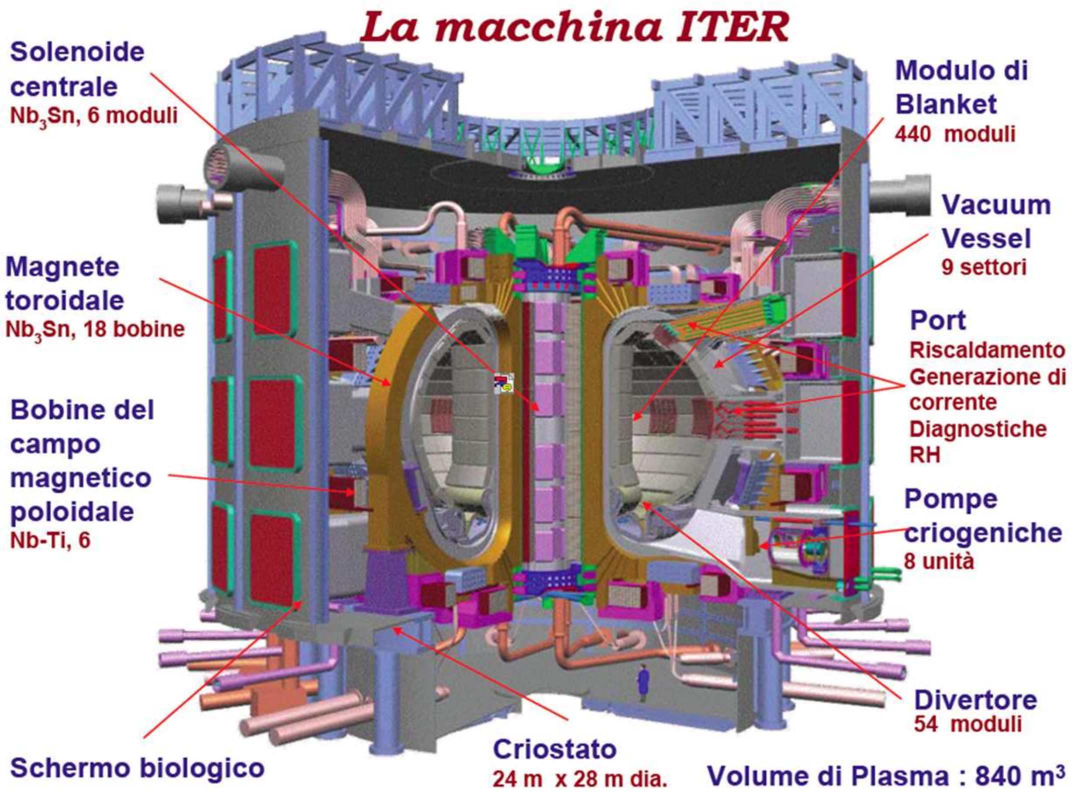

Massa: 23.350 ton

5/11 Country hosting ITER (EU)
1/11 each of 6 partner
Cost for EU for the construction~ 7B€ (2010)

80% to national industries

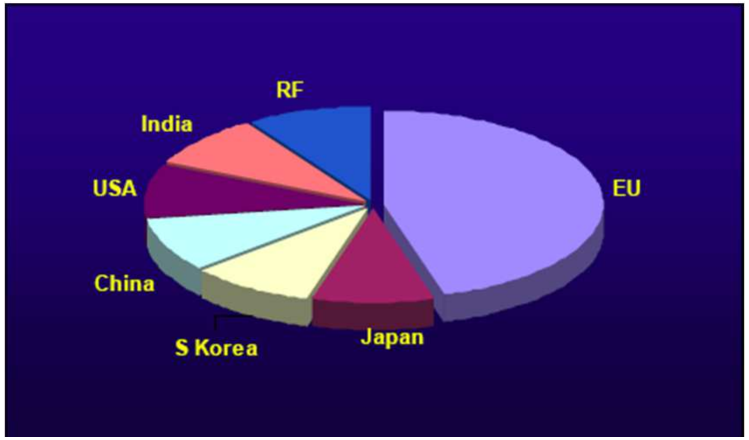

Istituto di Fisica del Plasma "Piero Caldirola"
Consiglio Nazionale delle Ricerche

ITER project

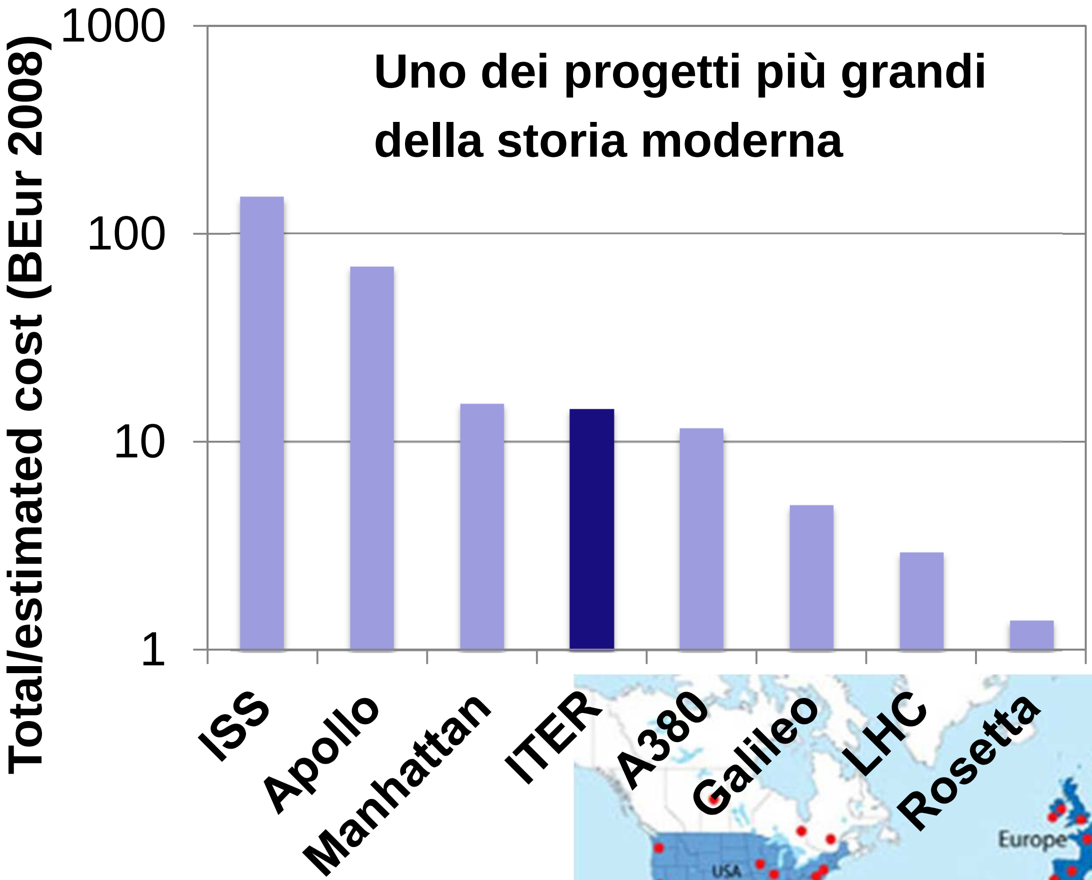

iter
china eu india japan korea russia usa

FUSION FOR ENERGY

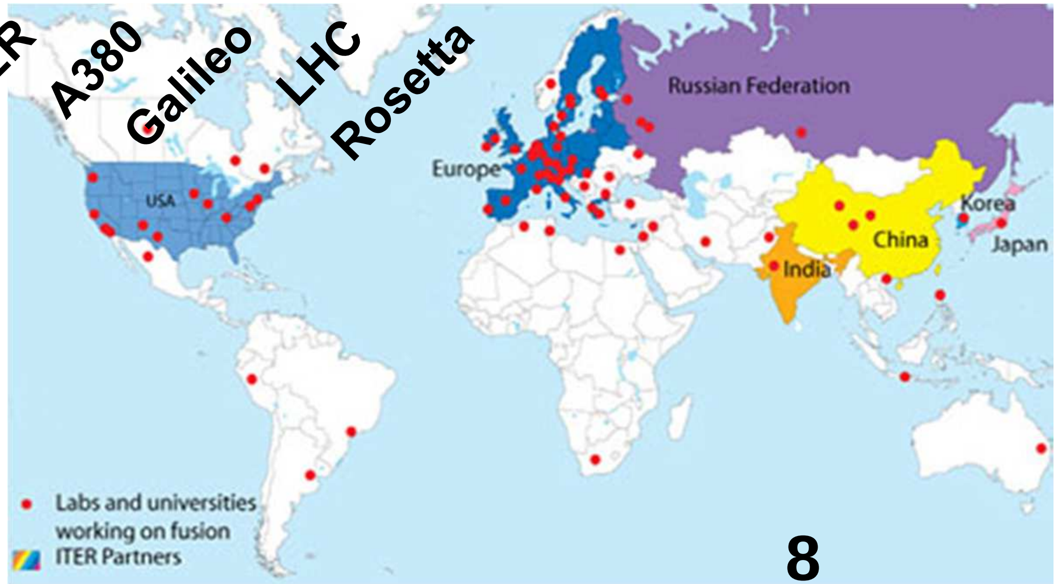

Road map and steps to fusion power reactor

ITER

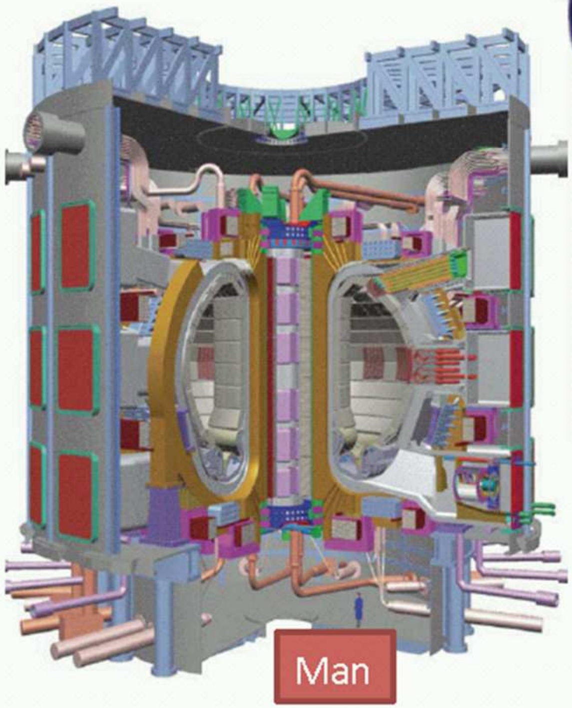

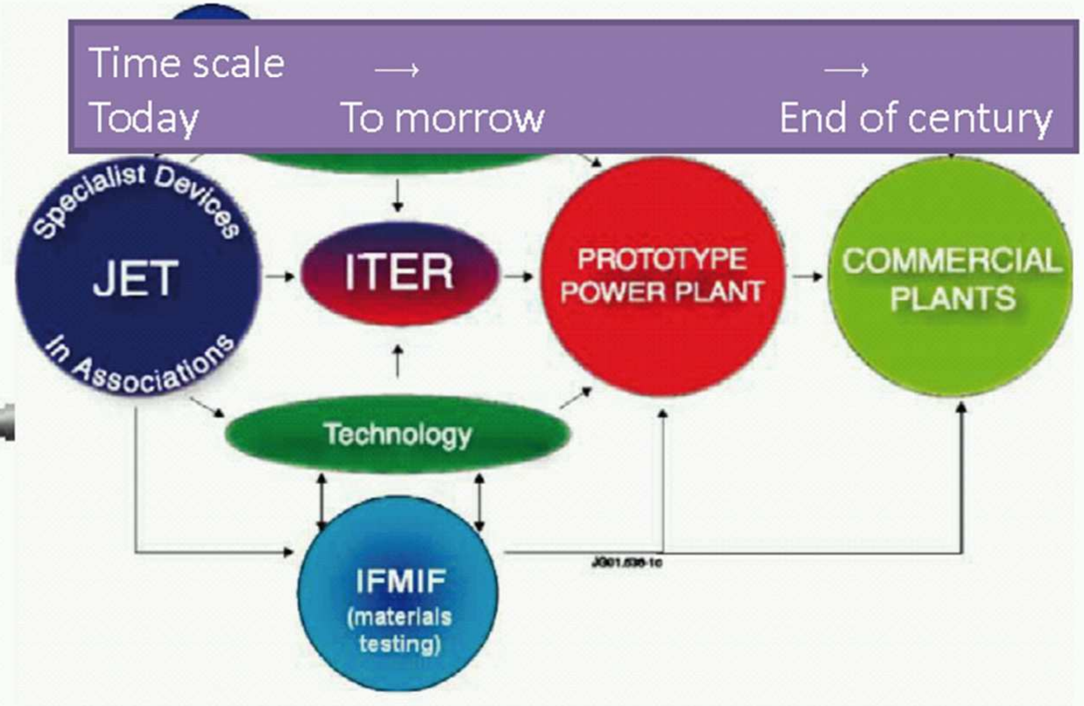

Neutron emission in fusion reactions

The energy distribution of fast ions needs to be known for reliable operation of a thermonuclear fusion reactor

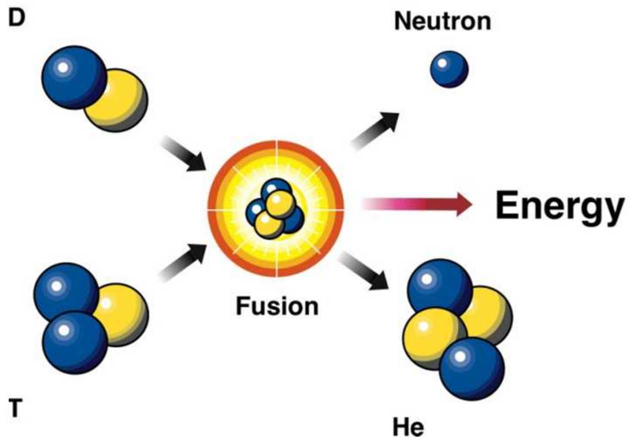

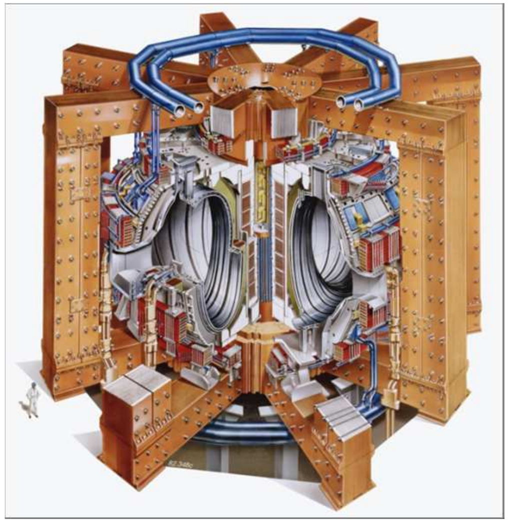

D + T $\rightarrow$ α +n +17.6 MeV

•α **particles** play a key role in the self sustainment of a fusion reactor

•**fast ion acceleration (NBI or RF)** needs to be assessed in in specific heating schemes to quantify efficiency of auxiliary heating (H, D, T, ^{3}He, ^{4}He accelerated ions)

•fast ions can drive MHD modes that may lead to their **redistribution and losses**

Istituto di Fisica del Plasma "Piero Caldirola" Consiglio Nazionale delle Ricerche

Neutron emission from thermonuclear plasmas

Neutron production

Neutrons are produced by fusion reactions

$d + d \rightarrow n + {}^3He$

$d + t \rightarrow n + \alpha$

In a **cold plasma** ($E_{reactants} \approx 0$)

$E_n = 2.45$ MeV for DD reaction

$E_n = 14.0$ MeV for DT reaction

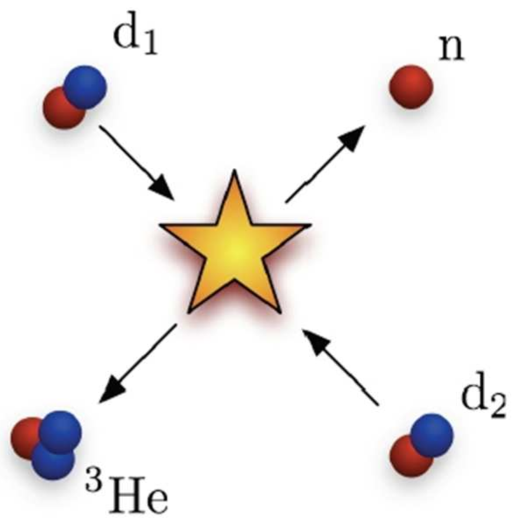

Neutron energy spectrum

The neutron energy depends on the **energy of the reactants**

$$E_{\mathrm{n}} = \frac{1}{2} m_{\mathrm{n}} v_{\mathrm{cm}}^2 + \frac{m_{\mathrm{R}}}{m_{\mathrm{n}} + m_{\mathrm{R}}}(Q+K) + v_{\mathrm{cm}} \cos(\theta) \left(\frac{2 m_{\mathrm{n}} m_{\mathrm{R}}}{m_{\mathrm{n}} + m_{\mathrm{R}}}(Q+K) \right)^{1/2}$$

Neutron emission spectroscopy (NES)

In a plasma in thermal equilibrium, the particles are distributed according to a Maxwellian distribution Neutron spectrum is well approximated as a Gaussian centered at 2.45 MeV (or 14.0 MeV) and with FWHM (W)

Ion Temperature T_i

$W = 82.5 \cdot \sqrt{T}$ for DD emission

$W = 177 \cdot \sqrt{T}$ for DT emission

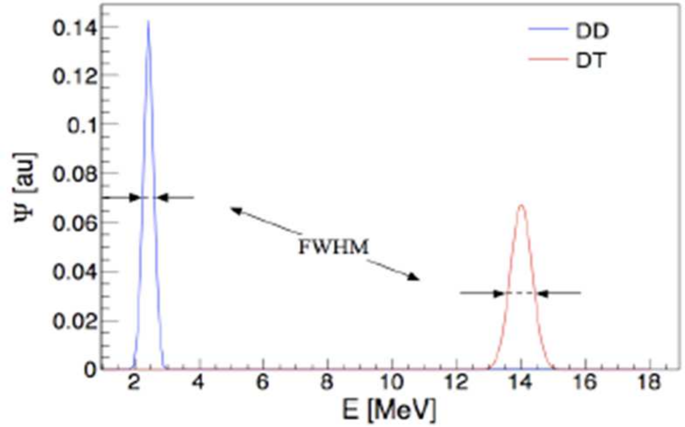

Fast fuel ions can be well diagnosed with NES due the enhanced reactivity

δ(E)-spectra

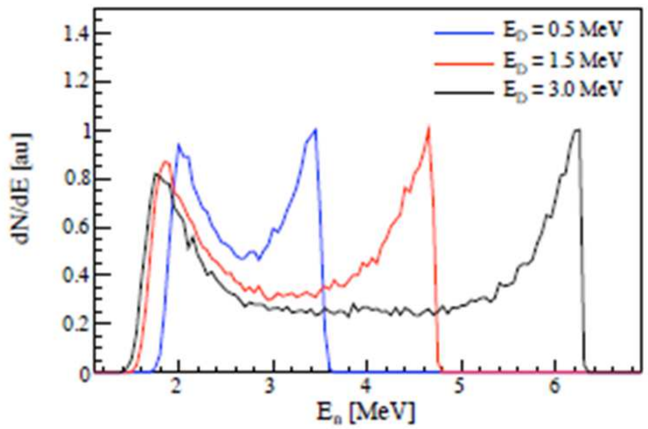

Need for dedicated spectrometers.
Energy resolution ($\Delta E_n/E_n$<5%)
Time resolution (count rate capability, >100 kHZ)

Fusion neutron spectrometry since the 50's

ZETA, 1958

- A cloud chamber was used in 1958 to measure the spectrum of the neutron emission from D-plasmas of ZETA.
- The spectrum was observed to be Doppler shifted depending on the plasma current direction, in consistence with an ordered center-of-mass velocity of the deuteron pairs producing the neutrons.
- It was concluded that the fusion reactions were not due to thermal but driven ions thus disproving that thermonuclear reactions had be attained.

Fusion neutron spectrometry since the 50's

PLT, 1979

- The first proof of thermonuclear reactions from NES was obtained with a ^3He ionization chamber at the PLT tokamak in 1979.
- Neutron spectra were recorded for D-plasmas injected with neutral beams (NB) of H or D atoms which allowed separation of neutrons from thermal and driven ion reactions.

Fusion neutron spectrometry since the 50's

ALCATOR C, 1981

- Doppler broadening of the neutron emission was measured with ^{3}He ionization chamber for Omically heated D-plasmas.
- Ion temperature (T_i) was derived from spectral width.
- This proof-of-principle experiment required summing many discharges to achieve statistics.

Fusion neutron spectrometry since the 50's

JET, 1985

- Time resolved (1s) ^{3}He NES at JET thanks to higher flux.
- Besides T_i the spectral amplitude could also be measured for a well collimated sight-line which allowed n_d to be determined and, hence, the fuel dilution factor, n_d/n_e <0.5.
- This proved unambiguously that the dilution was much worse than had been surmised due to impurities from the wall.

Fusion neutron spectrometry since the 50's

JET, 1989

- To improve NES data, a neutron time-of-flight (TOF) spectrometer was developed in the 80's which could operate at a significantly higher count rate (several kHz) and thus acquire better statistics.
- This made it possible to detect contributions to the fusion power due to reactions between thermal ions and those involving supra-thermal ions caused by injected power through neutral beams (NB) or radio-frequency waves (RF).
- This was the beginning of NES as a probe of the fuel ion population while the data quality was short of the limit for quantitative plasma information.

Fusion neutron spectrometry since the 50's

JET, 1997

- The MPR was designed specifically to attain maximum performance for ignited DT plasmas (IGNITOR) and was put to the test for the sub-ignited conditions reached in JET's DT experiments.
- This fourth generation NES diagnostic meant drastically improved data quality (up x10^3 count rate) which, e.g., permitted plasma information to be extracted from the shape of the neutron emission and not only the width.

Fusion neutron spectrometry since the 50's

TOFOR, 2004

- The MPR success indicated the development of the next step NES diagnostics towards
- further increase in sensitivity through proton detectors with better background handling (MPRu)
- capability and use of orthogonal sight-lines
- development of a high-performance 2.5-MeV spectrometer (TOFOR, for NES diagnosis of D plasmas.

Istituto di Fisica del Plasma "Piero Caldirola"
Consiglio Nazionale delle Ricerche

Neutron Detectors

Main reference on radiation detectors:
Glenn F KNOLL, *Radiation Detection and Measurement*

Istituto

Cons

ITER has a comprehensive set of diagnostic systems

Including some neutron diagnostics (not many, unlike fission)

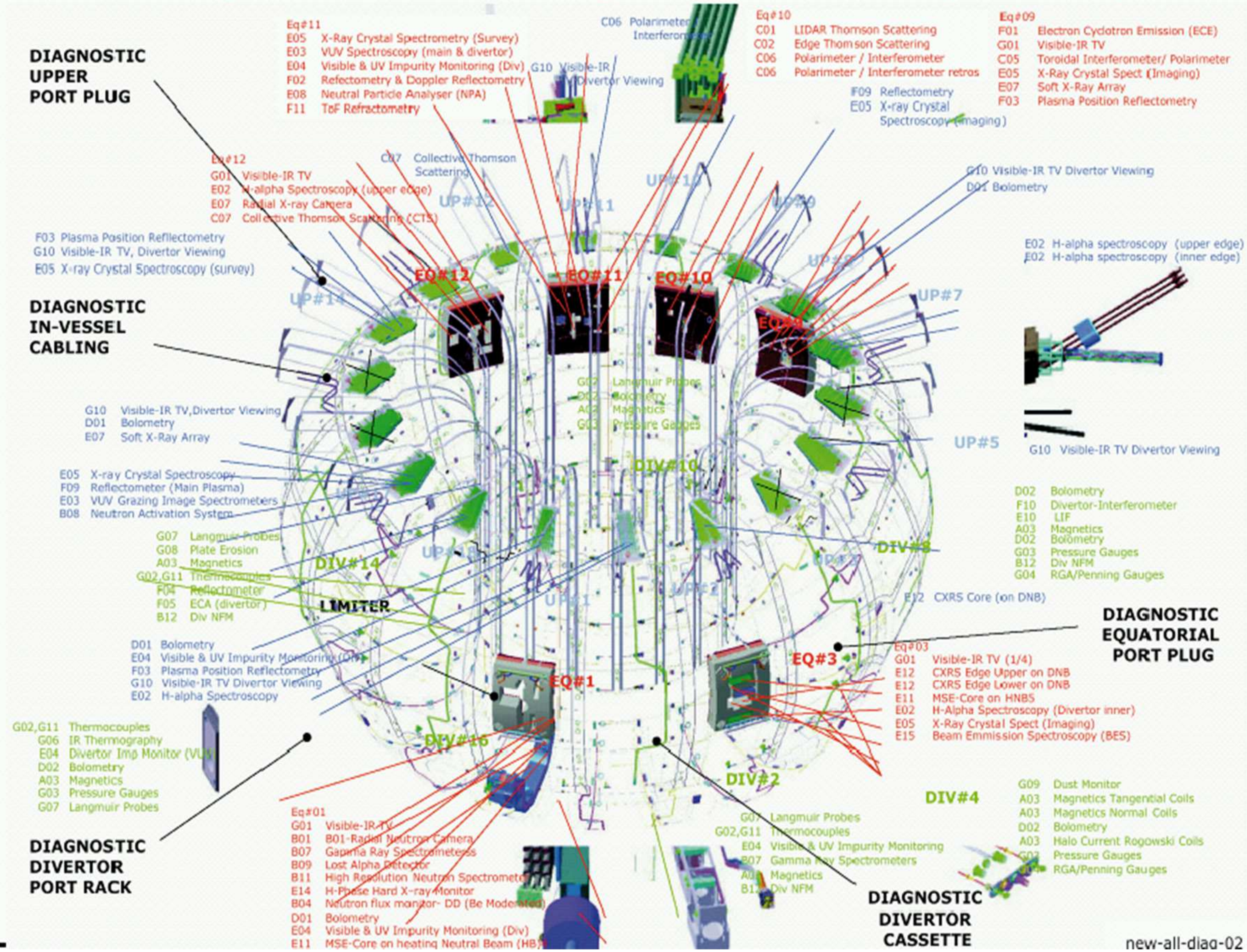

At any position around the fusion reactor the neutron field is an admixture of "uncollided" and "collided" neutrons

Three uncollided components: dt, dd, dt
Collided neutrons can easily overwhelm the uncollided component

Example 1: measurement of the dd uncollided component in a dt plasma

Example 2: measurement of dt component in the side channels of a neutron camera

The need for separation of different components must be kept in mind when designing a diagnostic system
Other considerations: gamma-ray background, environment (B, T)

=> Detectors must be DESIGNED for the specific application.

Challenges in neutron detection

- Neutrons have no charge: they do not produce ionizations or excitations in matter directly; neutrons are difficult to stop.

- Background : main component gamma-rays; discrimination against gamma-rays is not easy.

- High detection rates are often required: usually neutron detectors are used in a regions of high neutron (and gama) flux

- Cross-sections of neutron reactions on which neutron detectors can be based decrease with increasing neutron energy $\Rightarrow$ fast neutrons with high efficiency is particulary difficult

Interaction of neutrons with matter

- No electric charge → no electromagnetic interaction
- Only strong interaction with the nuclei

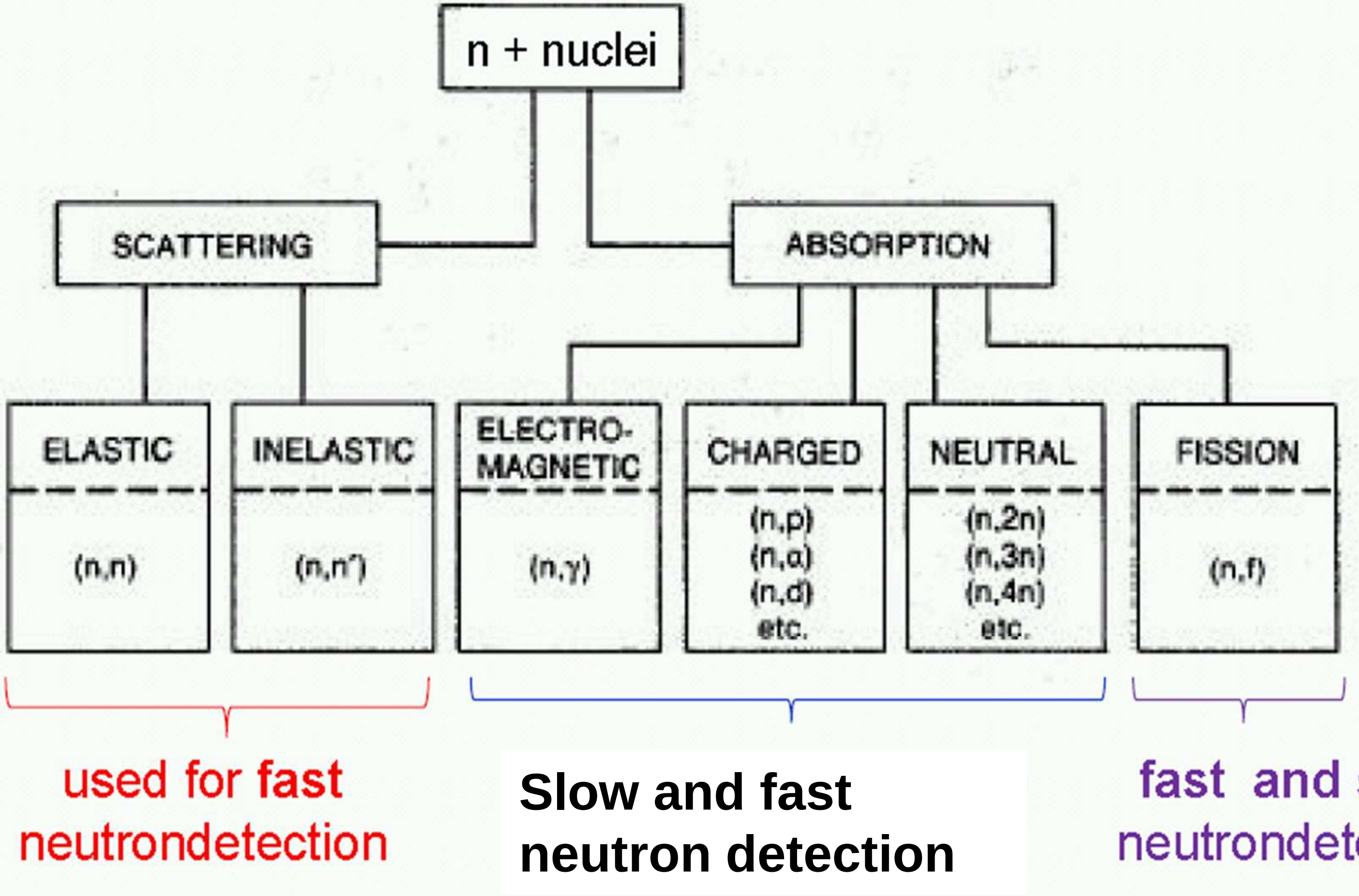

Fast Neutron Detection

- All neutron detection relies on observing a neutron-induced nuclear reaction
- The capture cross sections for fast-neutron induced reactions are small compared to those at low energies ($\sigma_{cap} \sim 1/v$)
- Approaches to detect fast neutrons:
  - Thermalize/ moderate & capture as before, only providing count rates (i.e. neutron flux)
  - Elastic scattering from protons at high energy
    - Protons are easy to detect in conventional detectors
    - Observe recoils for time-of-flight (ToF) enabling neutron energy measurements by measuring the velocity through ToF.

–.Nuclear reactions

Commonly Used Neutron Reactions

$n + {}^{3}He \rightarrow ({}^{4}He)^{*} \rightarrow p + {}^{3}H$, $Q = 0.765$ MeV, target abundance ~ $1.4\mathrm{x}10^{-4}$ % (5.3 kb) — (n,p)

$n + {}^{6}Li \rightarrow ({}^{7}Li)^{*} \rightarrow {}^{4}He + {}^{3}H$, $Q = 4.78$ MeV, target abundance ~ 7.5% (940 b) — (n,α)

$n + {}^{10}B \rightarrow ({}^{11}B)^{*} \rightarrow {}^{7}Li^{*} + {}^{4}He$, $Q = 2.31$ MeV, 94% branch, nat. abund. ~20 % (3.8kb) — (n,α)
$\rightarrow {}^{7}Li + {}^{4}He$, $Q = 2.79$ MeV, 6% branch

$n + {}^{113}Cd \rightarrow ({}^{114}Cd)^{*} \rightarrow {}^{114}Cd + \gamma$, $Q \sim 8$ MeV, target abundance ~ 12% (21 kb) — (n,γ)

$n + {}^{157}Gd \rightarrow ({}^{158}Gd)^{*} \rightarrow {}^{158}Gd + \gamma$, $Q \sim 8$ MeV, target abundance ~ 16% (255 kb) — (n,γ)

$n + {}^{235}U \rightarrow ({}^{236}U)^{*} \rightarrow$ (fission fragments), $Q \sim 200$ MeV, target abundance ~ 0.7% — (n,f)

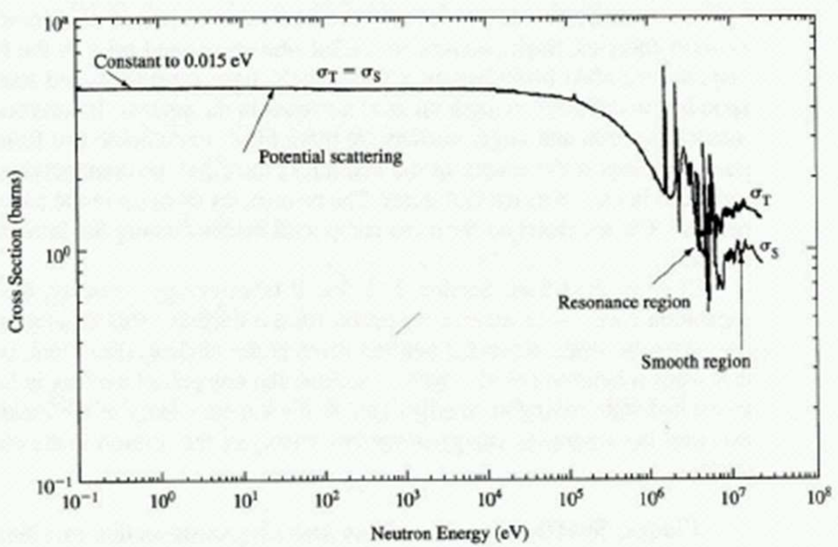

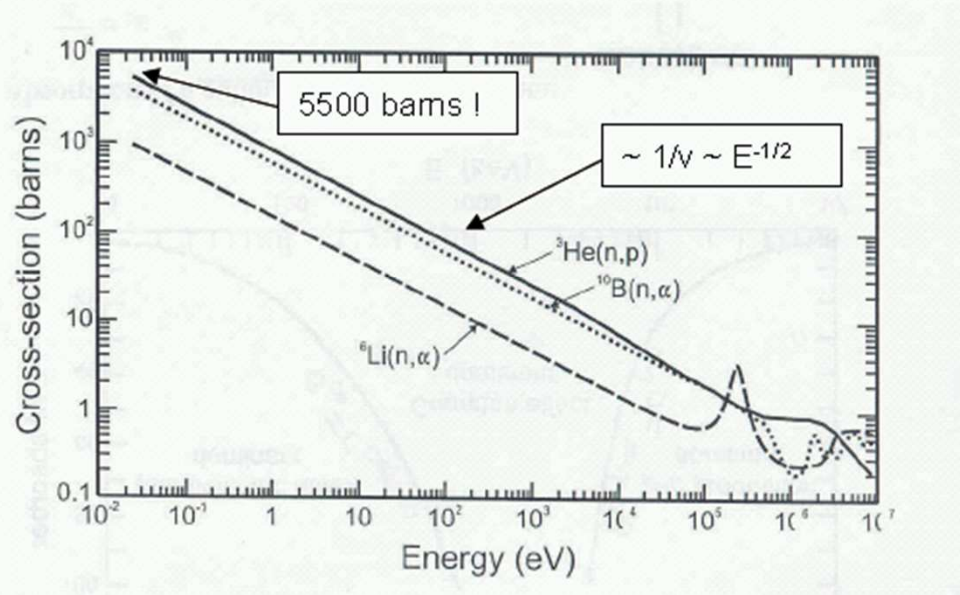

Istituto
di Fisica del Plasma
"Piero Caldirola"
Consiglio Nazionale delle Ricerche

Neutron flux measurements

Neutron –Induced Fission Reactions

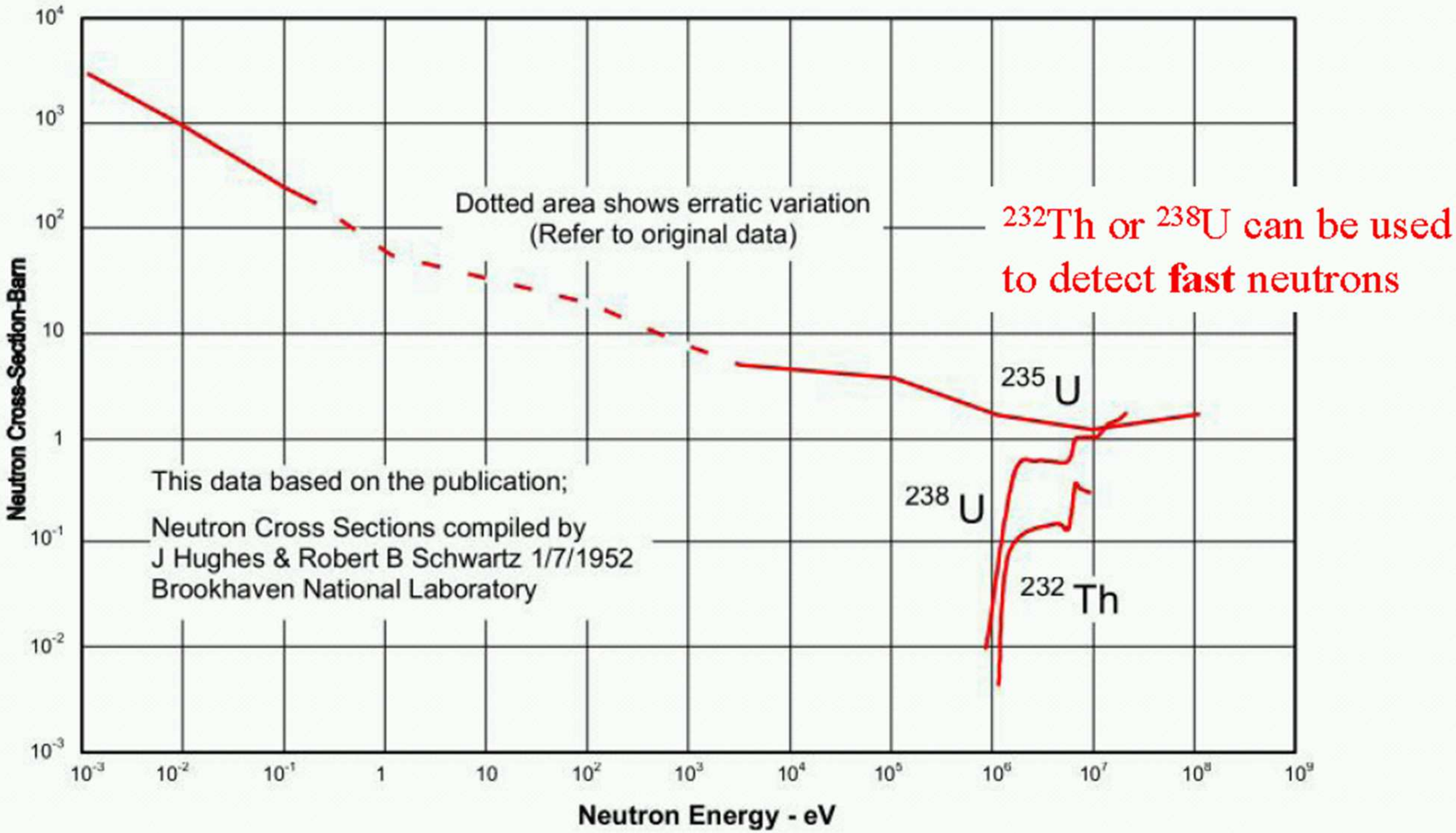

Fission chambers: principle of operation

Neutron cause fission of the material covering one (or both electrode) of the chamber

The high energy ionising products → output pulses of the ionization chamber.

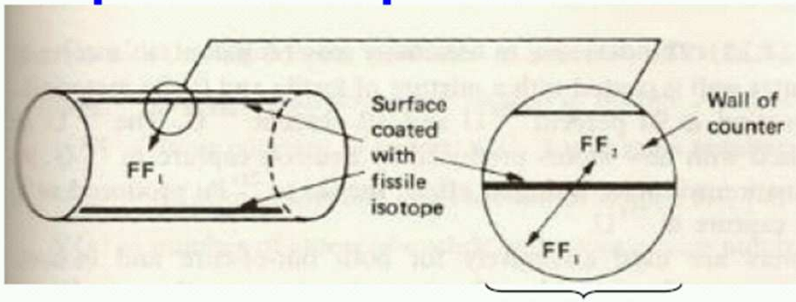

for slow neutrons, the two FF are emitted in oposite directions

Fission fragments (FF) are very energetic (for example ^{235}U : Q~200 MeV → FF share about 160 MeV);

α and γ background also present;

^{235}U is the most used material; ^{238}U and ^{232}Th are used for fast neutrons

Other fissionable isotopes are ^{239}Pu, ^{237}Np, ^{234}U and ^{233}U.

- The most common filling gas is Argon plus 10% methane (or 2% N_2), with filling pressures typically from 1 to 5 atm (pressure depending on the application). At this pressure the range of FF is ~ a few cm.

Fission chambers

Coating thickness should be as large as possible to increase efficiency

BUT

smaller than the range of fission fragments in the coating material (average range of FF from ^{235}U is ~7 μm ≡13mg/cm^2 coating;

- ➡ Typical coating thickness: 0.02 to 2 mg/cm^2
- ➡ Typical efficiency for thermal neutrons: 0.5 -1% (and even lower for fast neutrons)

Fission chambers can operate in pulse mode, DC or MSV mode.

- Pulse chambers are limited to count rates typically < 10^5 cps;
- for higher count rate, DC or MSV fission chambers are used.

Fission chambers: pulse mode

- allow direct α and γ discrimination based on amplitude threshold
  - The spectrum depends on the wall coating thickness
  - the wall thickness must be thin enough so that the pulses due to any of the fission fragments are greater than the pulses due to α particles (for α **discrimination**)

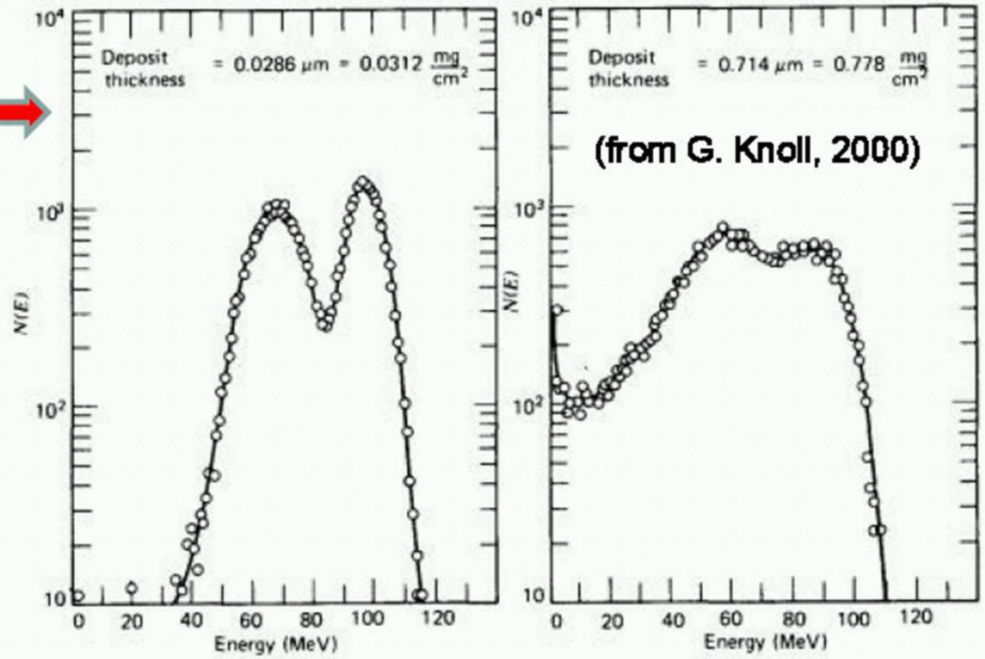

FF deposited energy >> gammas

→ Fission chambers have **high insensitivity** to gammas

but limited to count rates < 10^5 cps

Fission Chambers in MSV mode

In DC mode it is not possible to discriminate gamma-ray directly because all pulses, whether large or small, add some contribution to the measured current.

ALTERNATIVE: MSV (Mean Square Voltage) mode of operation:

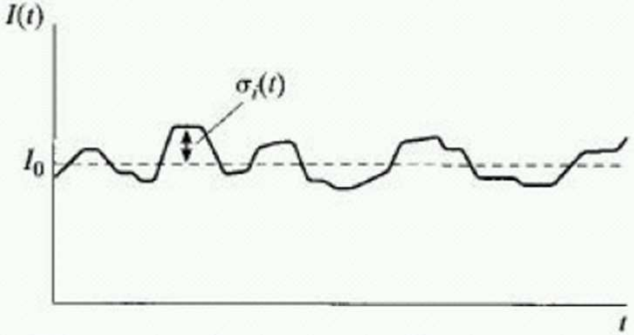

$$I_0 = rQ$$

r: rate of events
Q: charge produced per event

The variance in the current is:

$$\overline{\sigma_I^2(t)} = \frac{1}{T}\int_{t-T}^{t} [I(t') - I_0]^2 \, dt' = \frac{1}{T}\int_{t-T}^{t} \sigma_i^2(t') \, dt'$$

where T is the response time of the picoammeter
It is easy to conclude that

$$\overline{\sigma_I^2(t)} = \frac{rQ^2}{T}$$

Fission Chambers in MSV mode

By passing the current signal I(t) through a circuit element that blocks the average current I_0 *and only passes the fluctuating component* $\sigma_i(t)$*:*

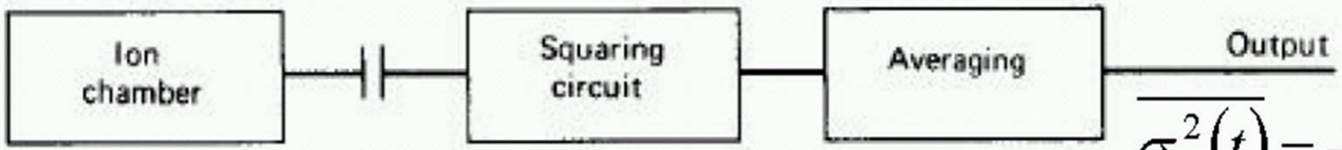

$$\overline{\sigma_I^2(t)} = \frac{1}{T}\int_{t-T}^{t} \sigma_i^2(t')\,dt'$$

$$\overline{\sigma_I^2(t)} = \frac{rQ^2}{T}$$

In MSV mode, the output is proportional to the *square of the charge per event.*

In a mixed radiation field, *the* detector response is weighted in favor of the type of radiation giving the larger average charge per event (e.g.,in a neutron and gamma mixed field the **neutron signal is enhanced** compared with the response due to smaller-amplitude gamma-ray events.

Fission Chambers in MSV mode

In a fission chamber, events may be due to neutrons, α particles or gamma-rays.

$$\overline{\sigma^2(t)} = \frac{rQ^2}{T}$$

$$= \frac{1}{T}\left(r_n q_n^2 + r_\alpha q_\alpha^2 + r_\gamma q_\gamma^2\right)$$

$$= \frac{q_n^2}{T}\left(r_n + r_\alpha \frac{q_\alpha^2}{q_n^2} + r_\gamma \frac{q_\gamma^2}{q_n^2}\right).$$

the electrical charges per pulse by neutron, α particle and γ-ray are defined as q_n, q_α and q_γ, respectively.

As $q_n \gg q_\alpha$ and $q_n \gg q_\gamma$,

$$\overline{\sigma^2(t)} \approx \frac{r_n q_n^{\;2}}{T}$$

Fission chambers in (fusion) reactors

Fission chambers are operated in pulse mode or current mode depending on the neutron flux to be measured:

Pulse mode:

1) easy gamma-ray discrimination with pulse amplitude discrimination;
2) the use of pulse mode is **limited to rates ~10^5 cps** (state-of-the-art techniques in chamber design and electronics are able to raise this limit to 10^7cps).

Current mode.

1) maximum rate limited by non-linear effects due to ion-electron recombination ;
2) lower limit of current operation is determined by the leakage currents in chamber insulators
3) **no chance of gamma-discrimination** (small pulses are also integrated and contibute to the current)

IN FISSION REACTORS:

- For the **startup range**, they are generally used in the **pulse mode**.
- For **power range**, core miniature ion chambers in the **DC mode**.
- They can be used over a wide range of neutron flux in **MSV mode**

Activation-based neutron detectors

A sample of a material with high cross-section for activation by neutrons is exposed to a flux of neutrons for a period of time and then removed so that the induced radioactivity (usually γ or β) may be counted.

For a thin foil irradiated with a contant flux of neutrons, the rate of activated species is:

$$R = \phi\sigma V$$

ϕ = neutron flux averaged over the foil surface
σ = activation cross section averaged over the neutron spectrum
V = foil volume

During irradiation the activity of the material:

$$A(t) = R\left(1 - e^{-\lambda t}\right)$$

λ = decay constant of the radioactive species formed under irradiation

$$\lim_{t\to\infty} A(t) = A_{\infty} = R = \phi\sigma V$$

After exposure to the neutron flux during a time t_0, the foil is transferred to an appropriate radiation counter for measurement of its activity.

Activation-based neutron detectors

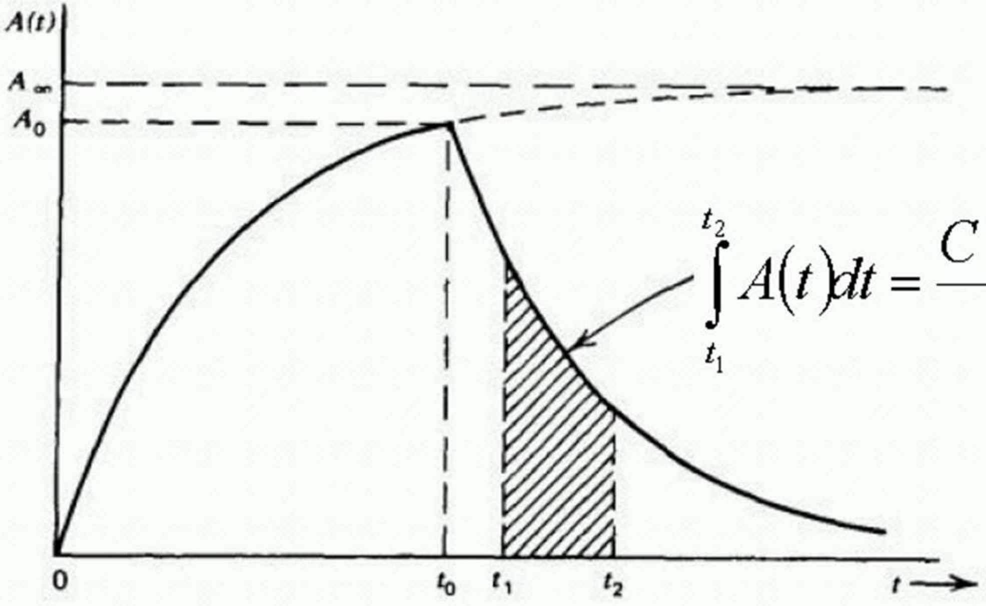

$$\int_{t_1}^{t_2} A(t)dt = \frac{C-B}{\varepsilon}$$

C = total number of counts in $t_2 - t_1$,

B = the number of background counts in $t_2 - t_1$,

ε = the overall counting efficiency (including any self-absorption effects);

• Because the activity is continuously decaying during this stage, careful account must be made of each of the times involved.

• If the counting is carried out over an interval between t_1 and t_2, **the number of counts,** C,

$$C = \epsilon \int_{t_1}^{t_2} A_0 e^{-\lambda(t - t_0)}\, dt + B$$

$$\boxed{A_\infty = \frac{\lambda(C-B)}{\epsilon(1-e^{-\lambda t_0})e^{\lambda t_0}(e^{-\lambda t_1} - e^{-\lambda t_2})}}$$

from A_∞ the neutron flux can be determined

Activation-based neutron detectors

Table 19.3 Materials Useful as Slow Neutron Activation Detectors (by (n,γ) reactions)

Element	Isotope (Abundance in Percent)	Thermal Activation Microscopic Cross Section (in 10^{-28} m^2)	Induced Activity	Half-Life
Manganese	^{55}Mn (100)	13.2 ± 0.1	^{56}Mn	2.58 h
Cobalt	^{59}Co(100)	16.9 ± 1.5	^{60m}Co	10.4 min
		20.2 ± 1.9	^{60}Co	5.28 y
Copper	^{63}Cu(69.1)	4.41 ± 0.20	^{64}Cu	12.87 h
	^{65}Cu(30.9)	1.8 ± 0.4	^{66}Cu	5.14 min
Silver	^{107}Ag(51.35)	45 ± 4	^{108}Ag	2.3 min
	^{109}Ag(48.65)	3.2 ± 0.4	^{110m}Ag	253 d
Indium	^{113}In(4.23)	56 ± 12	^{114m_1}In	49 d
		2.0 ± 0.6	^{114}In	72 s
	^{115}In(95.77)	160 ± 2	^{116m_1}In	54.12 min
		42 ± 1	^{116}In	14.1 s
Dysprosium	^{164}Dy(28.18)	2000 ± 200	^{165m}Dy	1.3 min
		800 ± 100	^{165}Dy	140 min
Gold	^{197}Au (100)	98.5 ± 0.4	^{198}Au	2.695 d

Source: K. H. Beckurts and K. Wirtz, *Neutron Physics*. Copyright 1964 by Springer-Verlag. New York. Used with permission.

Activation-based neutron detectors

Table 19.4 Materials Useful as Threshold Activation Detectors (useful for fast neutrons)

Material	Reactions of Interest	Isotopic Abundance (at %)	Half-Life	γ Energy (MeV)	γ Abundance (%)	Threshold (MeV)
F	$^{19}F(n,2n)^{18}F$	100.0	109.7 min	0.511⁺	194°	11.6
Mg	$^{24}Mg(n,p)^{24}Na$	78.7	15.0 h	1.368	100	6.0
Al	$^{27}Al(n,\alpha)^{24}Na$	100.0	15.0 h	1.368	100	4.9
Al	$^{27}Al(n,p)^{27}Mg$	100.0	9.46 min	0.84–1.01	100	3.8
Fe	$^{56}Fe(n,p)^{56}Mn$	91.7	2.56 h	0.84	99	4.9
Co	$^{59}Co(n,\alpha)^{56}Mn$	100.0	2.56 h	0.84	99	5.2
Ni	$^{58}Ni(n,2n)^{57}Ni$	67.9	36.0 h	1.37	86	13.0
Ni	$^{58}Ni(n,p)^{58}Co$	67.9	71.6 d	0.81	99	1.9
Cu	$^{63}Cu(n,2n)^{62}Cu$	69.1	9.8 min	0.511⁺	195°	11.9
Cu	$^{65}Cu(n,2n)^{64}Cu$	30.9	12.7 h	0.511⁺	37.8°	11.9
Zn	$^{64}Zn(n,p)^{64}Cu$	48.8	12.7 h	0.511⁺	37.8°	2.0
In	$^{115}In(n,n')^{115m}In$	95.7	4.50 h	0.335	48	0.5
I	$^{127}I(n,2n)^{126}I$	100.0	13.0 d	0.667	33	9.3
Au	$^{197}Au(n,2n)^{196}Au$	100.0	6.18 d	0.33–0.35	25–94	8.6
Li	$^{7}Li(n,\alpha n')t$	92.58	12.3 y	0–0.019ˣ	100ˣ	3.8

⁺Annihilation radiation.

°Yield of annihilation photons assuming all positrons are stopped.

ˣβ particle energy and percent abundance.

Activation foils as neutron detectors

\- They are **integrating** detectors ⇒ no information on any time variation of neutron flux

\+
- can be small in size
- insensitive to gamma-rays
- low cost
- can be installed in very harsh enviroments regarding temperature, pressure and high radiation fluxes (e.g. the core of a reactor)
- do not require any electrical connections (so they are handy)

⇓

They are widely used for mapping the spatial variation of steady-state neutron fluxes in reactor cores

^3He Proportional Counter

- $^3He(n,p)$ reactions due to
  - slow neutrons (moderated in detector environment) leading to epithermal peak
  - Fast reactions (no moderation) leading to full energy peak: $E_n + Q$
- Elastic scattering $n \rightarrow {}^3He$ leading to recoil distribution with maximum energy $E_R = 0.75\ E_n$
  - Cross section is larger than (n,p) reaction

Pulse-height spectrum by neglecting wall effects

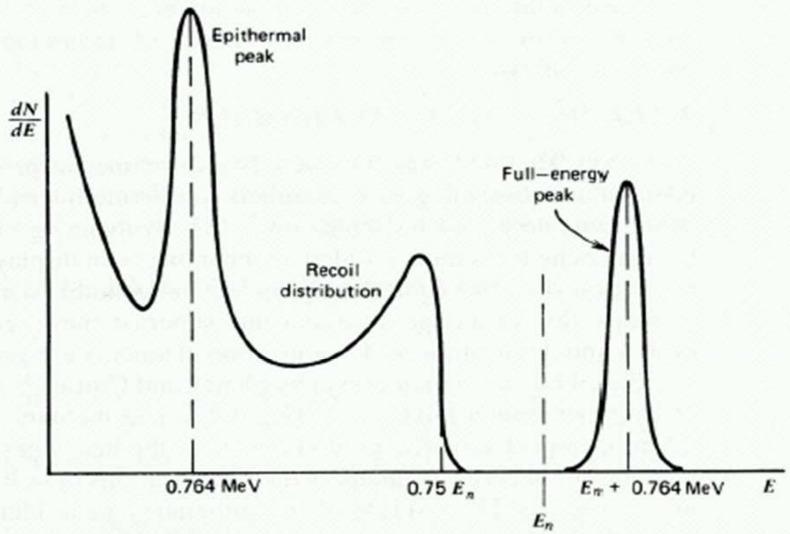

Fast Neutron Scattering and Kinematics

- Most common detection method for fast neutrons is by elastic scattering of neutrons on light nuclei producing a recoiling nucleus that can be easily detected (hydrogen → proton recoil)

- Elastic scattering
  - ⇨ Q-value not important
  - ⇨ Target nuclei masses are important!
    - ⇨ How much energy can be deposited per interaction ?

$$\frac{E_R}{E_n} = \frac{4A}{(1+A)^2}\cos^2\theta_{lab}$$

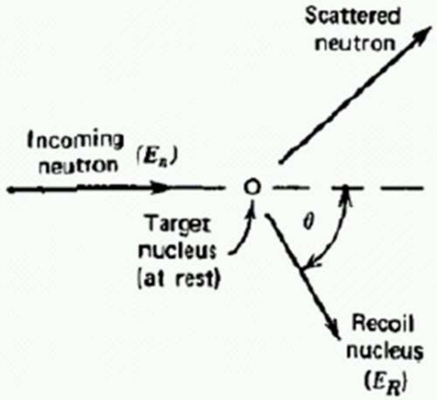

Tgt	A	$4A/(1+A)^2$
^{1}H	1	1
^{2}H	2	8/9=0.889
^{4}He	4	16/25=0.64
^{12}C	12	48/169=0.284

Liquid scintillator

The schematic diagram of the neutron spectrometer

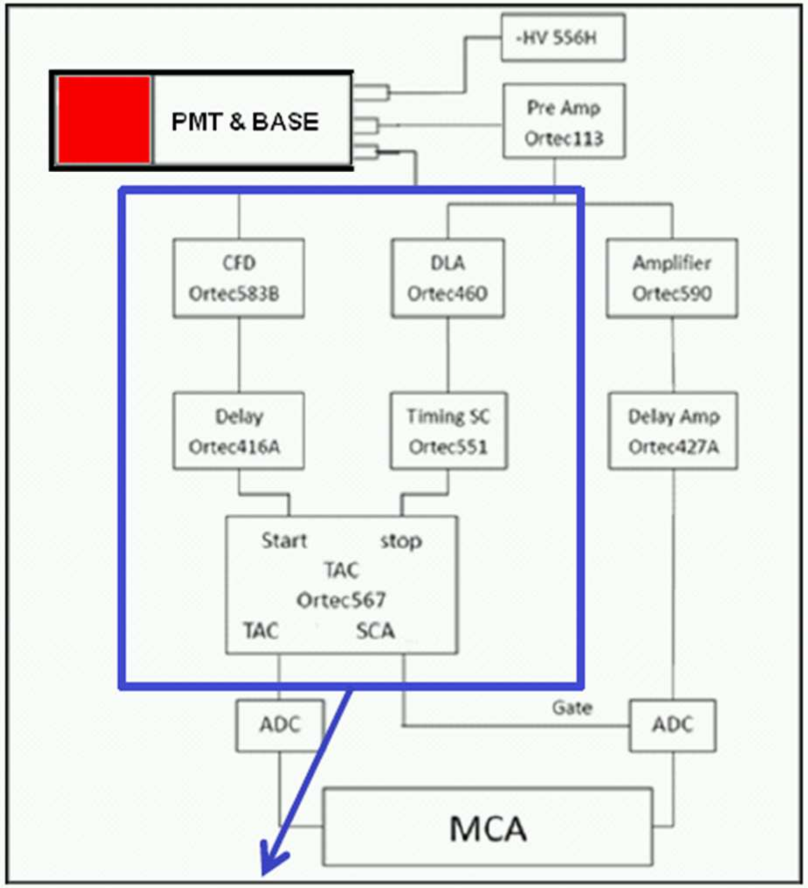

Neutron/ γ ray discrimination module

Three different scintillators:

- ✓ 2 inch×2 inch EJ301 liquid scintillator
- ✓ 5 inch×2 inch BC501A liquid

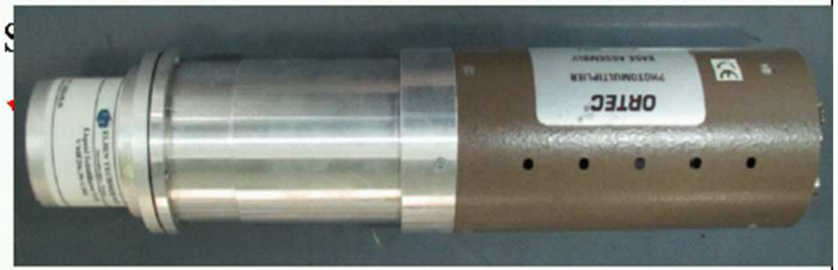

Detailed calibration of the neutron energy spectrometer via mono-energetic neutron source

✓ Totally 16 mono-energetic neutron filed were generated for the calibration

✓ Van de Graaff accelerator @ Peking University

✓ Neutron energy range: from 0.6 MeV to 16 MeV

✓ Key parameters:

- energy calibration result
- light output functions
- resolution function

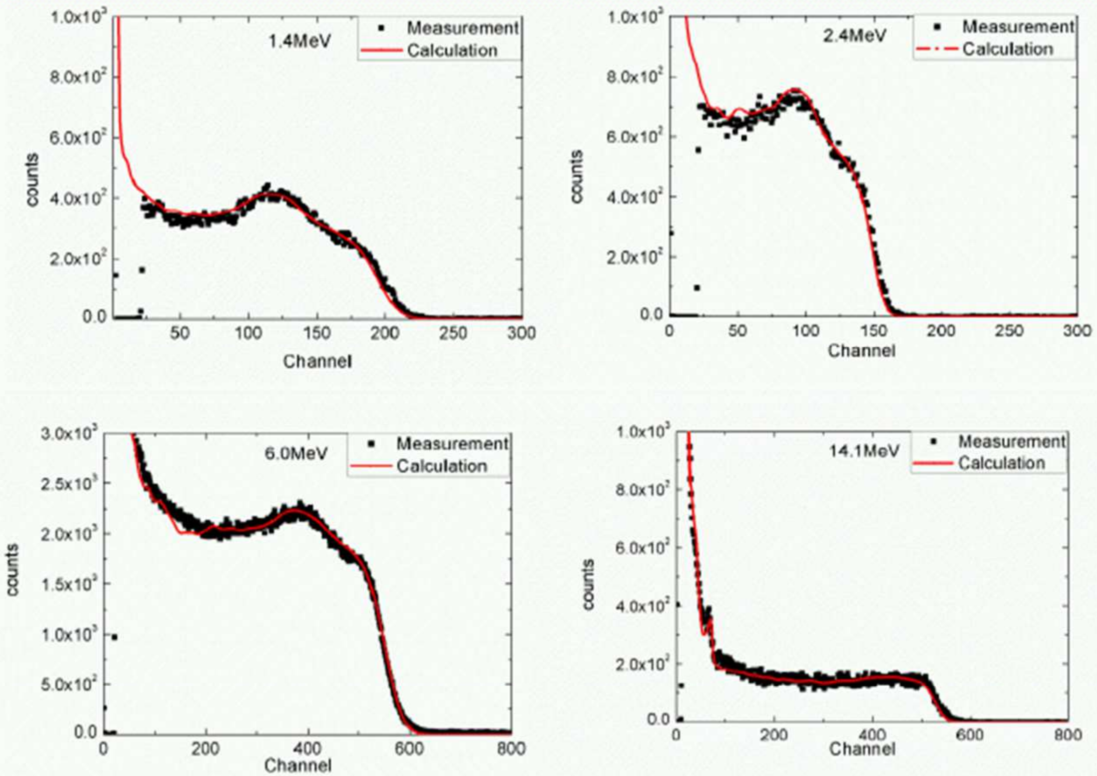

Istituto di Fisica del Plasma "Piero Caldirola"
Consiglio Nazionale delle Ricerche

Liquid scintillator

Neutron/gamma Discrimination: Charge Integration Method

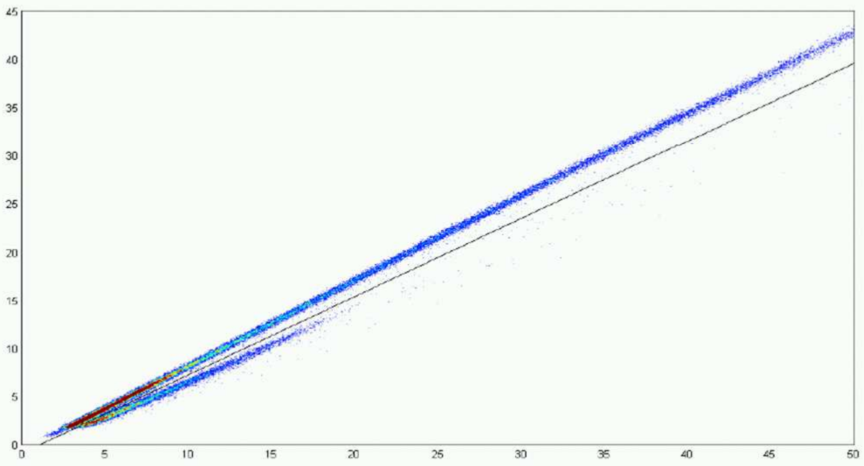

Pulse Height Spectrum from 300 EAST pulses

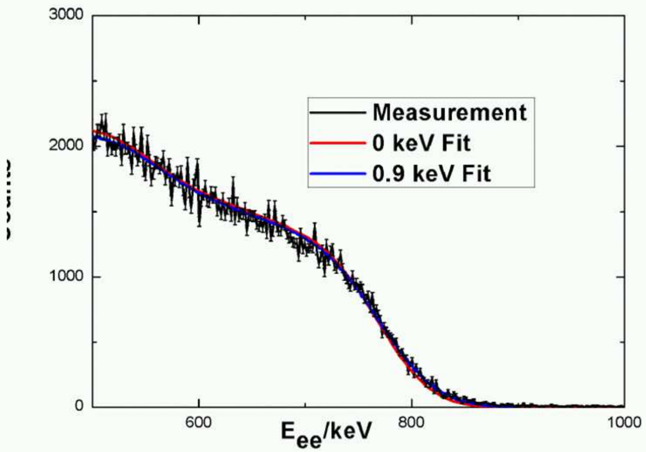

Role of scattered neutrons

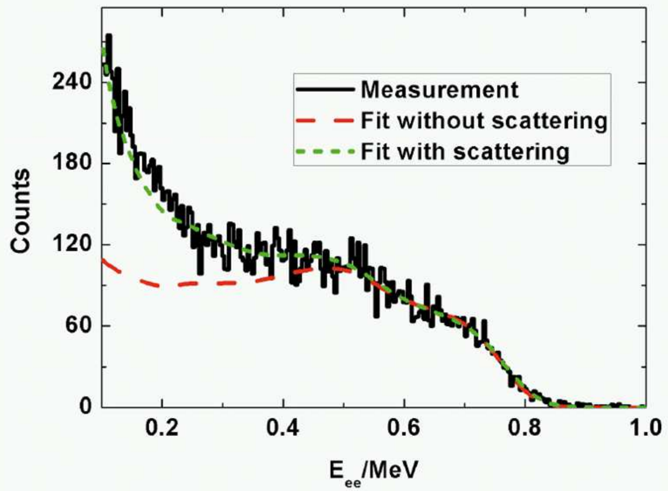

Istituto di Fisica del Plasma "Piero Caldirola"
Consiglio Nazionale delle Ricerche

JET neutron/gamma camera

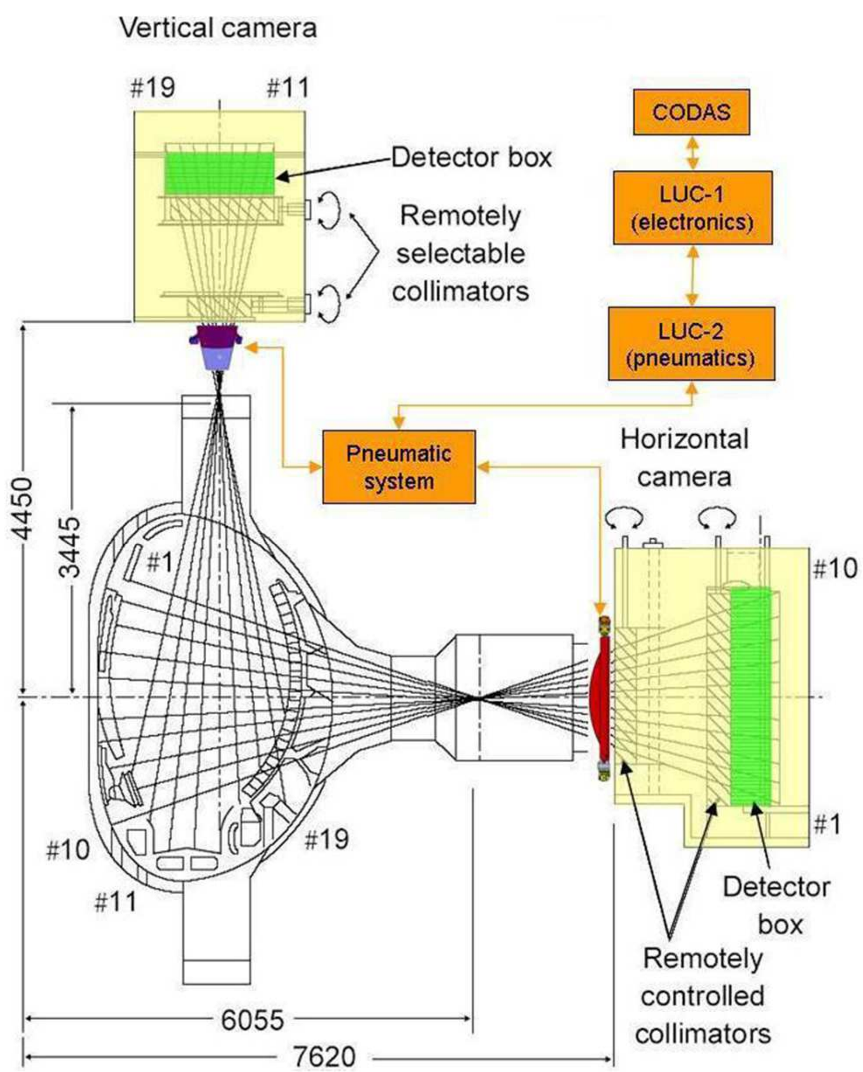

- Two cameras
- Vertical: 9 lines-of-sight
- **Horizontal: 10 lines-of-sight**
- **upgrade for DT**
- Fan-shaped array of remotely adjustable collimators with two apertures (Ø10 and 21mm)
- Space resolution: (8-15)cm (in the center)
- Detectors
- NE213 liquid scintillators (2.5 & 14 MeV)
- Bicron-418 plastic scintillators (14 MeV)
- **CsI(Tl) photo-diodes** (hard X-rays and γ-rays)

Operation in high neutron fluxes

Approximate attenuation factors

Neutron attenuator	Material	Neutron energy	
		2.45 MeV	14.1 MeV
Horizontal	H_2O	10^2	15
Vertical (normal)	H_2O	$10^{2\,(*)}$	15
Vertical (long version)	H_2O	10^4	10^2

Neutron emissivity spatial reconstruction

Neutron camera @ JET

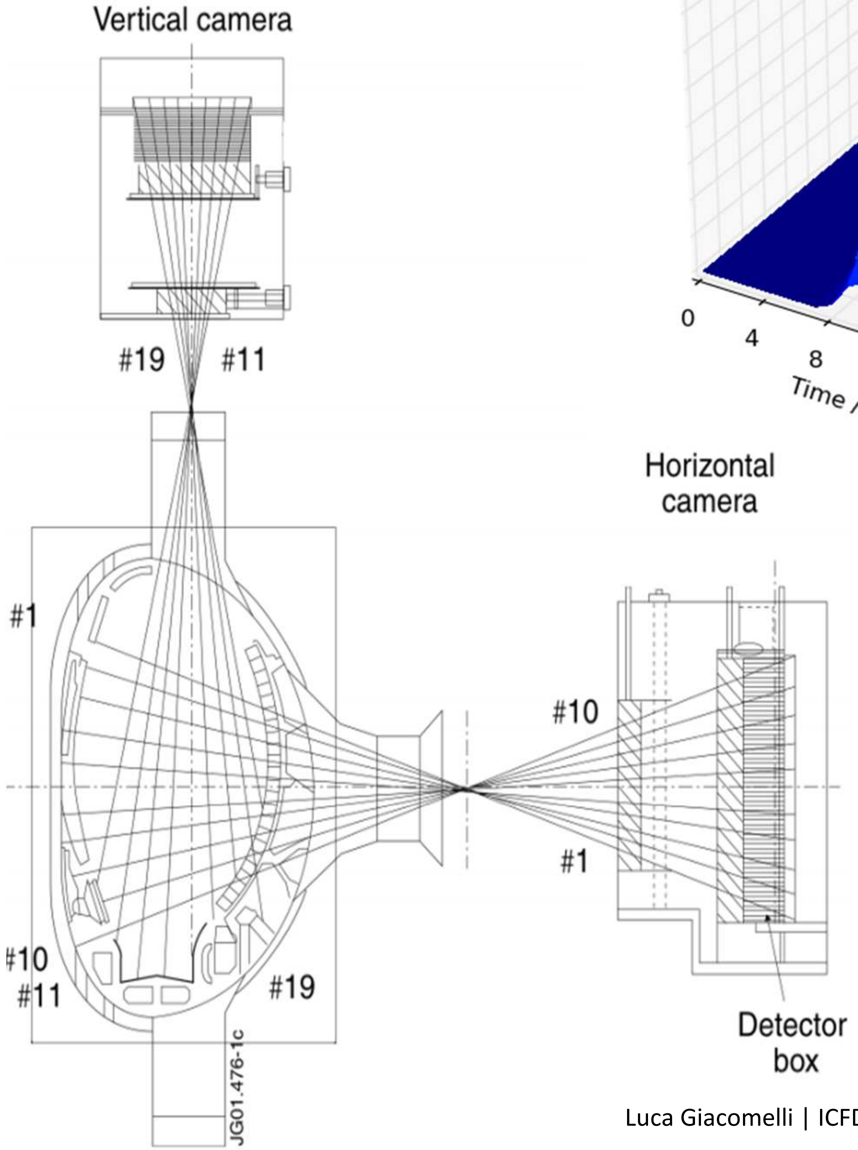

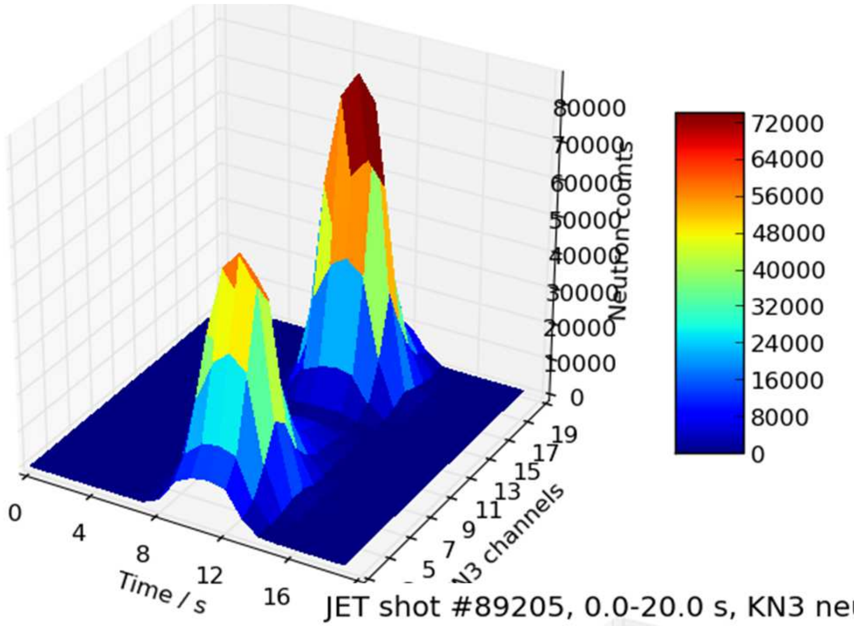

JET shot #89205, 0.0-20.0 s, KN3 neutron counts

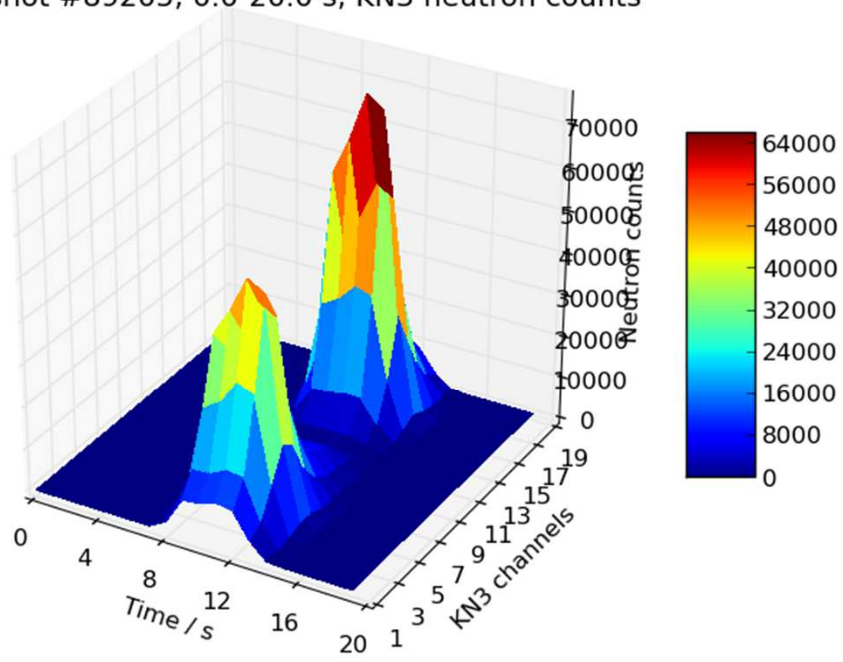

Neutron camera @ JET

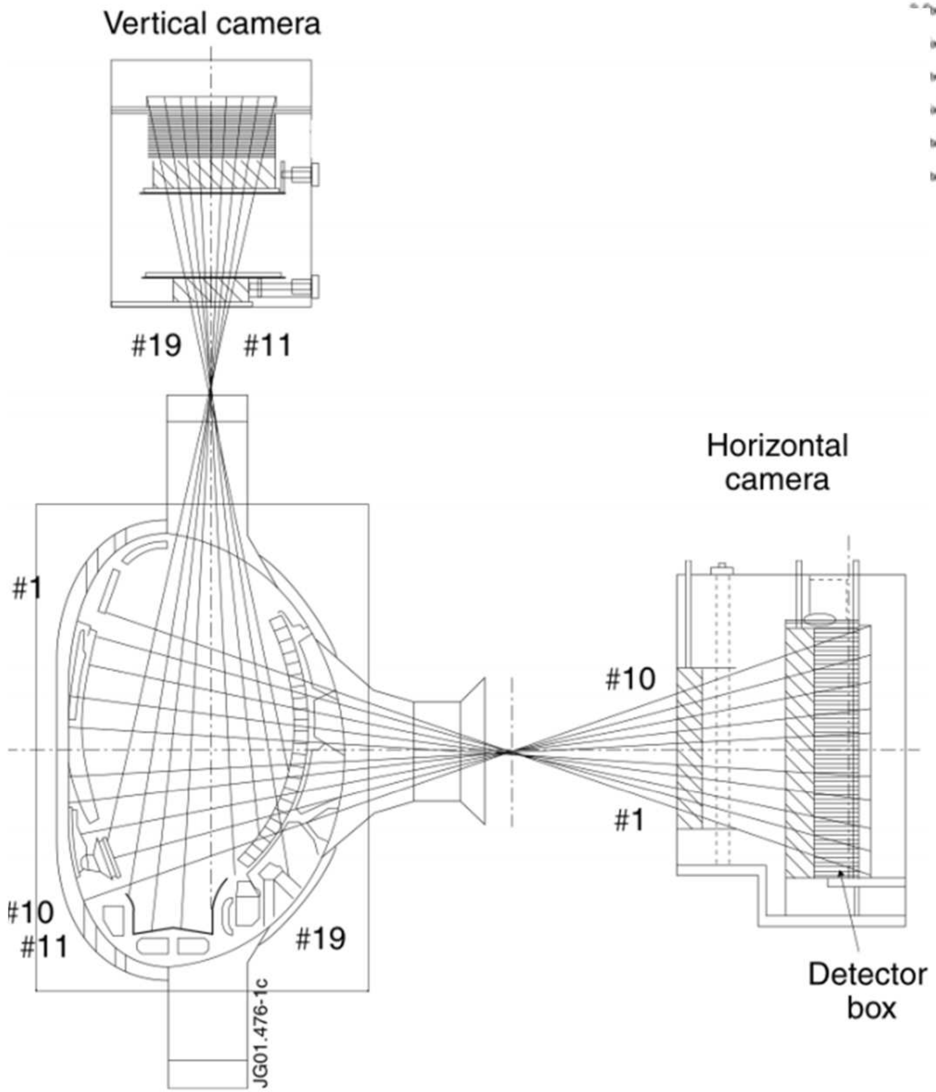

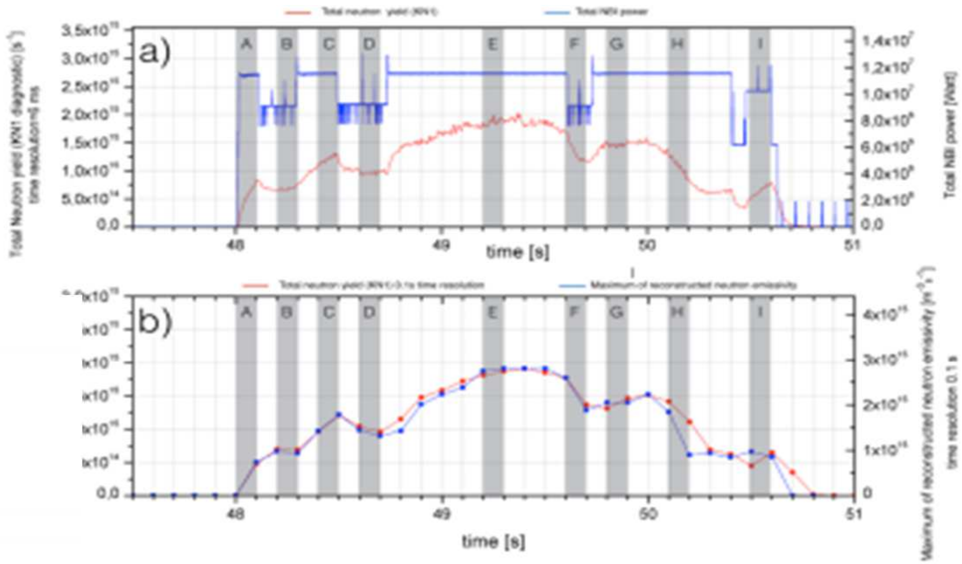

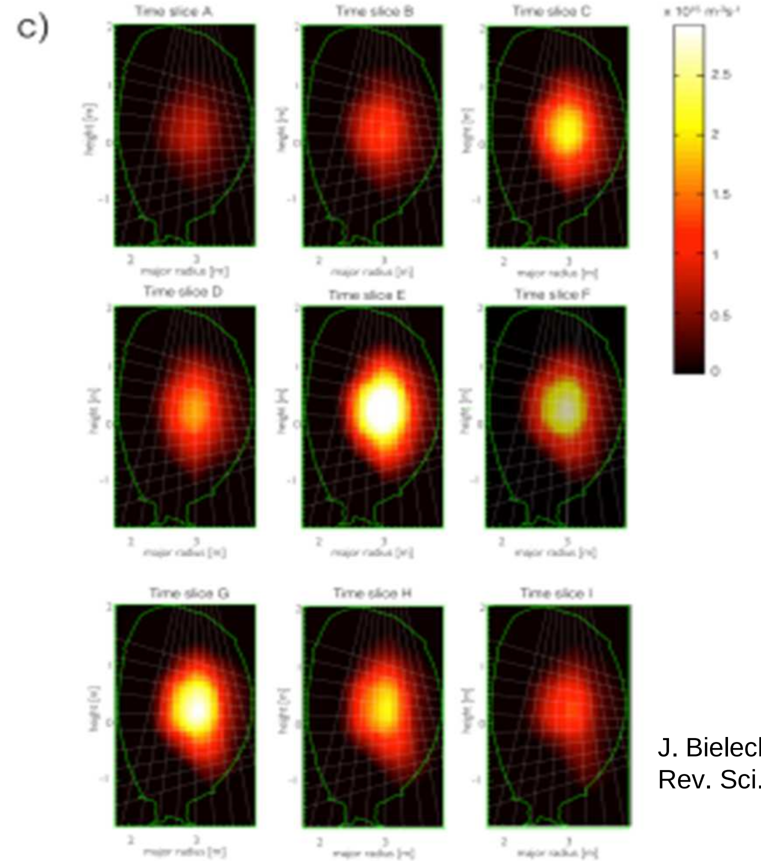

J. Bielecki
Rev. Sci. Instrum. 86 (2(

Spectrometer systems

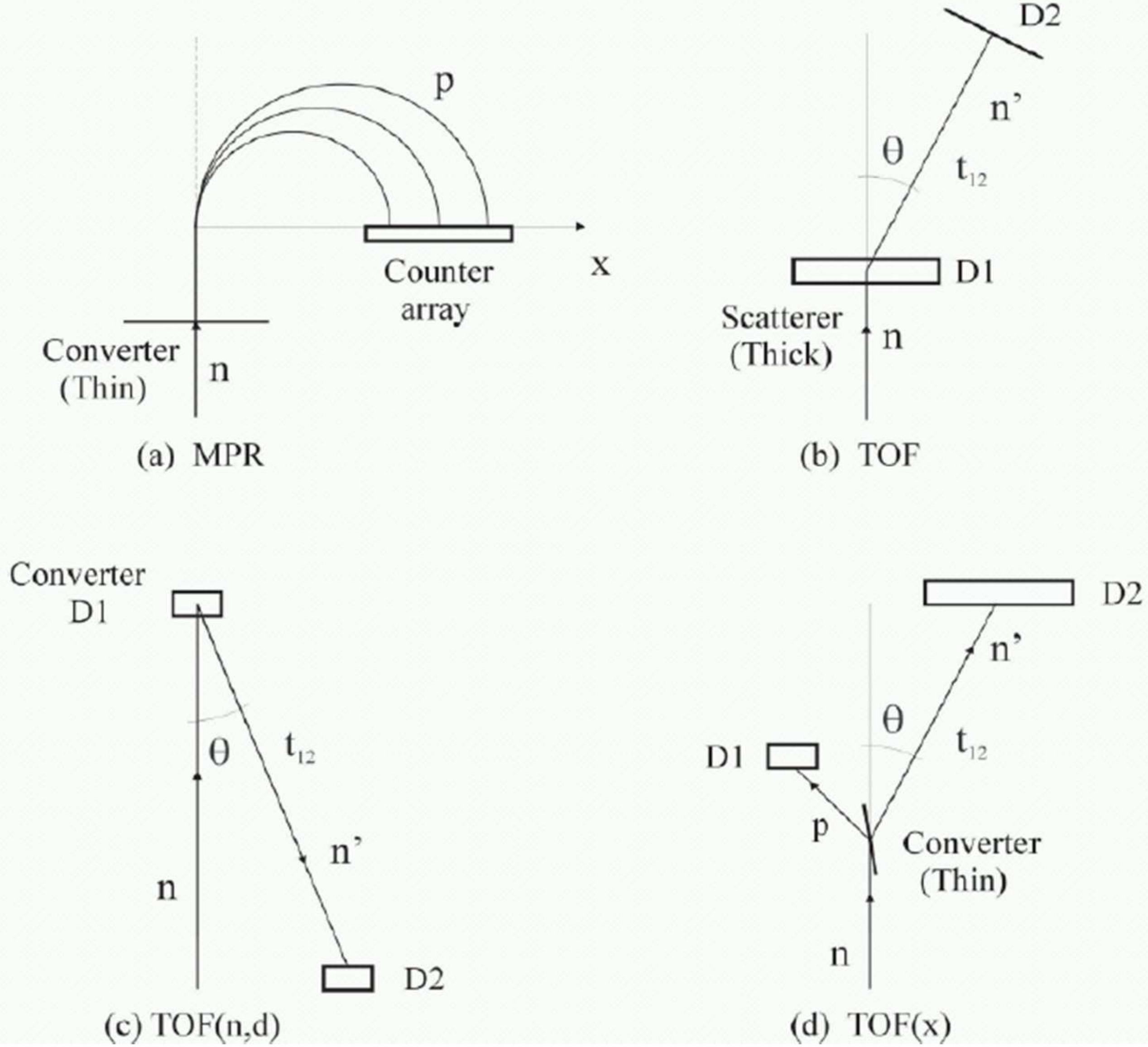

(a) MPR
(b) TOF
(c) TOF(n,d)
(d) TOF(x)

Another Spectrometer configuration: TPR

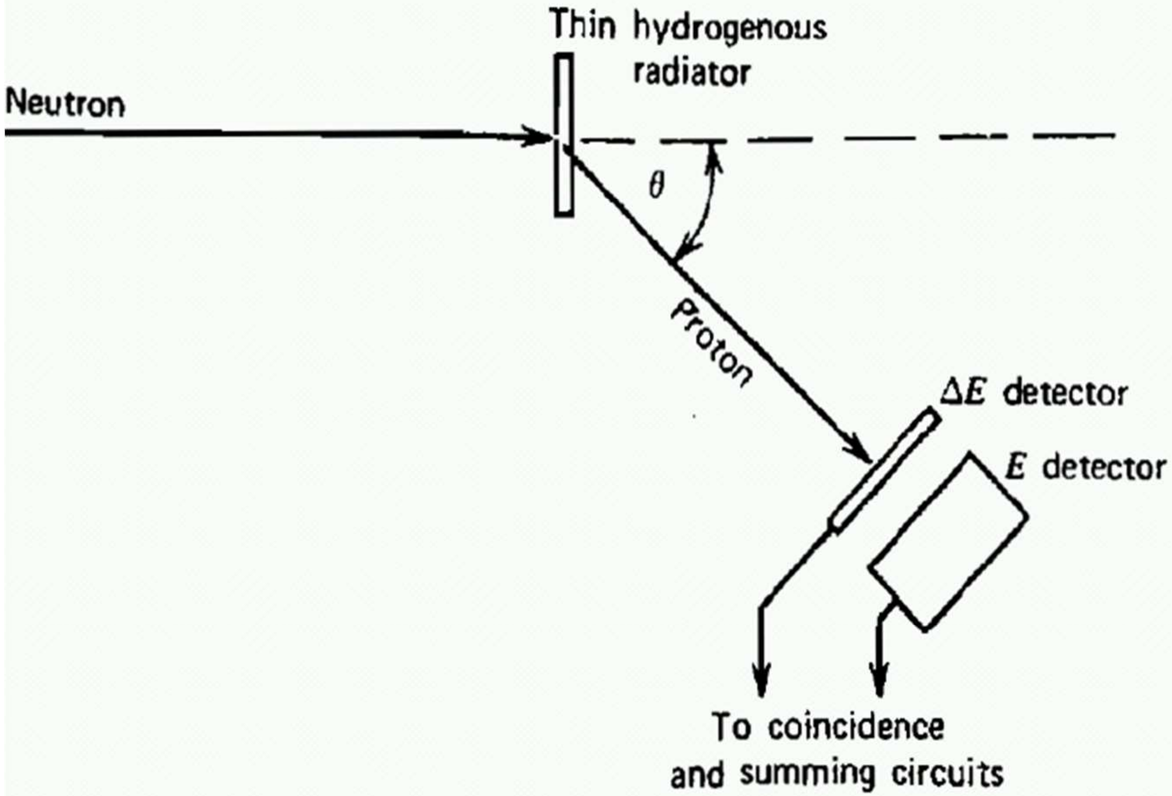

Figure 15.25 A proton reco
telescope.

Measurements of neutron spectrum

Neutron emission spectroscopy measurements on fusion plasmas

-**Recoil protons** from elastic scattering (n,p) can be measured. The energy of a recoil proton is given by: $E_{\mathrm{p}} = E_{\mathrm{n}}\ cos^2\theta$
Requires measurement of both the energy and angle of the recoil protons

-**Compact spectrometers** (scintillator) measure only the recoil energy $\rightarrow$ Need of advanced unfolding codes to reconstruct the incoming neutron energy spectrum from the measured recoil spectrum

-Thin film recoil spectrometers (**MPR**), only recoil protons scattered in a small angle interval are measured. simple response function, very high high count rate capability (DT operations), low efficiency

-Time of Flight (**TOFOR**) : measure the neutron energy from the time difference between the neutron elastic scattering in start and stop detectors. simple response function, optimized for 2.5 MeV neutrons

-**Diamond spectrometers: combine in a compact spectrometer high energy resolution, high rate operation**

Istituto di Fisica del Plasma "Piero Caldirola"
Consiglio Nazionale delle Ricerche

NES spectrometers installed at JET in 1997-2012

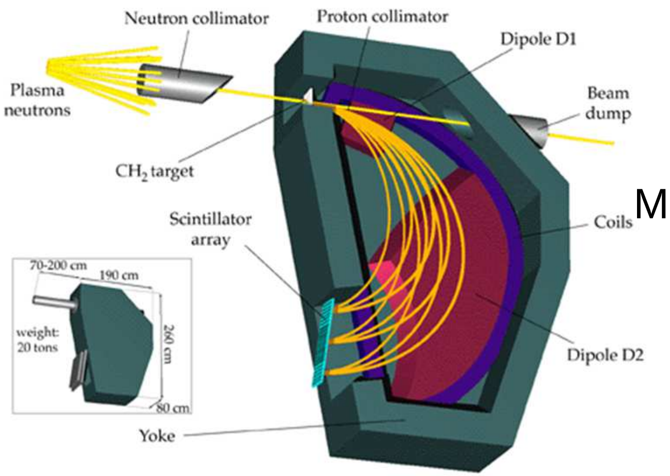

Magnetic proton recoil

MPR for 14 MeV neutrons
MPRu also for 2.5 MeV neutrons

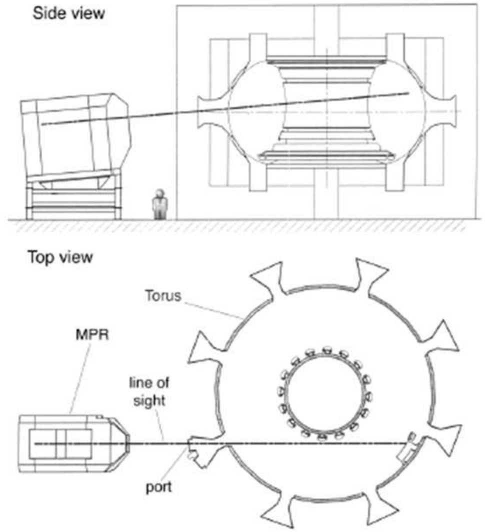

G. Ericsson, at al, RSI (2006); A. Sundén, at al, NIM A610 (2009)682

Time of flight optimized rate

TOFOR for 2.5 MeV neutrons

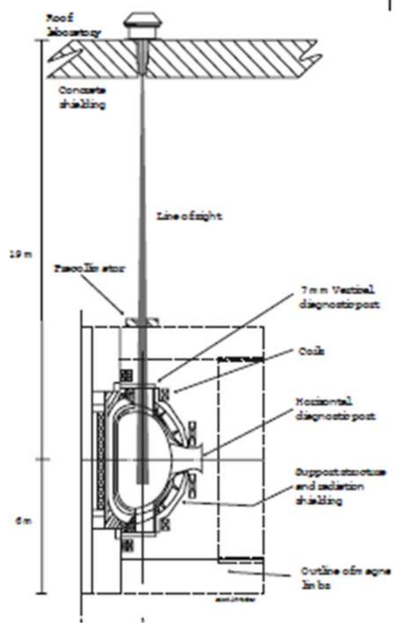

M. Gatu Johnson, NIM A591 (2008)417

Recent development later!

TOFOR

- Time-Of-Flight neutron spectrometer Optimized for Rate
- Measures neutron flight time between two detector sets;
- Designed for study of 2.5 MeV neutron emission spectrum from d+d fusion reactions
- Installed in JET roof laboratory in 2005

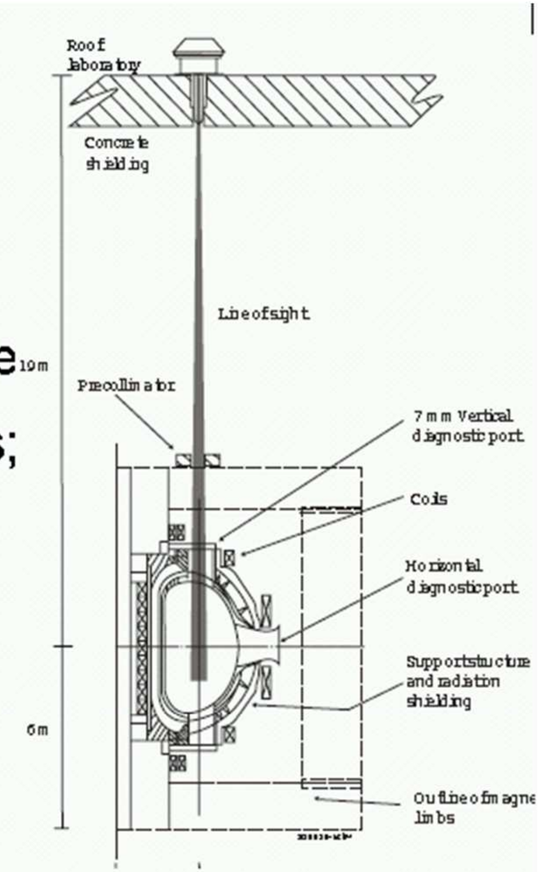

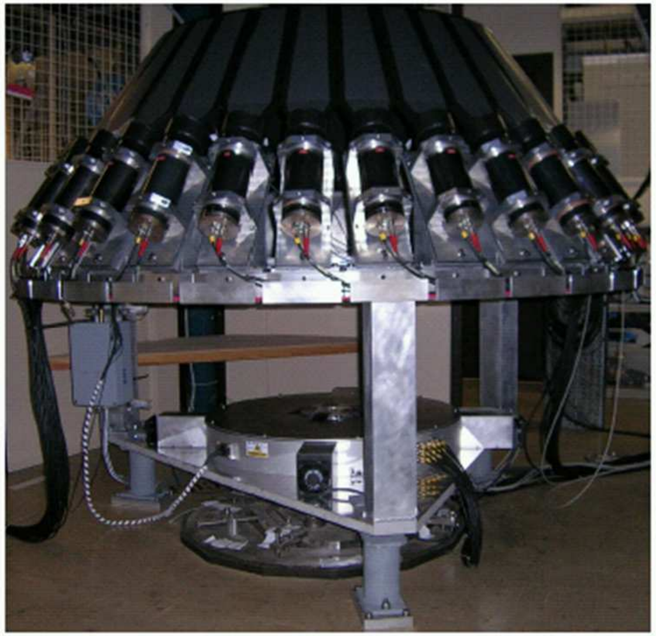

$$E_n \sim 2mR^2/t_{TOF}^2$$

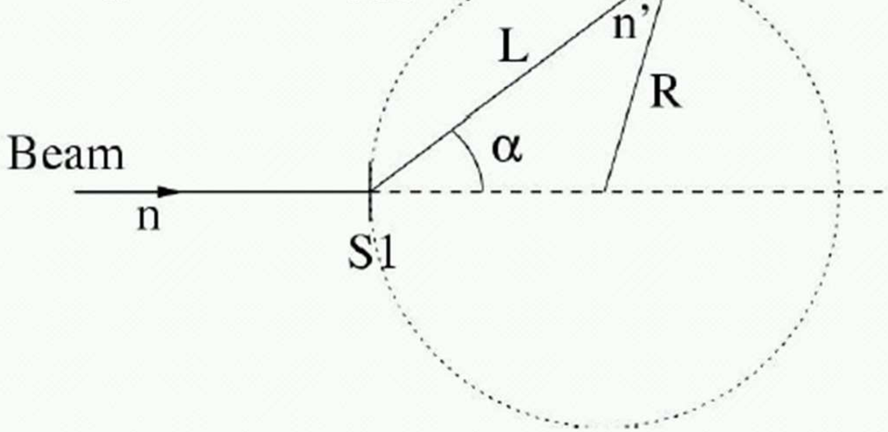

Constructing the t_{TOF} spectrum

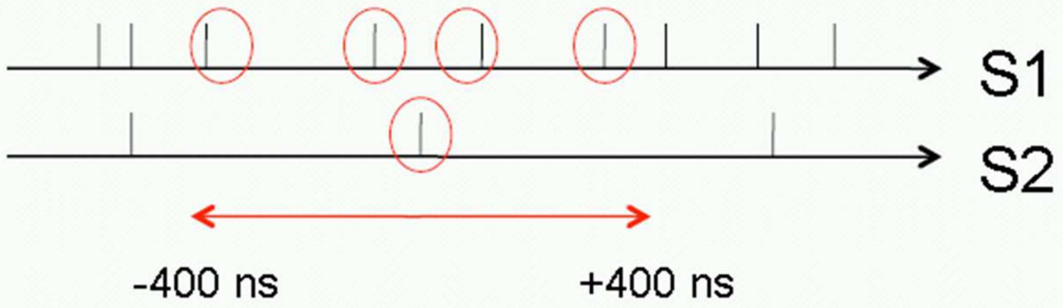

- All events individually recorded for each detector
- $t_{TOF}=t_2-t_1$
- Both true and random coincidences constructed in this way
  - Random rate proportional to rate(S1) and rate(S2) = rate²
  - True rate proportional to rate in S2
  - Ratio Random/True proportional to S1 rate => optimize catching factor S2/S1
  - Background B<<S2: need well shielded S2
- Energy cuts (thresholds) set to avoid recording events of certain energies, to minimize random (and other) background
  - Old settings: Window of energies allowed, with upper and lower cuts
  - New settings: Only lower cut; the high energy events are the interesting ones!

Features of the t_{TOF} spectrum

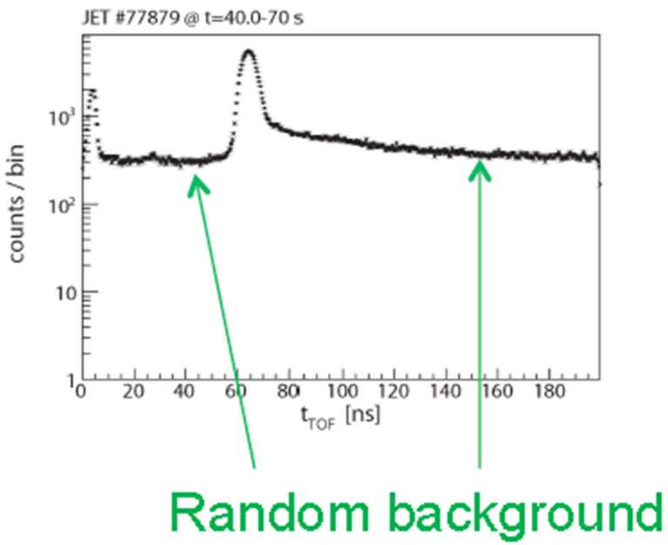

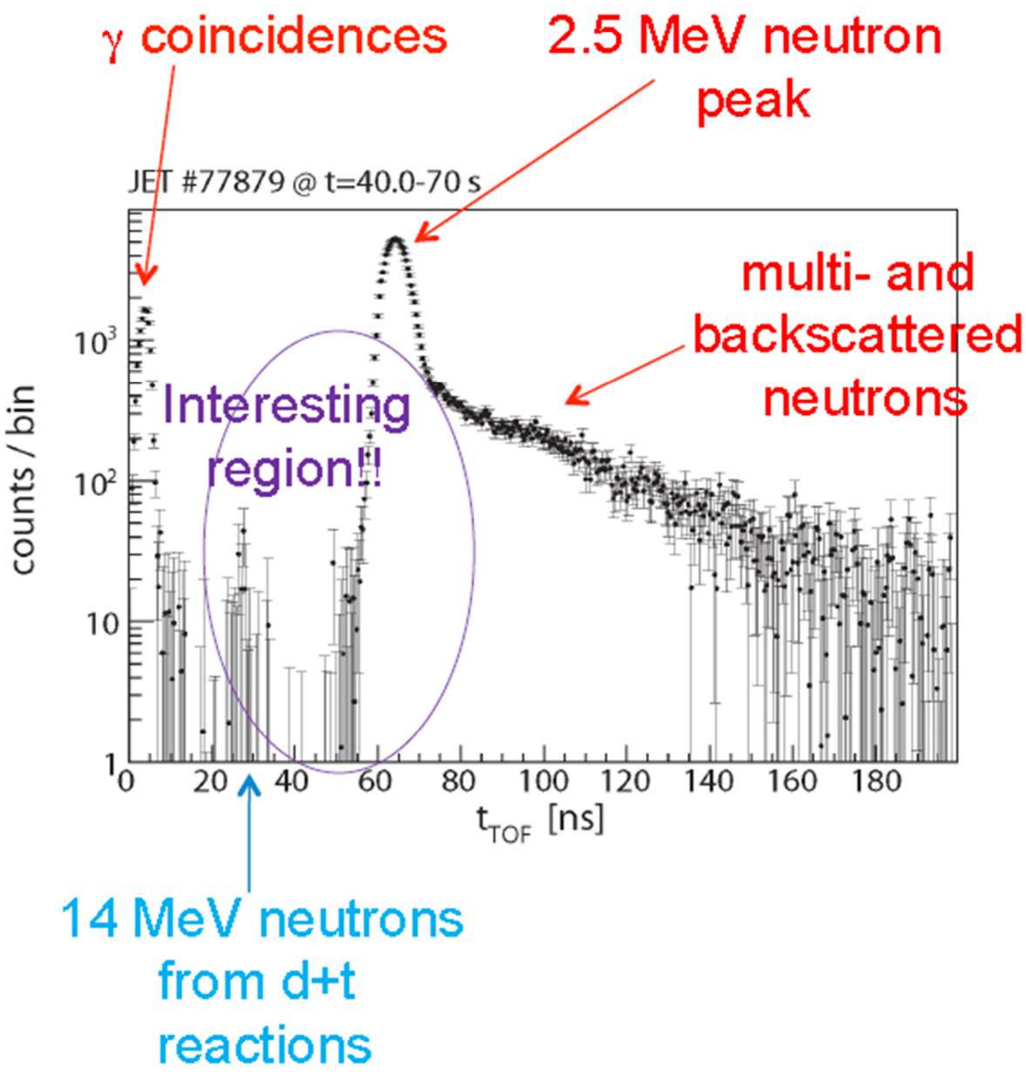

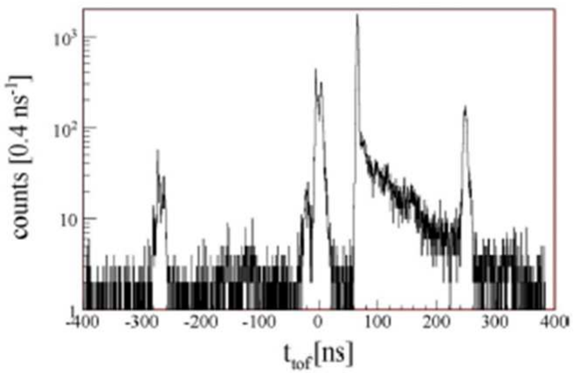

Measured spectra - examples

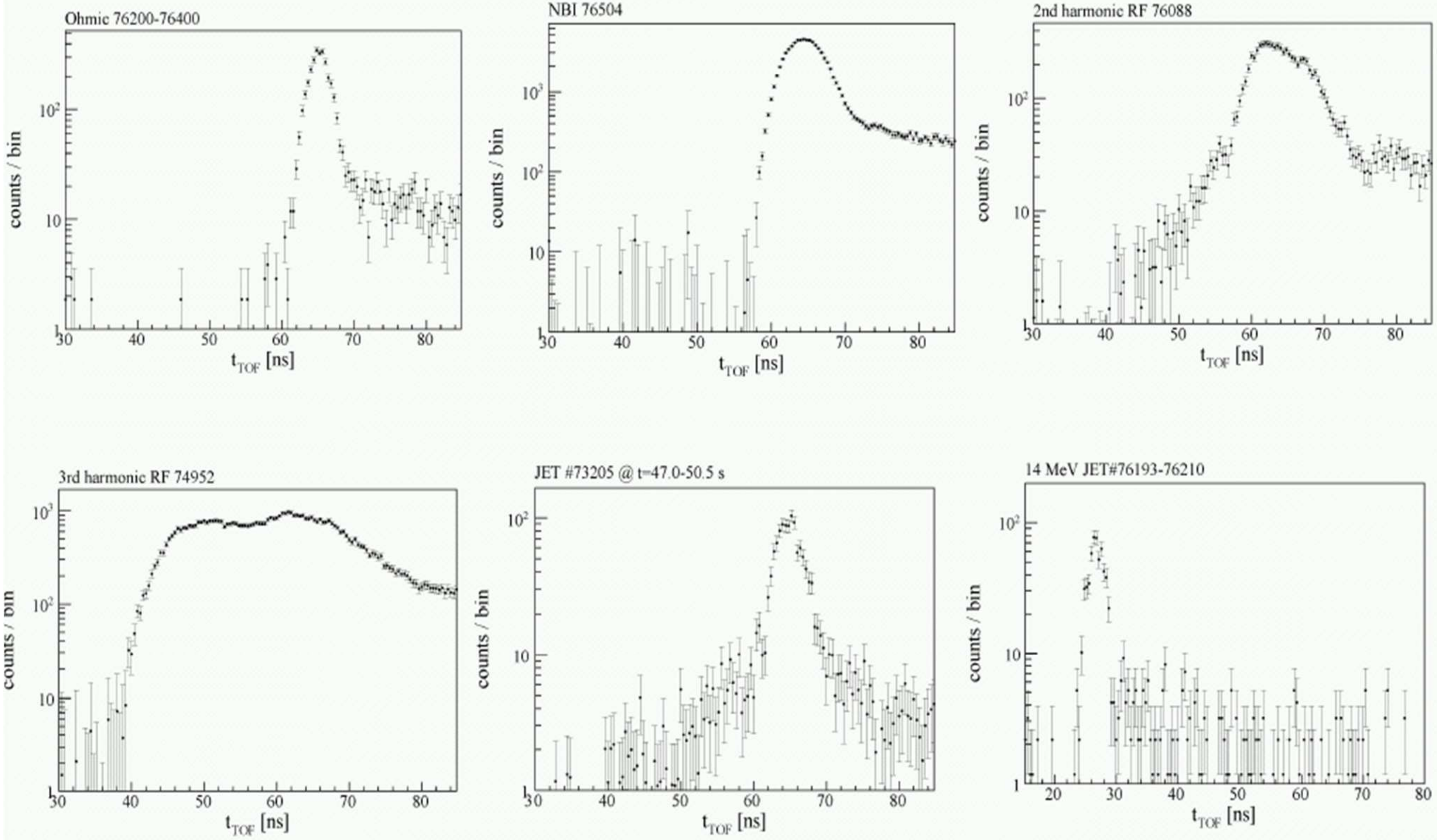

Spectral analysis

- Use physics knowledge to create components on neutron energy scale that describe represented parts of the fuel ion population
  - Bulk reaction component: Maxwellian defined by bulk ion temperature and intensity
  - NB heating component:
    - Simplest case: ”half box” defined by beam injection energy and intensity
    - TRANSP can be used to create more advanced components
  - RF heating components: isotropic and anisotropic Maxwellians
  - Other components can be constructed as needed:
    - Beam-beam, knock-on, ...
- Fold components with response function to get them on t_{TOF} scale
- Fit to data using Cash statistics

MPR principle

From neutron energy distribution to proton position histogram

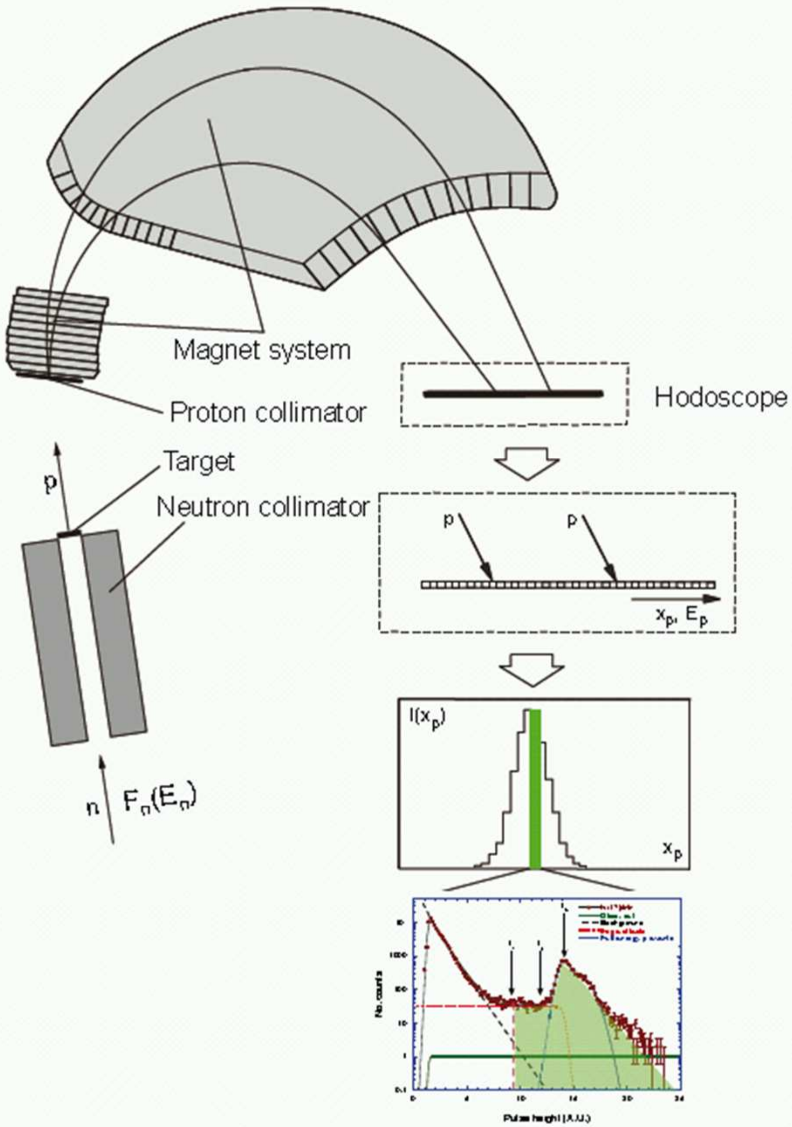

- Passive n-to-p conversion in "target" (CH_2)
- Passive momentum dispersion in B-field
- 37-element hodoscope, fast scintillators
- Active counting of protons in detectors
- Time resolved p position histogram:
  Scaler data, no dead-time
- Pulse height distribution:
  ADC data, spectral shape

Spectrometer components (I)

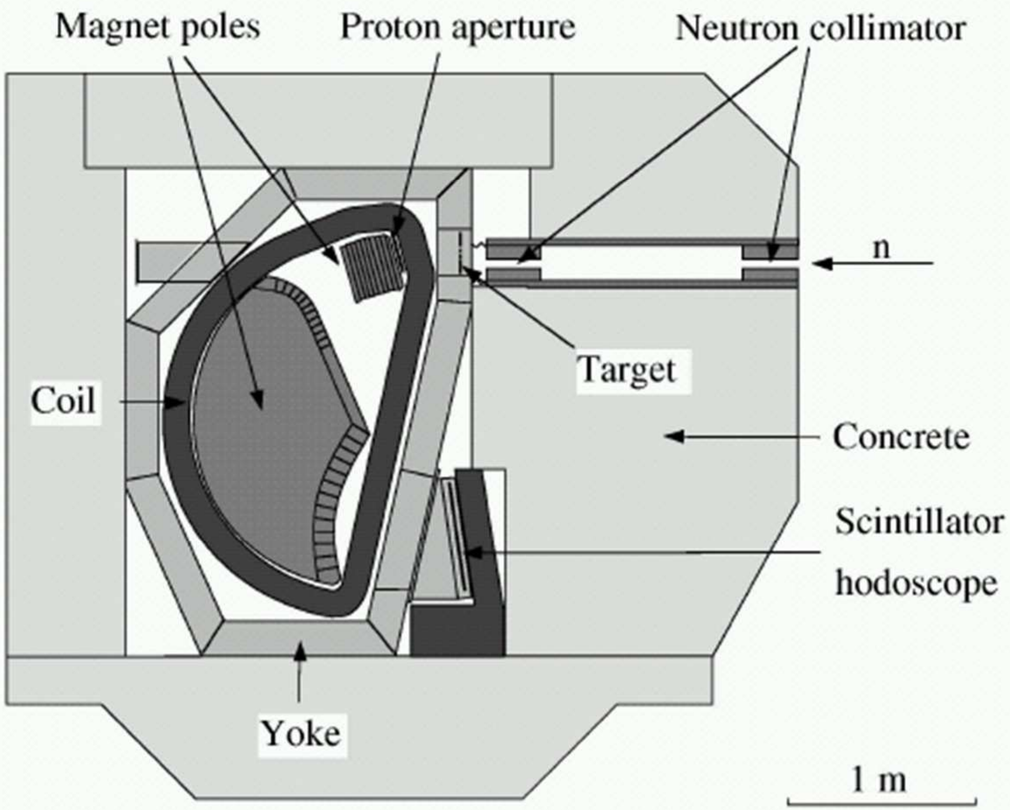

- High resolution, high efficiency magnetic spectrometer (20T)
- Flexible B-field, 0 – 1.3T: $0 < E_0 < 17$ MeV
- Energy bite $E_0 \pm 20\%$
- Flexible settings for 14-MeV and 2.5-MeV n: 5 targets, 5 p apertures
- Yoke is vacuum chamber with $p < 10^{-3}$ mbar
- Radiation shield of concrete and lead (65T)

Spectrometer components (II)

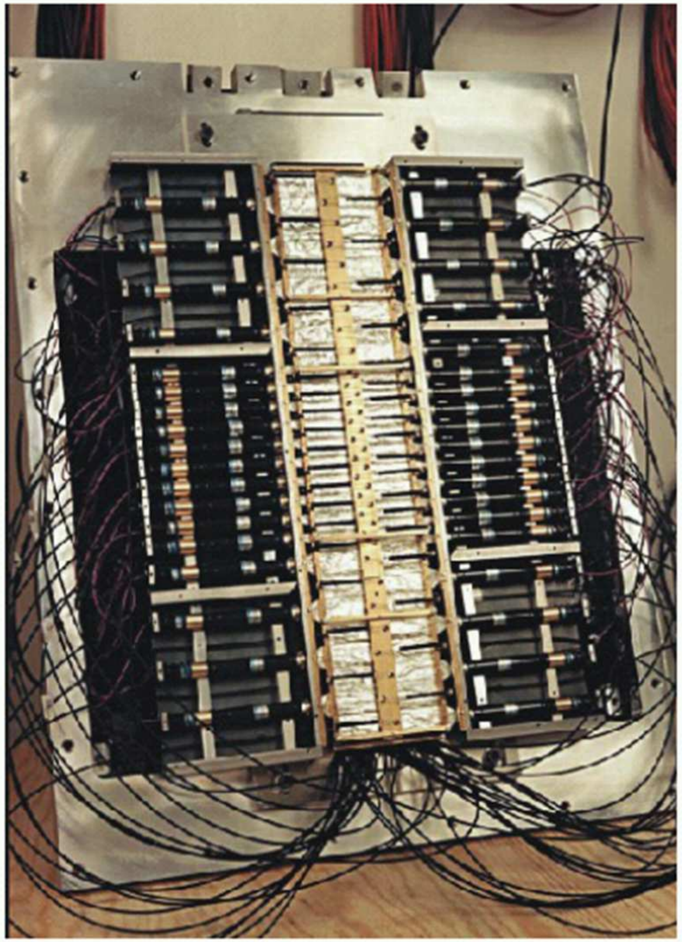

Assembled hodoscope

MPR assembly in AH

MPR in the JET Torus Hall

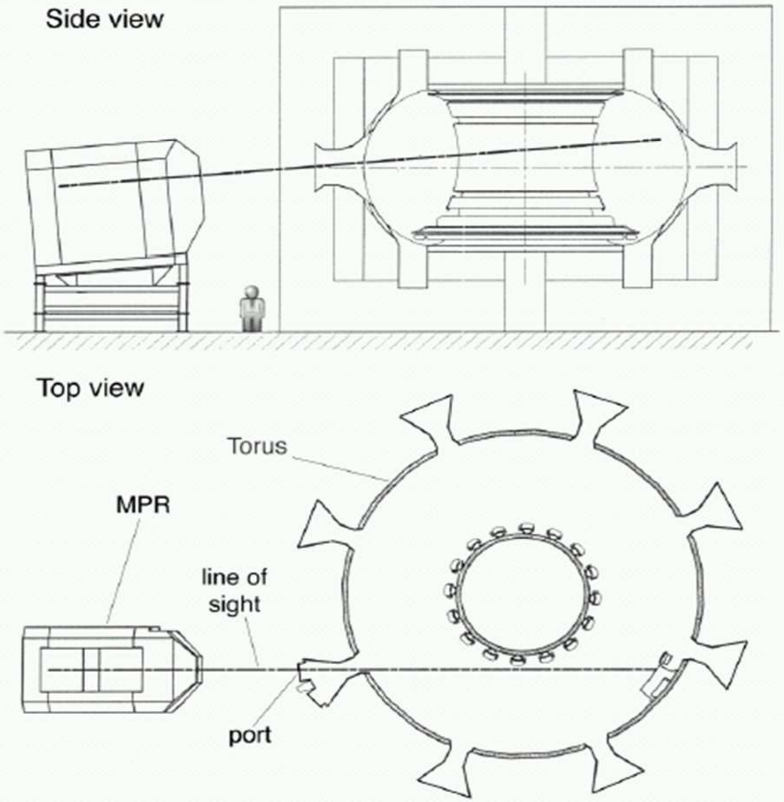

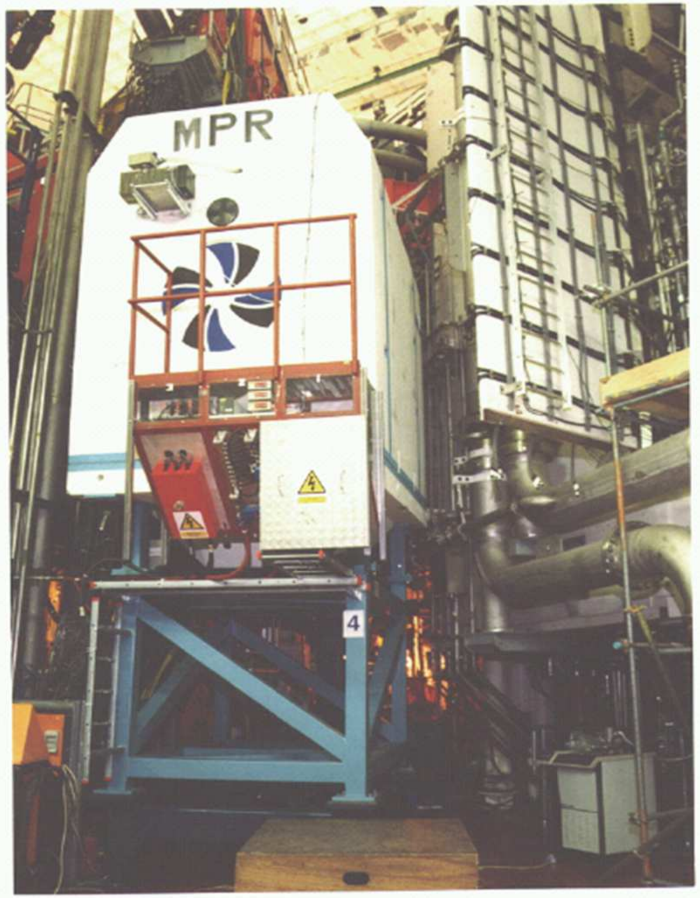

Istituto
di Fisica del Plasma
"Piero Caldirola"
Consiglio Nazionale delle Ricerche

NES results on JET plasmas

Istituto di Fisica del Plasma "Piero Caldirola"
Consiglio Nazionale delle Ricerche

NES results on DT plasmas

Ohmic and ICRH at $2\omega_{CD}$

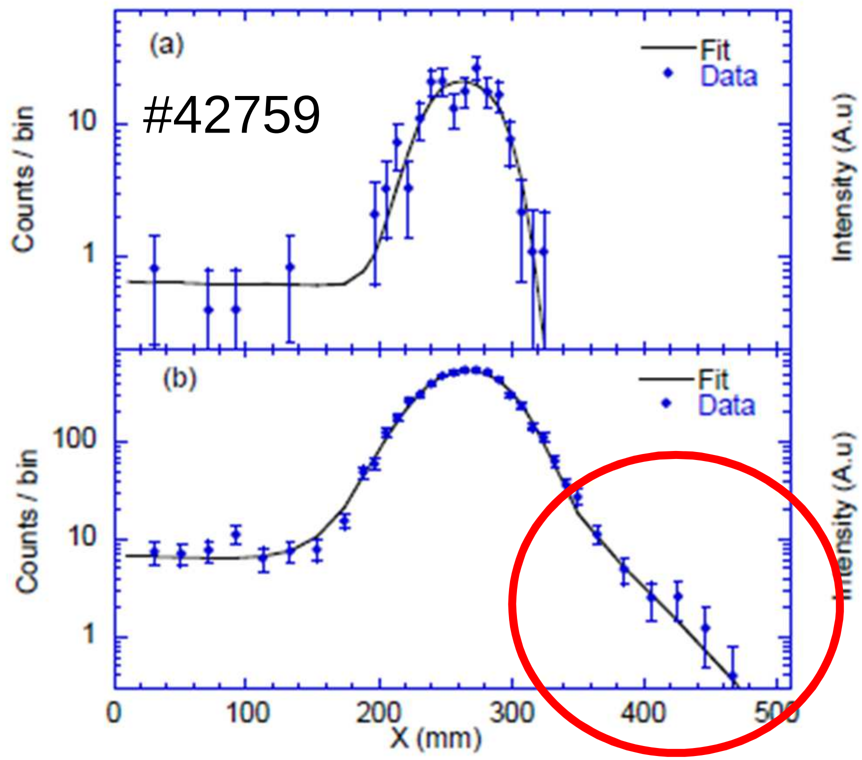

Spectral components inferred from fit

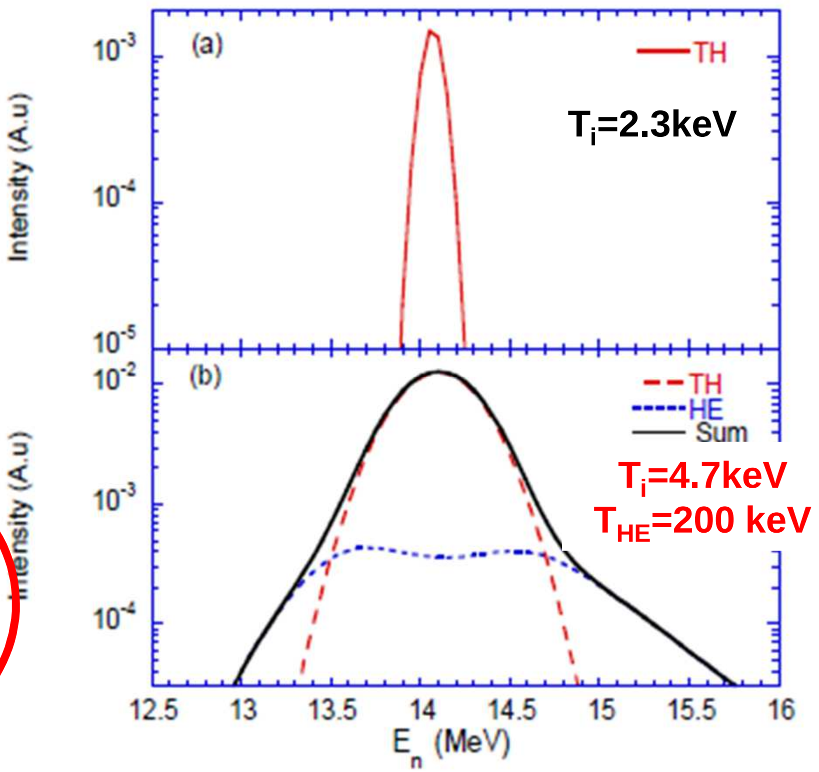

M.Tardocchi, PhD thesis,Uppsala (2000)

Measure high energy tail temperature of fast D

Model describes deuterium velocity distribution with an anisotropic "cut" Maxwellian
-thermal component for the main bulk ions.
-Tail temperature T_{HE} and pitch angle distributed as a Gaussian centred at 90° ±10°

***M. Tardocchi** et al, Nuclear Fusion 42 (2002) 1273.*

Diagnostic capabilities

- Neutron rate/yield determination – R_p
- Toroidal rotation of fuel ions – dE (shift)
- Temperature of thermal plasmas – ΔE (width)
- Fuel ion distribution functions for aux. heated plasmas
- Studies of weak components in the neutron spectrum:
  - Triton Burn-Up (TBN) in D plasmas – 2nd order process
  - Alpha Knock-On (AKN) in DT plasmas – 3rd order process
  - Tritium retention in D plasmas – $c_t > 10^{-5}$

AKN evidence (single pulse)

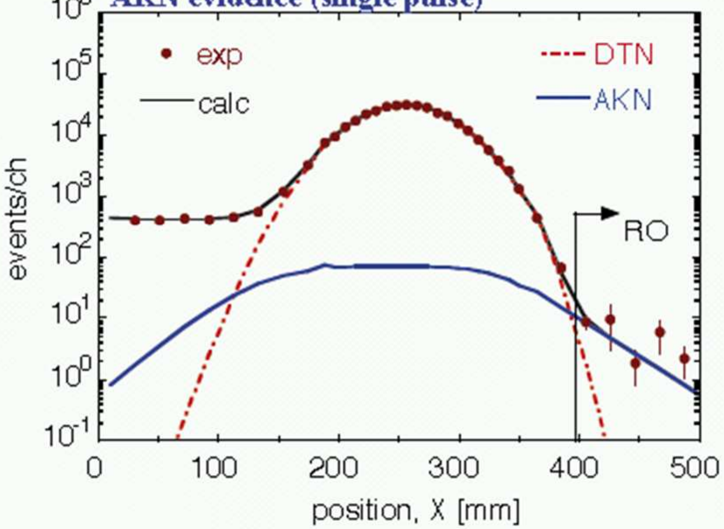

Tritium retention results (note non-uniform time axis)

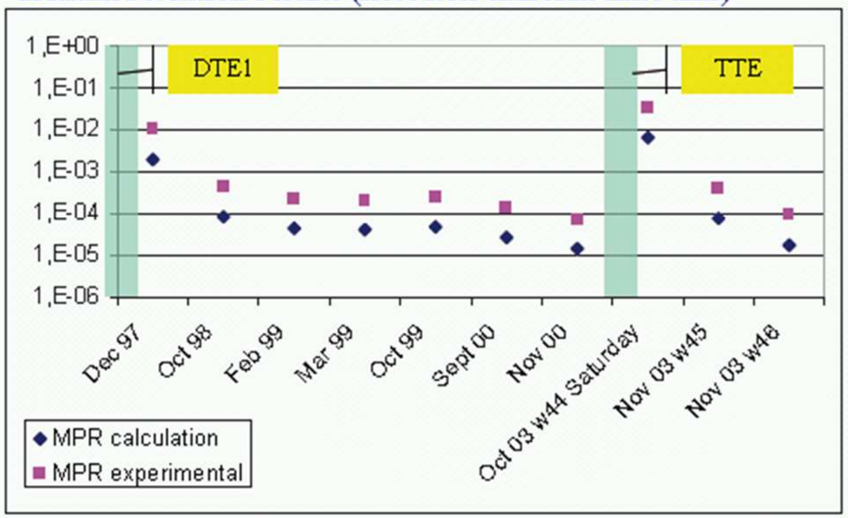

Istituto di Fisica del Plasma "Piero Caldirola"
Consiglio Nazionale delle Ricerche

NES results on ICRH D plasmas

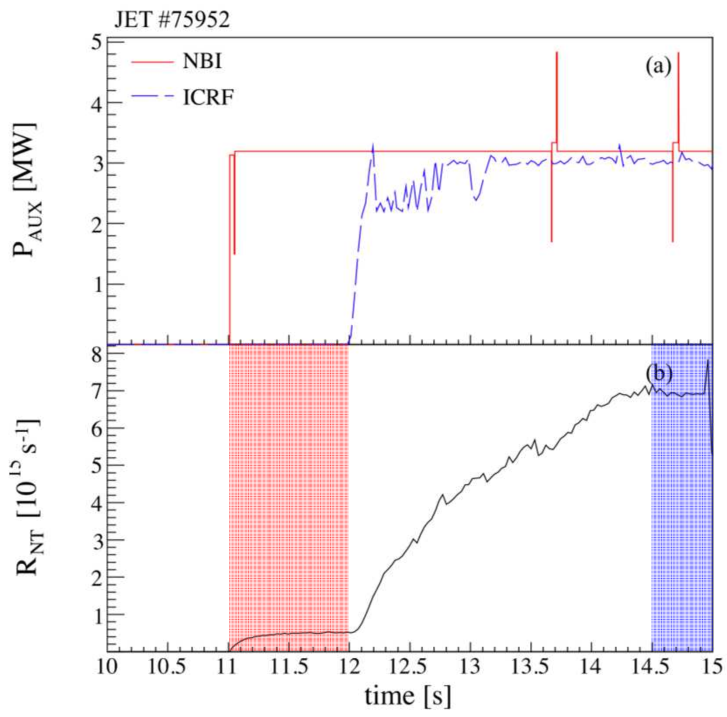

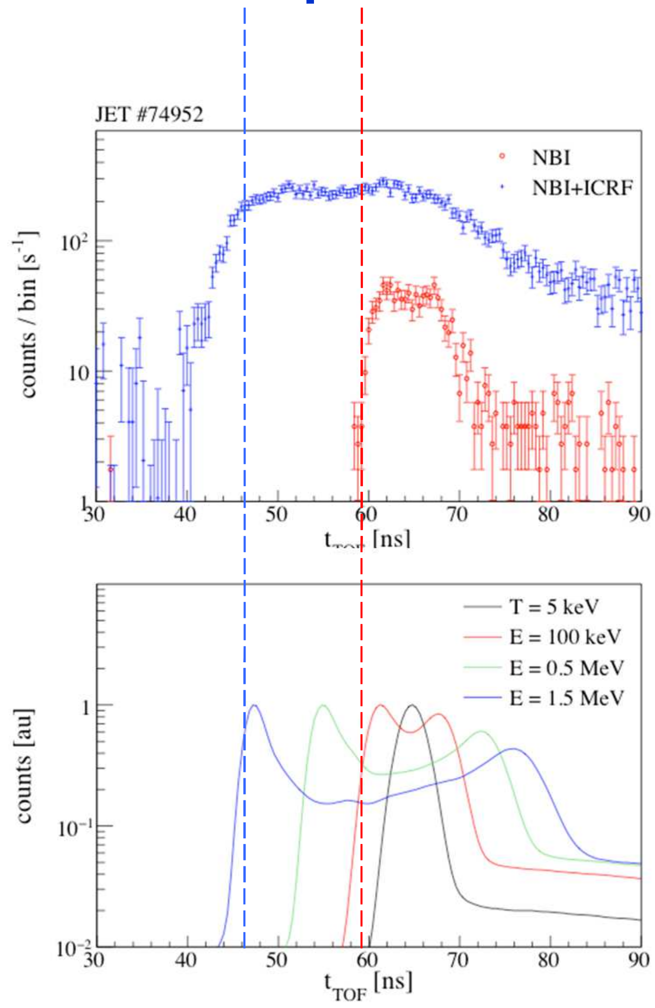

RF heating tuned to 3rd harmonic D resonance
Adding 3 MW RF to 3 MW NBI increased neutron rates by 14 times! $R_{NT}=5\cdot10^{14}\rightarrow7\cdot10^{15}$ n/s

Among the highest neutron yield/MW heating ever produced at JET (without tritium)

C. Hellesen et al, Nucl. Fusion letter (2010)022001

Deriving D distribution in 3rd harmonic ICRH plasmas

Use high energy neutrons to probe high energy ions

Highest energy of neutron spectrum given by reactant energy

Integration of TOFOR spectrum **below** a fixed t_{TOF} is equivalent to select D ions above a cerain E_D

Two of such probes:

t_{TOF} < 55 ns, E_d > 0.5 MeV

t_{TOF} < 48 ns, E_d > 1.3 MeV

Similar to threshold reactions in gamma ray spectroscopy (but with thresholds can be set arbitrarily)

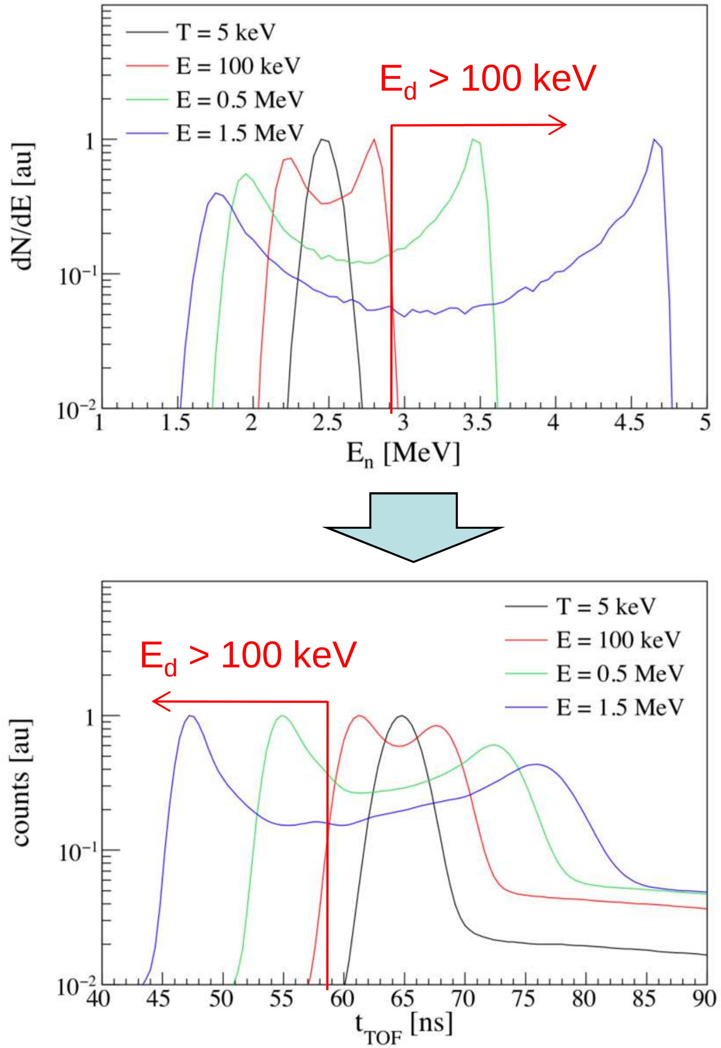

Deriving the fast ion distribution

- Iteratively fit the weights of monoenergetic $\delta(E)$-spectra to match the TOFOR data
  - Ion distribution can be derived from measured data
- Demonstrate on synthetic data (TOFOR response function)
  - Use predefined fast-ion distribution, two maxwellians
  - Fold neutron spectrum with response function and add Poisson errors
  - Thermal component treated as Gaussian centred at 2.5 MeV
  - HE component fitted to the high energy tail

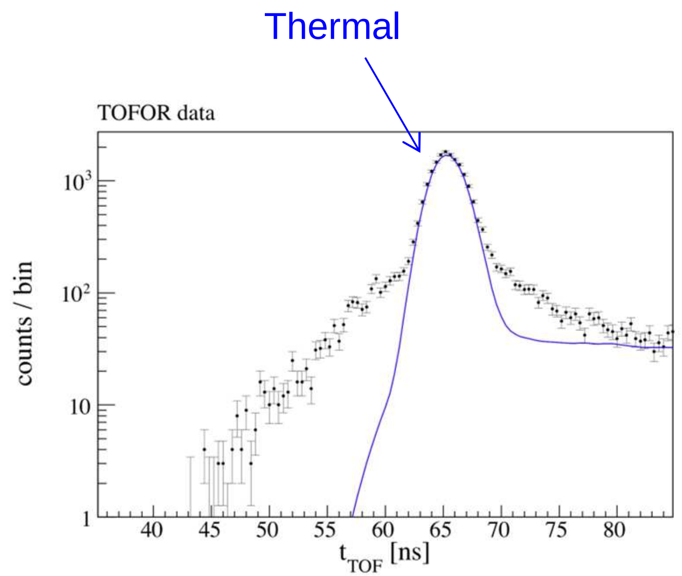

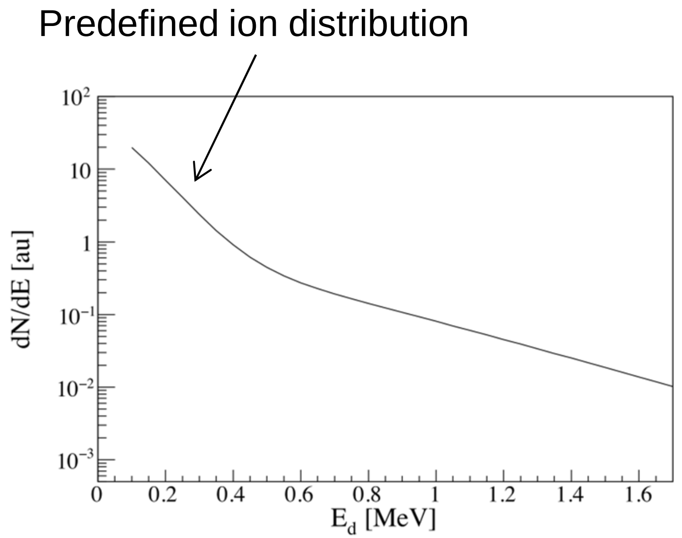

Deriving the fast ion distribution

Thermal

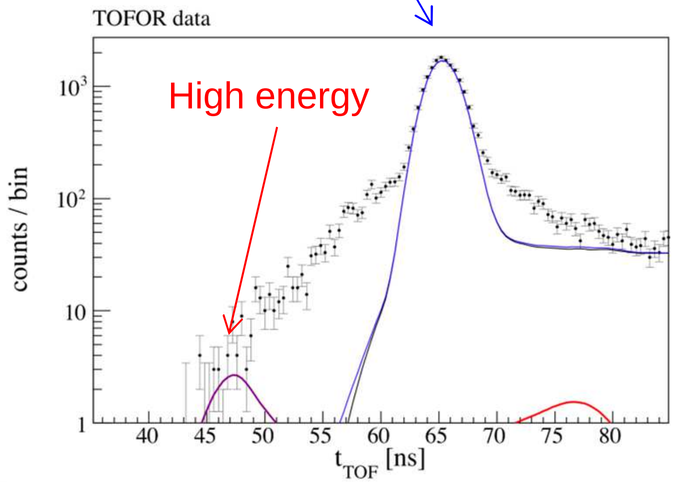

Predefined ion distribution

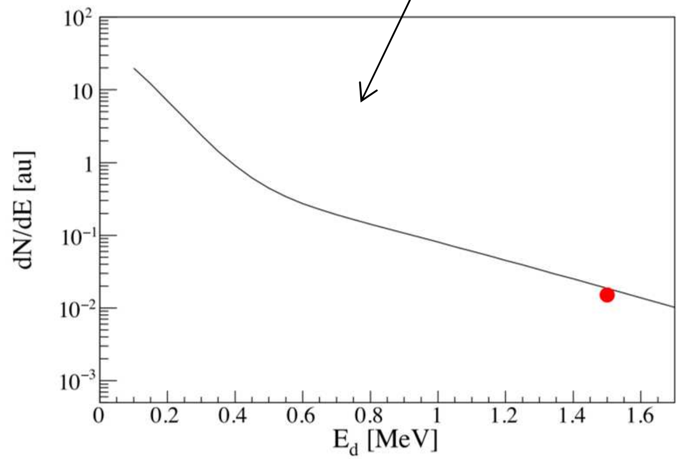

C. Hellesen et al, Nucl. Fusion letter (2010)022001

Deriving the fast ion distribution

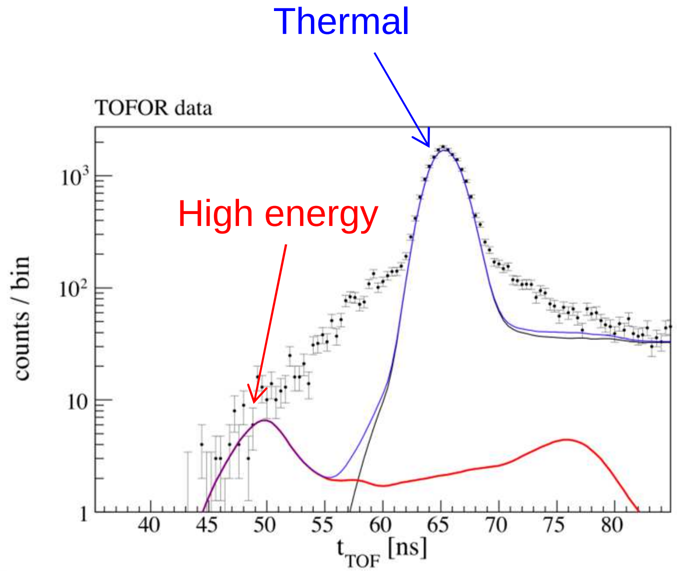

Predefined ion distribution

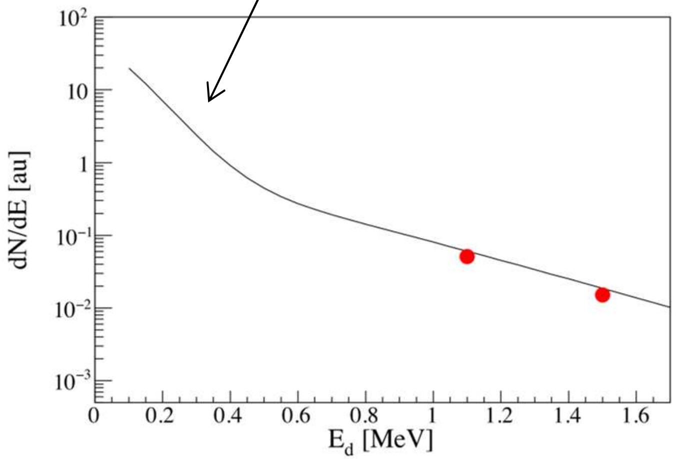

Deriving the fast ion distribution

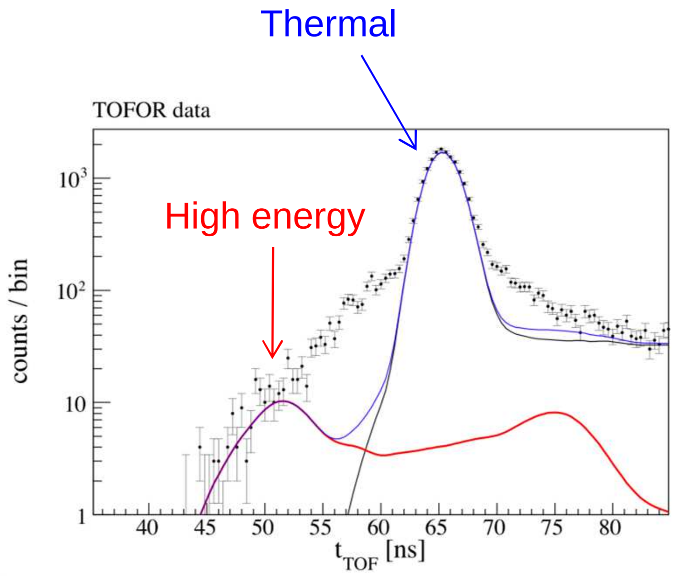

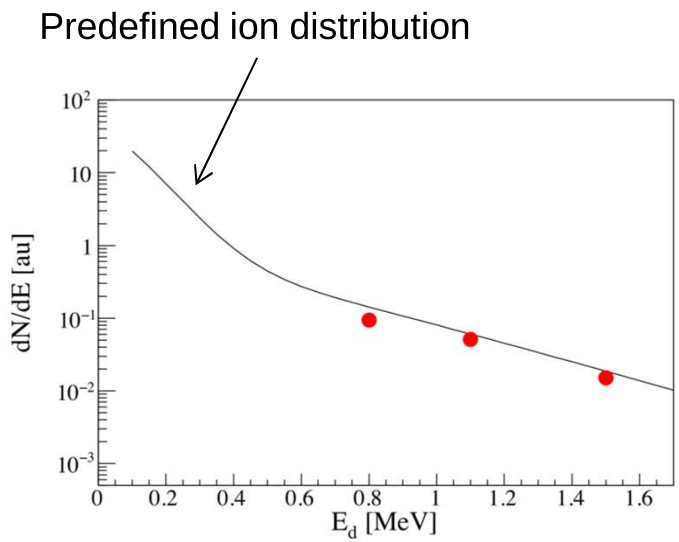

Istituto
di Fisica del Plasma
"Piero Caldirola"
Consiglio Nazionale delle Ricerche

Deriving the fast ion distribution

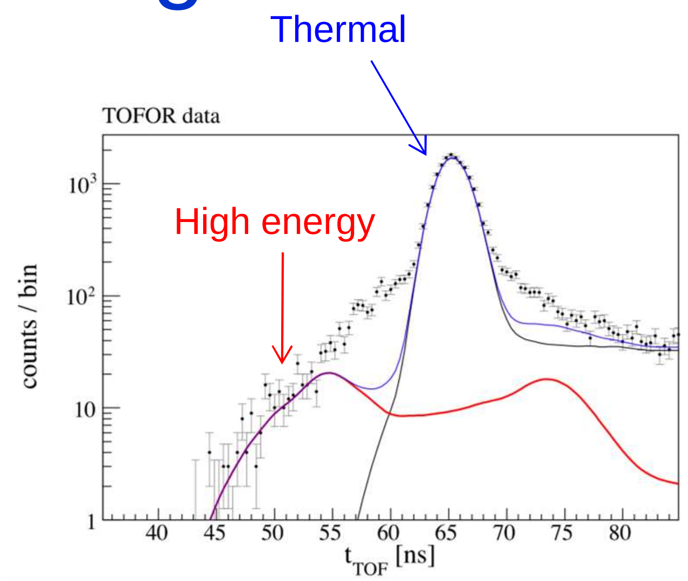

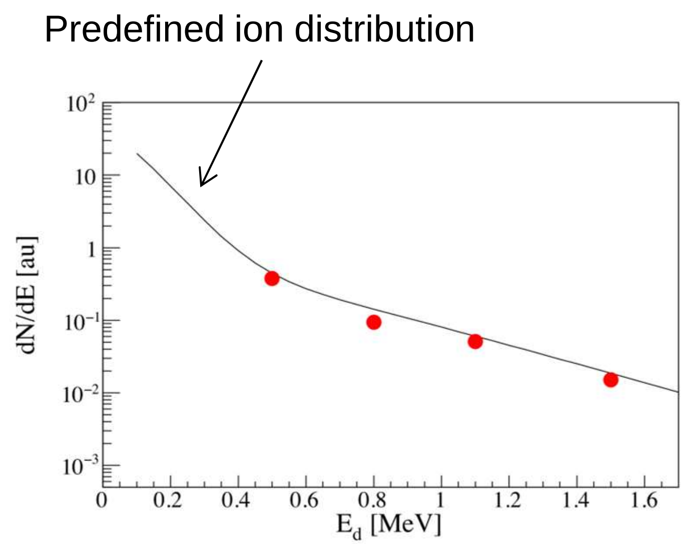

Istituto di Fisica del Plasma "Piero Caldirola"
Consiglio Nazionale delle Ricerche

Deriving the fast ion distribution

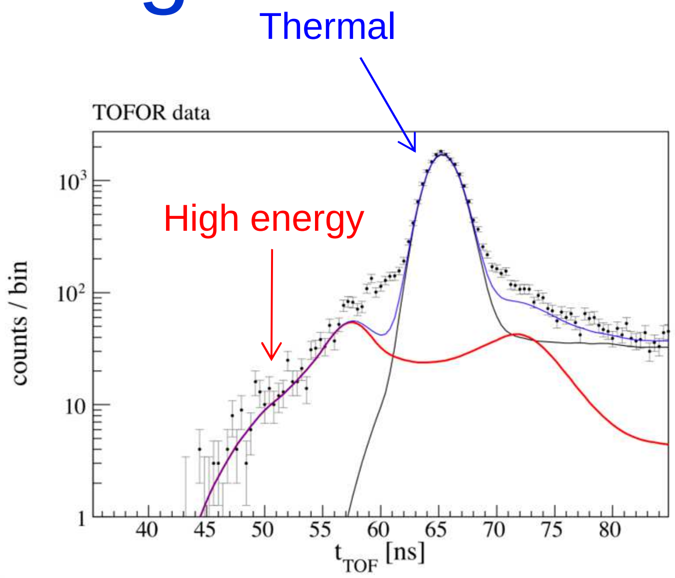

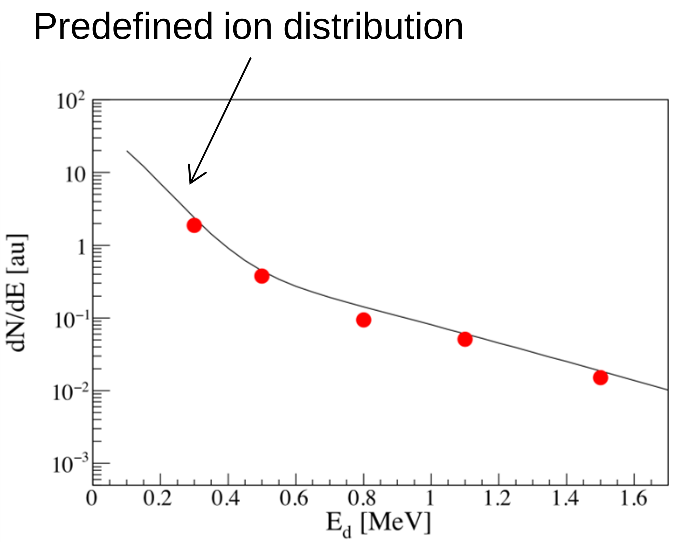

Istituto di Fisica del Plasma "Piero Caldirola"
Consiglio Nazionale delle Ricerche

Deriving the fast ion distribution

Thermal

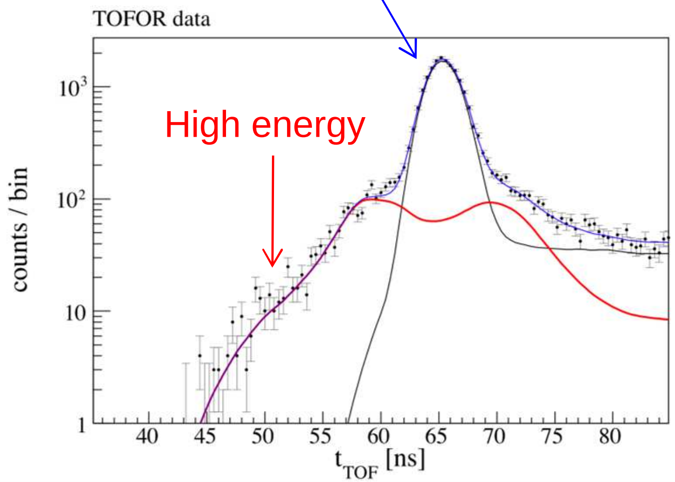

Predefined ion distribution

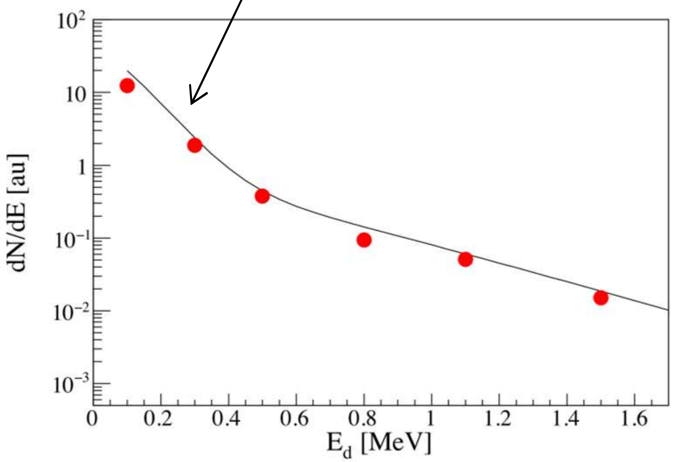

NES time resolved results

Integrating TOFOR data below a certain t_{TOF} gives a probe of neutrons above a certain energy

$t_{TOF} < 55$ ns $\rightarrow E_d > 0.5$ MeV

$t_{TOF} < 48$ ns $\rightarrow E_d > 1.3$ MeV

Good statistics $\rightarrow$ high time resolution, down to 25 ms

- After the start of RF (t=12 s) both 0.5 and 1.3 MeV signals rise.

At t=16.5 s TAE activity begins and 0.5 MeV continue to rise while 1.3 MeV starts decaying

n=4,3,2 TAEs resonate with E_d=1.1, 1.4 and 2.1 MeV

Apossible explanation is redistribution of fast ions which interact with TAE resonances.

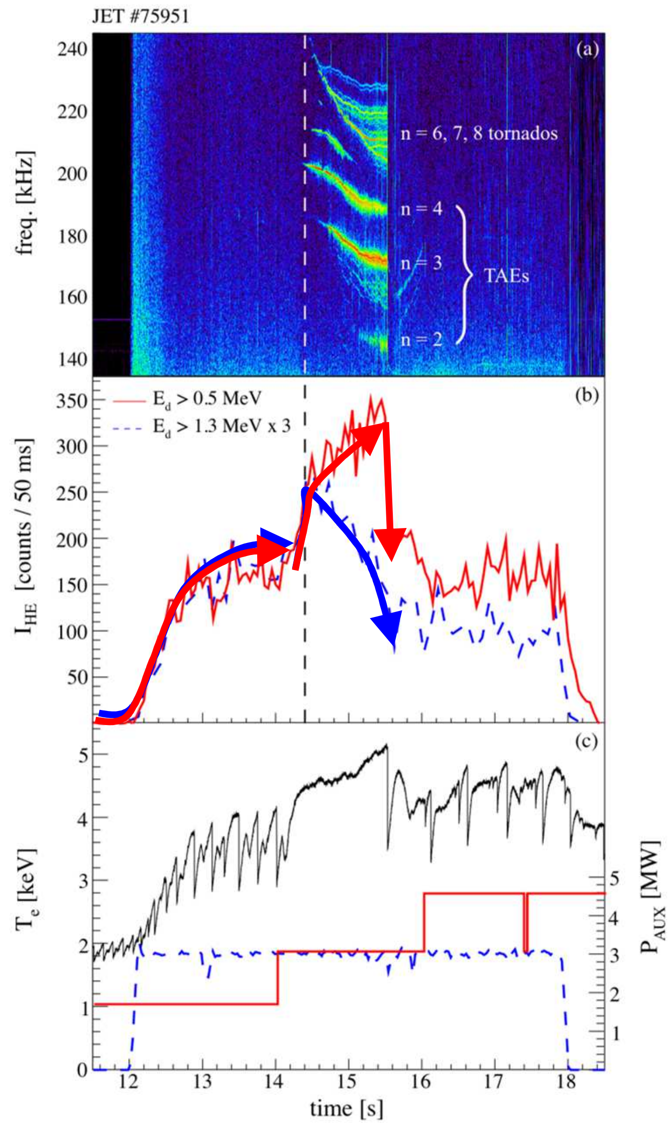

C. Hellesen et al, Nucl. Fusion 50 (2010)084006

A compact neutron spectrometer based on single crystal diamonds for DT plasmas at JET

- Good energy resolution in DT plasmas at $E_n > 6$ MeV via **$^{12}C(n,\alpha)^{9}Be$** reaction.

- JET Vertical Neutron Spectrometer (VNS) project
- Application in the ITER RNC
- Detector array built within CNR
- **<u>Fully digital fast DAQ</u>**– allows for count rate >1MHz

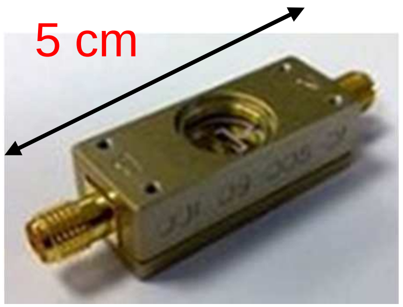

Picture of a SDD prototype

Single Crystals Diamond spectrometers

- Radiation hardness.
- High mobility of free charges (→fast response, comparable to Si, Ge).
- Room temperature operation (E_g=5.5 eV)→ No Cooling.
- Compact volume solid state detector.

A charged particle passes through the diamond and ionizes it, generating electron–hole pairs ($E_{e\text{-}h}$=13 eV)

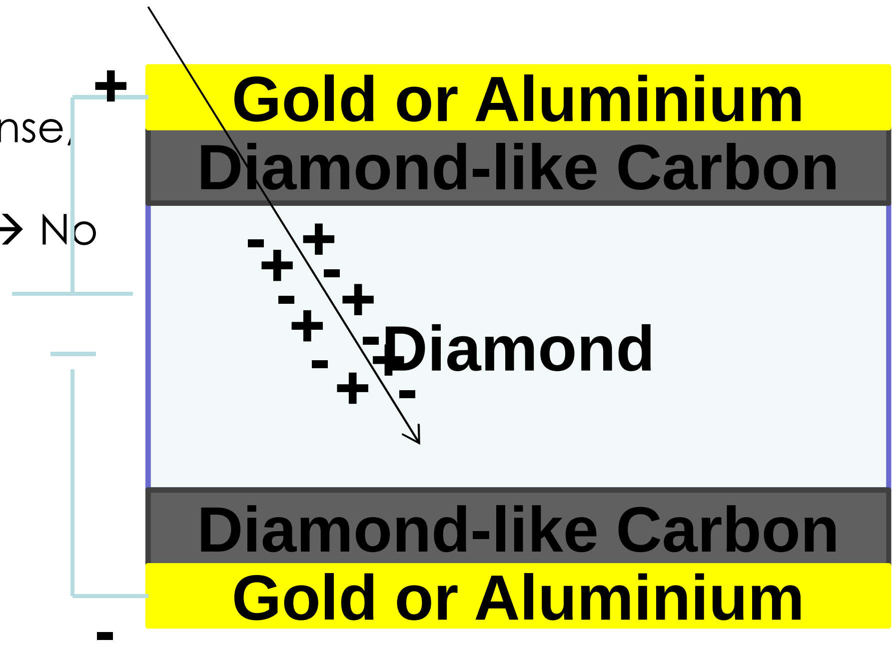

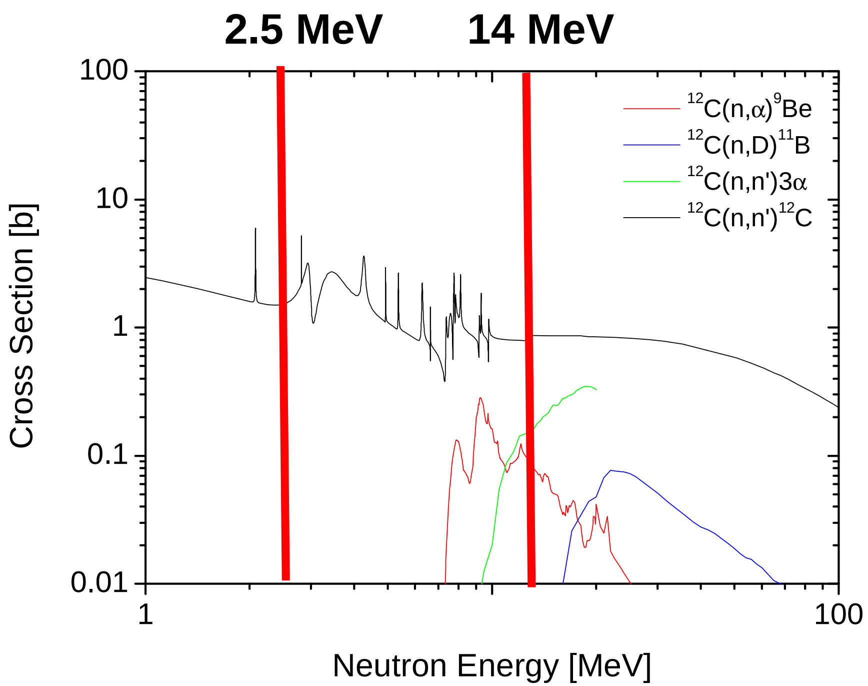

→ **Fast neutron detection**

- **$^{12}C(n,a)^{9}Be$ (Q_{value}=5.7 MeV, E_{thr}=6.17 MeV) good for 14 MeV neutron spectroscopy.**
- **$^{12}C(n,n')3a$ (Q_{value}= 7.23 MeV, E_{thr}=7 MeV)**
- **$^{12}C(n, D)^{11}B$ (Q_{value}= 13.7 MeV, E_{thr}=13.8 MeV)**
- **$^{12}C(n, n')^{12}C^{*}$ is the only possible for 2.5 MeV neutrons.**

The detector and the electronic chain

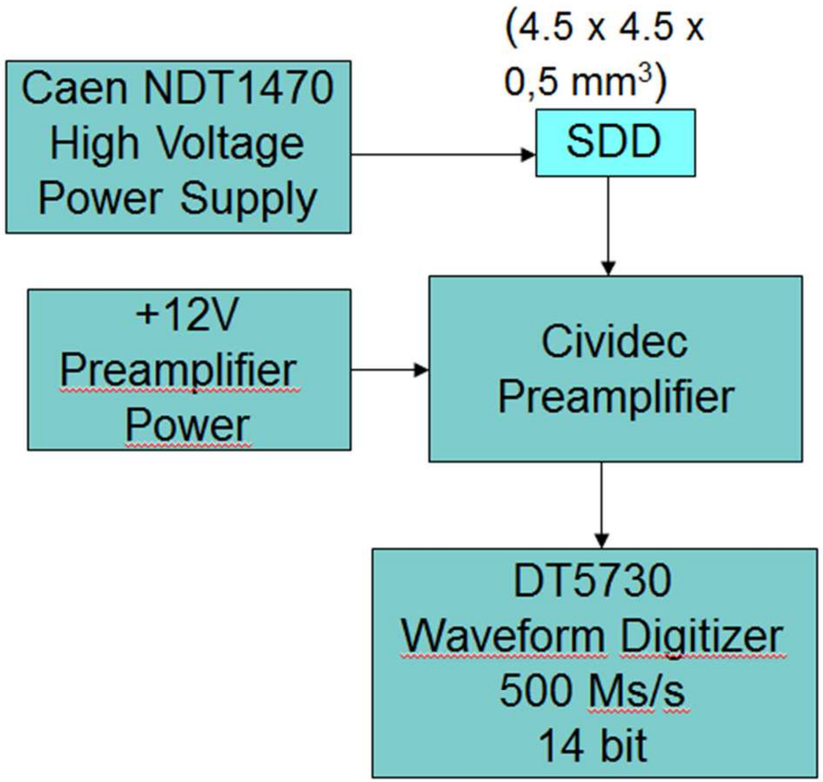

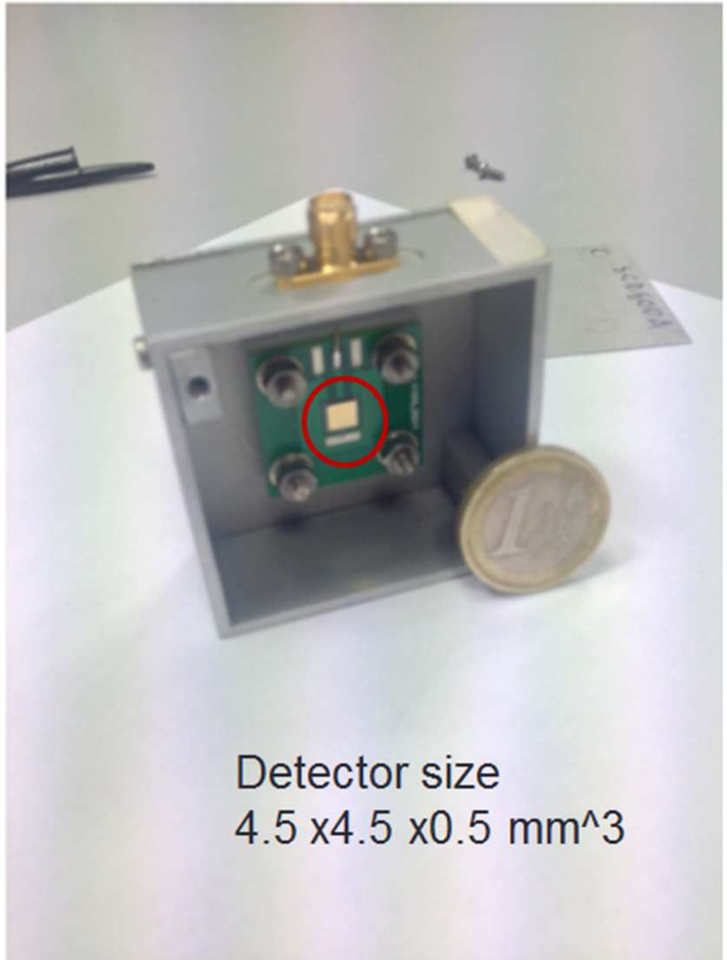

Read-out electronic built ad hoc to combine the **high counting rate** capability with the **good energy resolution.**

Waveform Digitizer (500 Msps - 14 bit) equipped with a real time analysis software on FPGA

Istituto di Fisica del Plasma "Piero Caldirola"
Consiglio Nazionale delle Ricerche

Detector response at monoenergetic neutron energies in the range 2-20 MeV

Detector response at different neutron energies

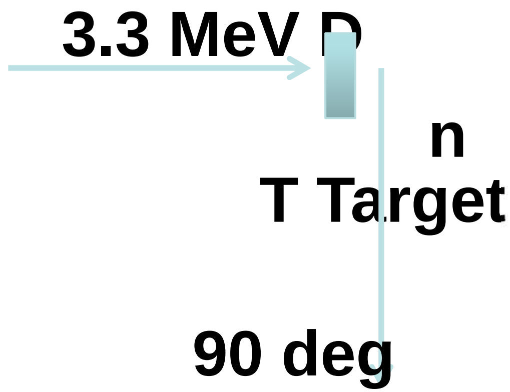

FWHM=220 keV

Thick target (run43)

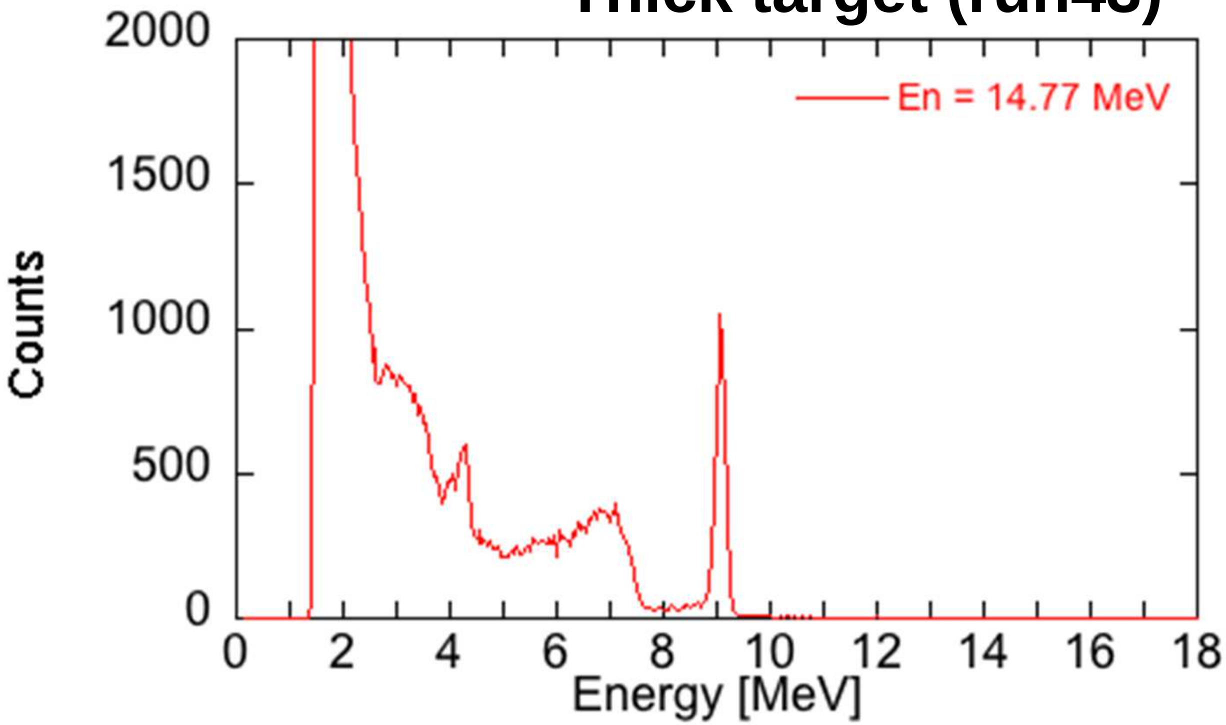

Istituto di Fisica del Plasma "Piero Caldirola"
Consiglio Nazionale delle Ricerche

UNIVERSITA' DEGLI STUDI DI MILANO BICOCCA

Detector response at different neutron energies

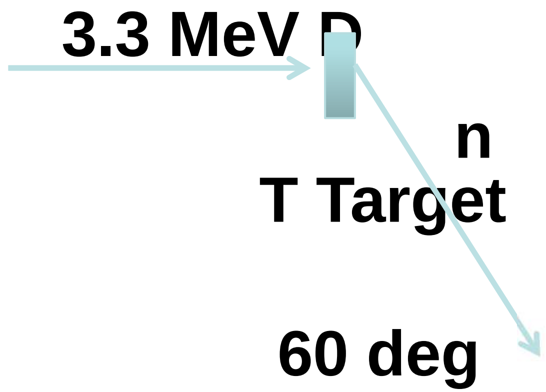

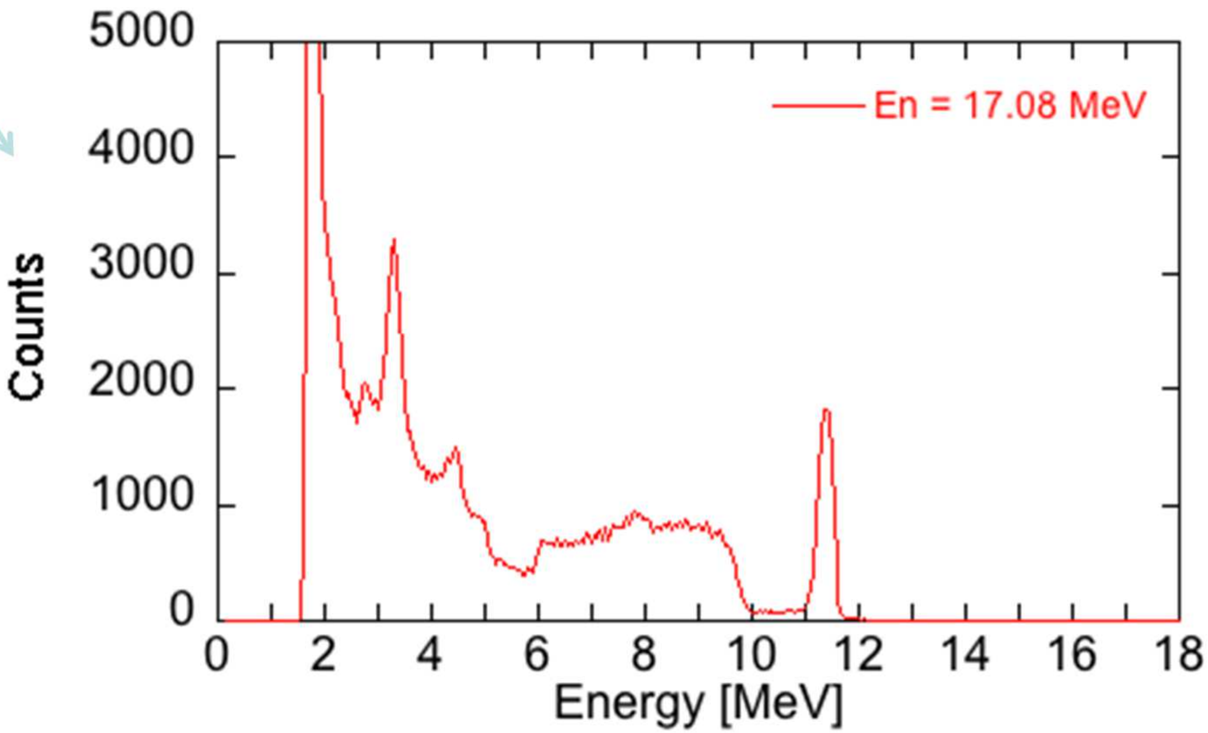

FWHM 296 keV (3cm)

Istituto di Fisica del Plasma "Piero Caldirola"
Consiglio Nazionale delle Ricerche

Detector response at different neutron energies

UNIVERSITÀ DEGLI STUDI DI MILANO BICOCCA

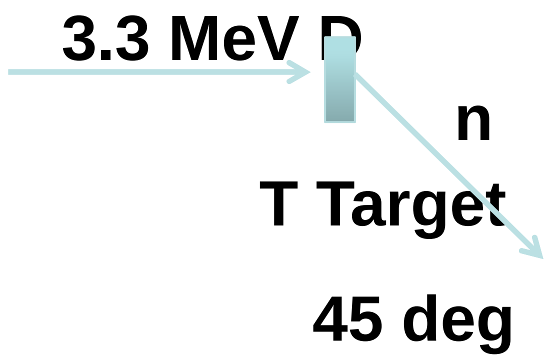

Energy resolution

Thick target (run41)

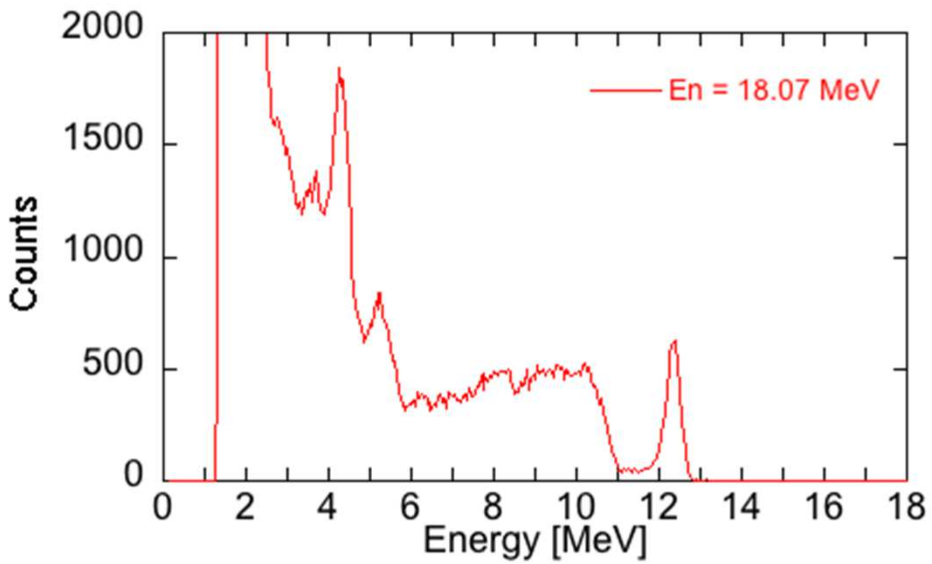

Detector response at different neutron energies

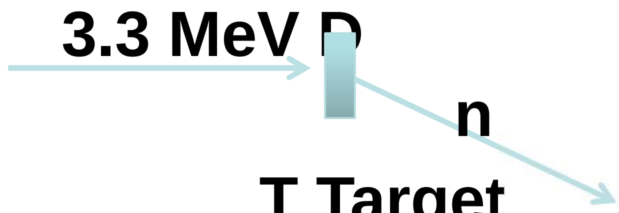

30 deg

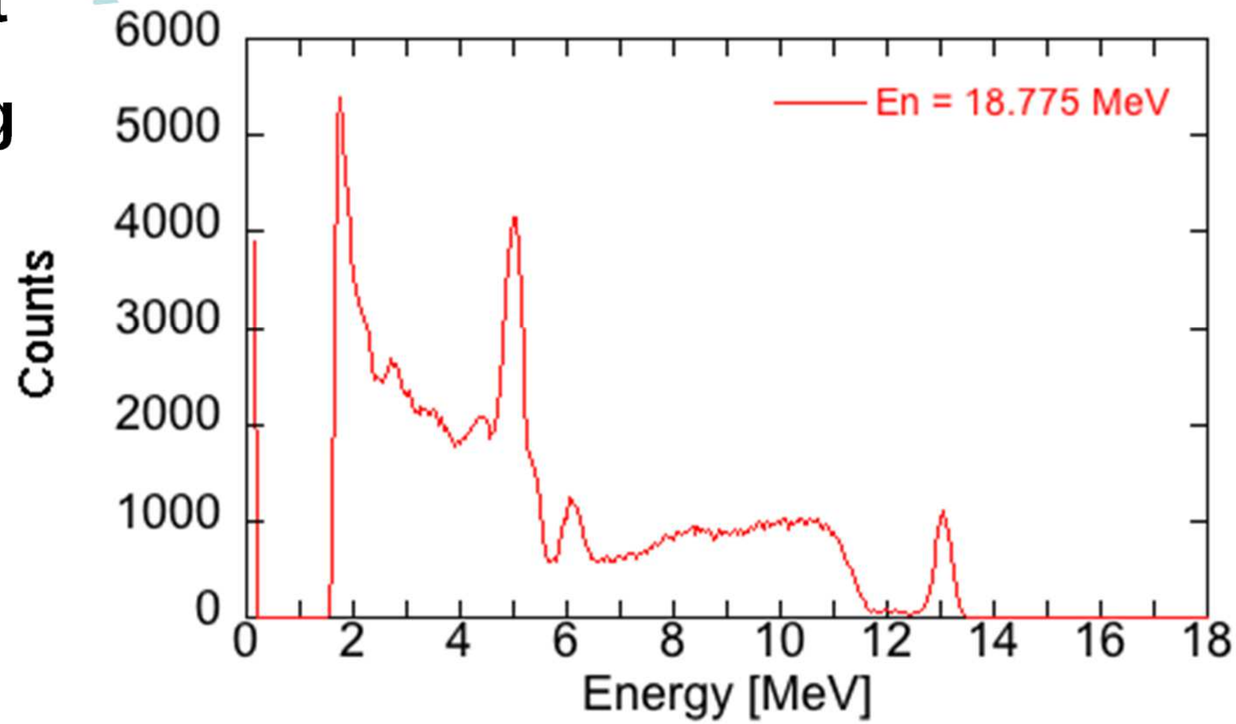

FWHM 361 keV

Detector response at different neutron energies

3.3 MeV D

n

T Target

0 deg

20 MeV neutrons
FWHM 180 keV

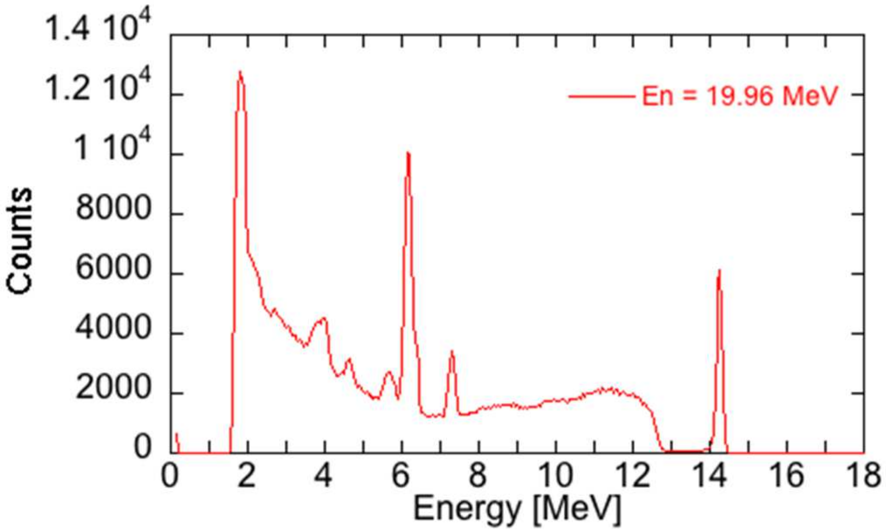

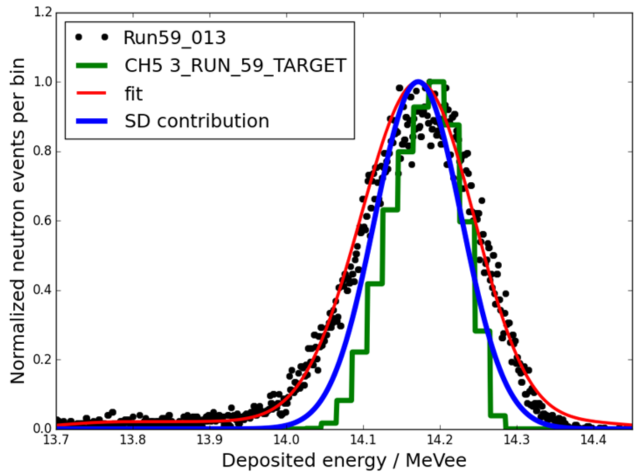

FIG. 2. (Color online). Detail of FIG. 1: Fit (red line) of the $^{12}C(n,a)^{9}Be$ peak with a FWHM = 174 keV as a result of the convolution of a Gaussian (blue line), which mimic the SD response function, with the TARGET neutrons of E_n = 20 MeV.

Istituto di Fisica del Plasma "Piero Caldirola"
Consiglio Nazionale delle Ricerche

Detector response at different neutron energies

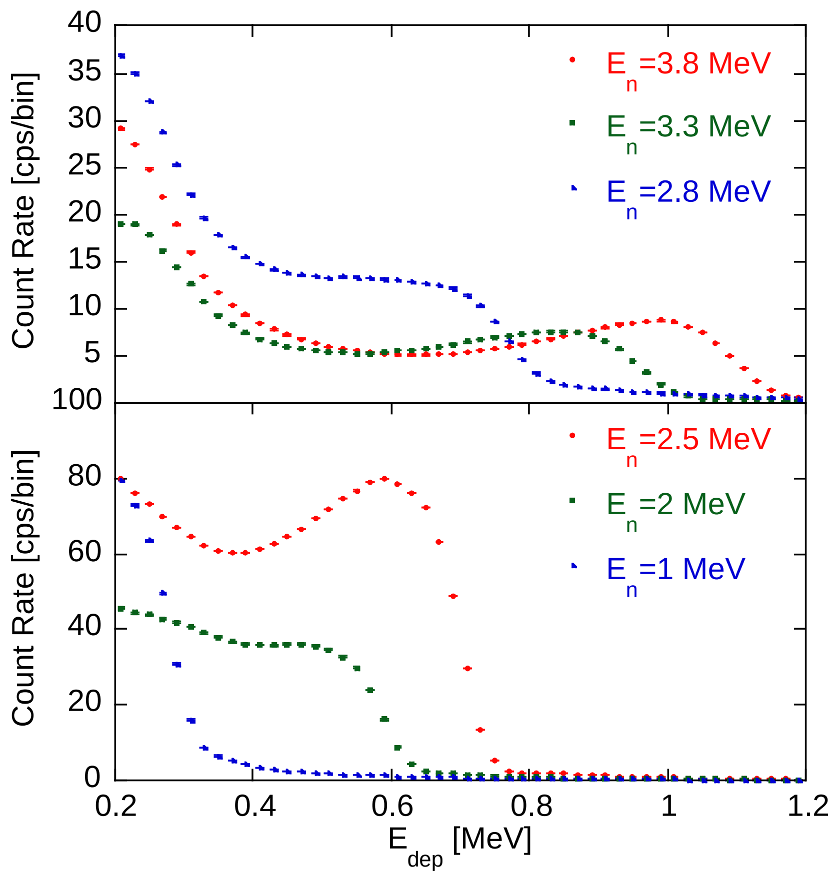

Pulse height spectra of a Single-crystal Diamond Detector irradiated at the INFN-LNL facility (top) and at the Pecking University (bottom). Neutron energies are reported in the legend.

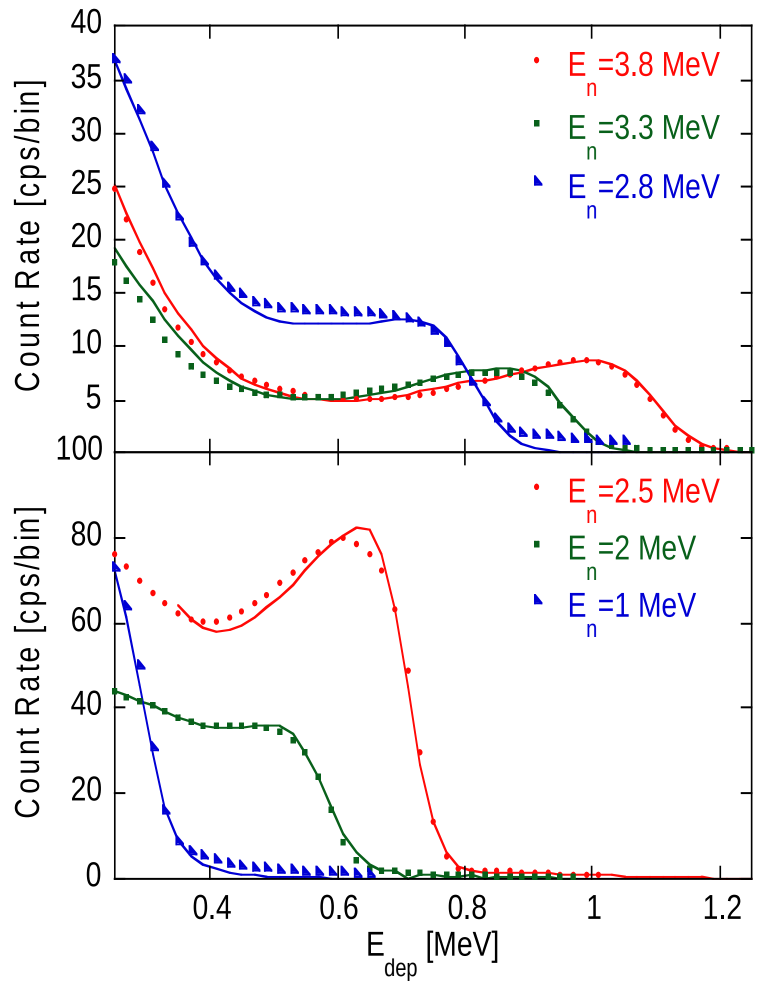

Fits on the whole experimental data set.

Istituto di Fisica del Plasma "Piero Caldirola"
Consiglio Nazionale delle Ricerche

Measured pulse height energy resolution 1-5 MeV

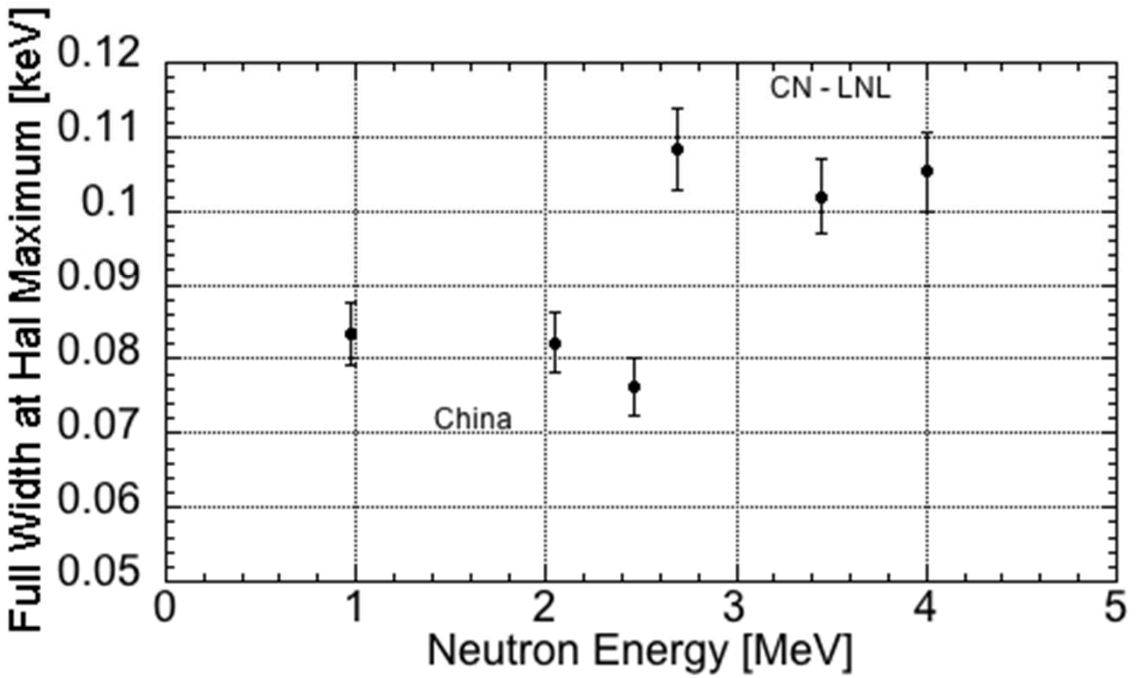

Energy resolution measured. Values are related to the FWHM of the Gaussian used to convolve the response function.

"Response function of single crystal synthetic diamond detectors to 1-4 MeV neutrons for spectroscopy of D plasmas", M. Rebai et al, submitted to Rev. Sci. Instr. (2016)

Istituto di Fisica del Plasma "Piero Caldirola"
Consiglio Nazionale delle Ricerche

Diamond spectrometer prototype installed at JET

SDD prototype installed behind KM9

SDD ready for mounting with preamp

SDD setup in the MPR after-burner

Istituto di Fisica del Plasma "Piero Caldirola"
Consiglio Nazionale delle Ricerche

Diamond spectrometer signals

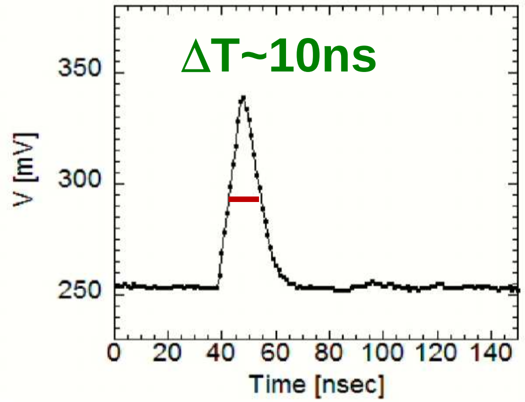

Pulse of a 14 MeV neutron events digitized by a 10 bit/1GS digitizer.

Optimization between **fast shape** preamplification and **high resolution** pulse height spectroscopy

Energy resolution=120-140 keV

($\Delta E/E$=0.9–1.0 %)

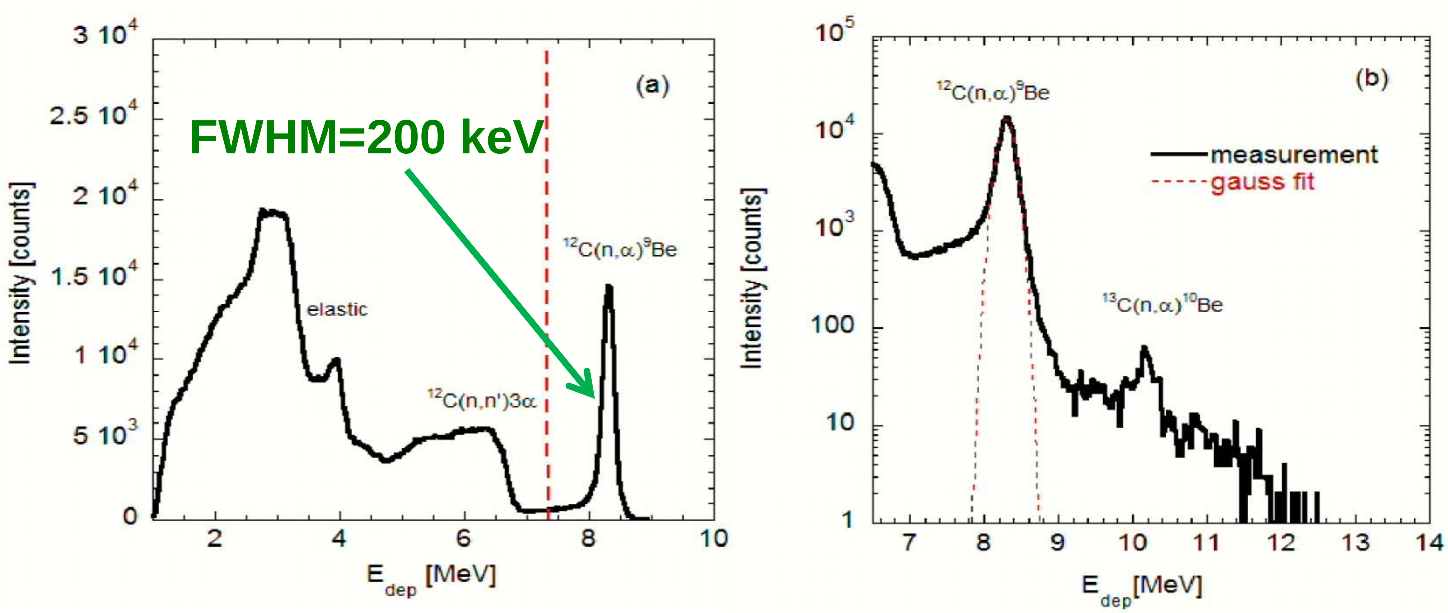

Deposited energy spectrum of **mono-energetic 14 MeV neutrons** in lin (a) and log (b)scale measured at the Frascati Neutron Generator.

C. Cazzaniga, M. Nocente et al., Rev. Sci. Instrum. 85 (2014) 11E101

Istituto di Fisica del Plasma "Piero Caldirola" Consiglio Nazionale delle Ricerche

Calibration with ^{241}Am alpha source

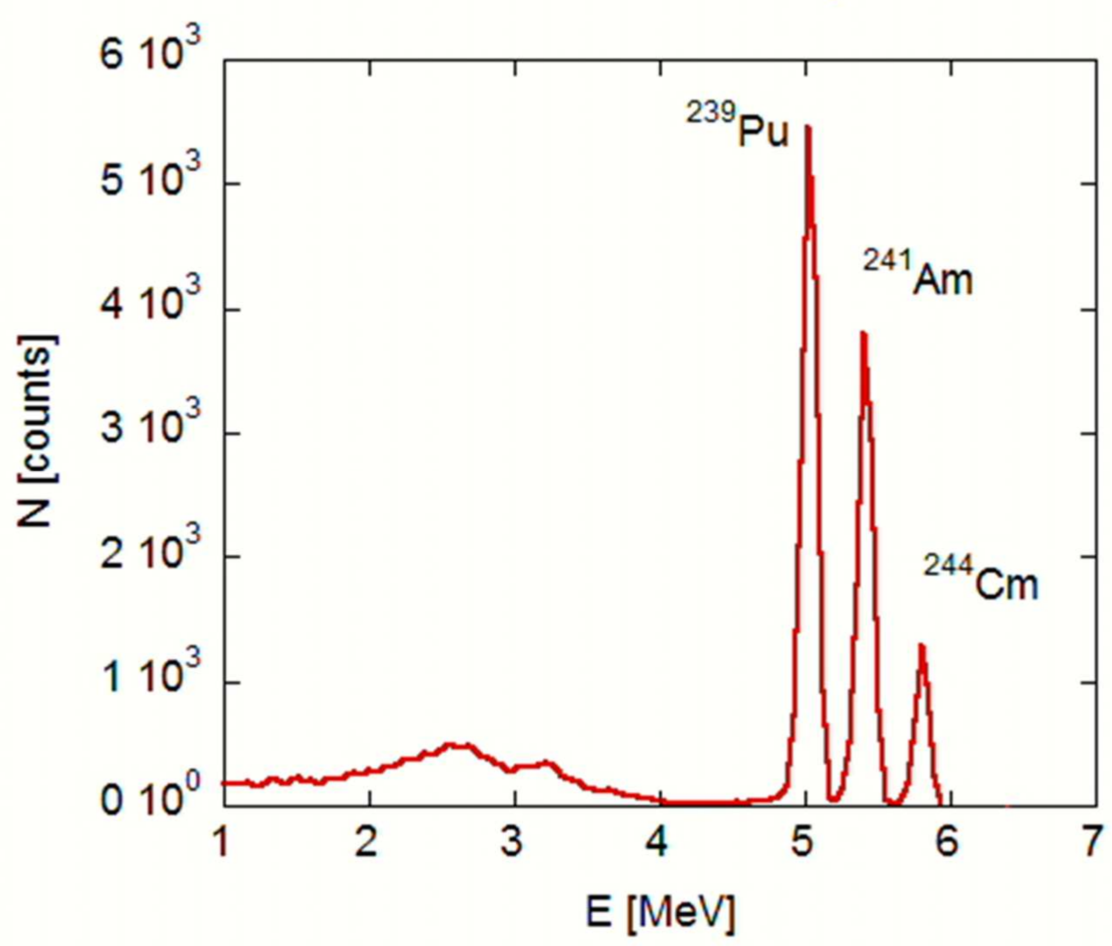

Calibration with final setup → digital acquisition in the Diagnostic Hall after about 120 meters cables.

Energy resolution is 2.2% at 5.2 MeV
→ Obtained with system that allows for MHz count rate

Istituto di Fisica del Plasma "Piero Caldirola"
Consiglio Nazionale delle Ricerche

Pulse Height Spectrum from D plasma

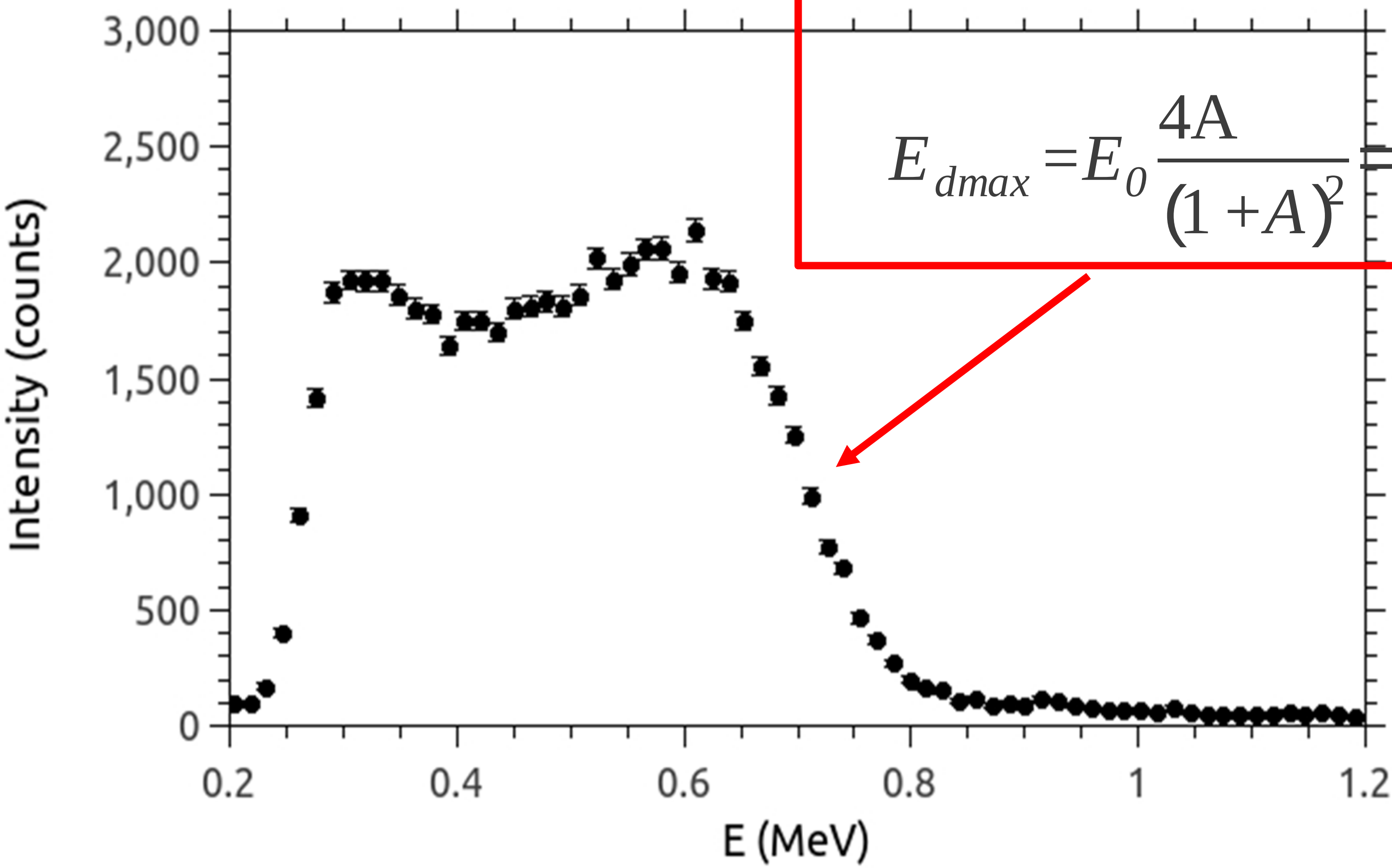

$$E_{dmax} = E_0 \frac{4A}{(1+A)^2} = 0.69\,MeV$$

- 45 shots added (12-14 july 2013)

Broadening is due to (1) Detector resolution (2) Plasma

2.5 MeV neutron NBI measurement vs simulations

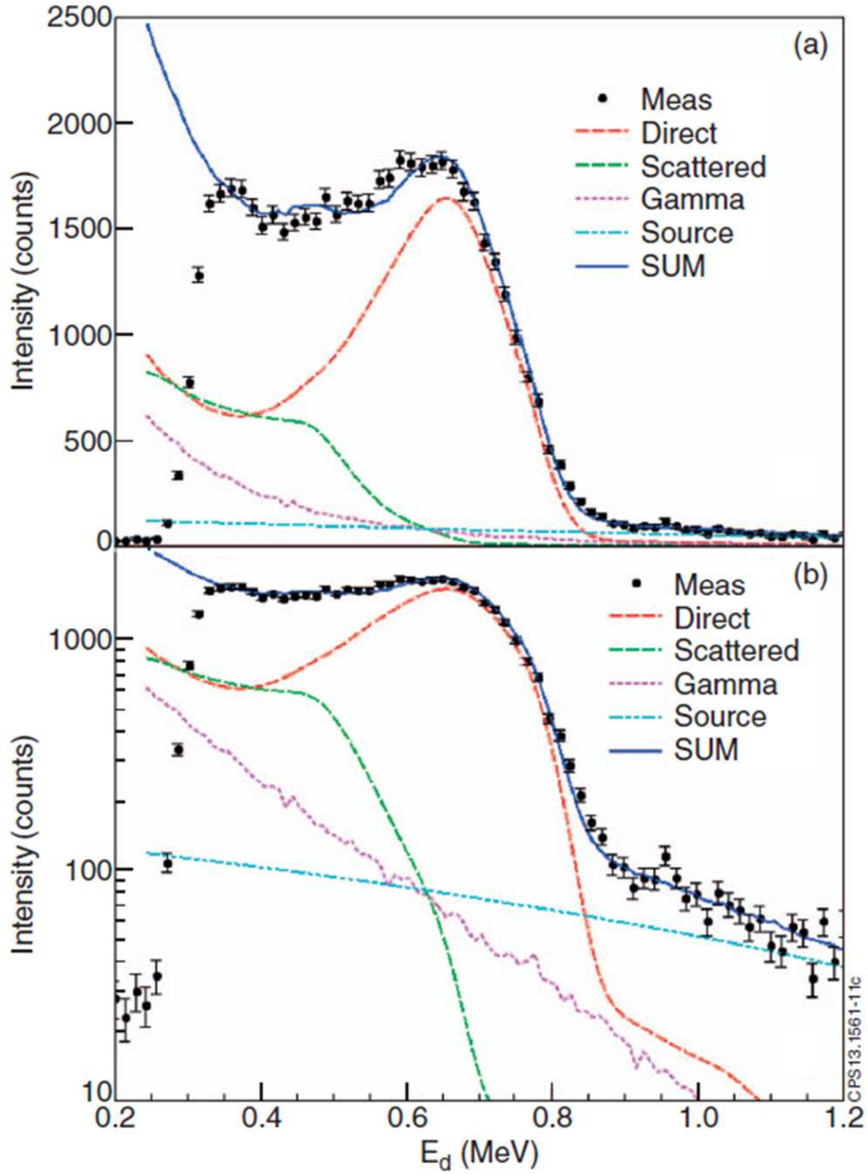

Highly non Gaussian spectrum reflecting a highly non-Maxwellian fast ion distribution

The same 1D model of TOFOR based on 3rd harmonic RF acceleration theory provides a relatively good description of the data.

Cazzaniga et al. Rev. Sci. Instrum. **85**, 043506 (2014)

Istituto di Fisica del Plasma "Piero Caldirola" Consiglio Nazionale delle Ricerche

Matrix diamond spectrometer

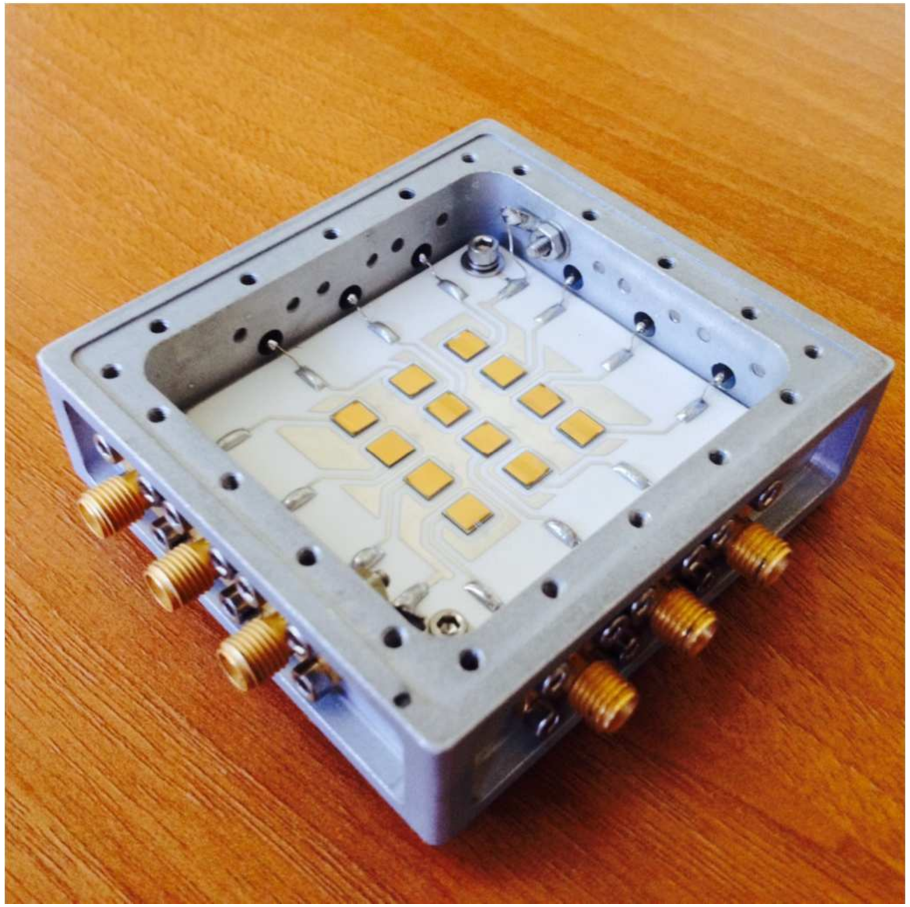

12 Pixels equipped with 12 standard SMA connectors.

The Single Cristal CVD Diamond is produced by the Element Six Ltd

Thickness: 0.5 mm
Area: 4.5x4.5 mm^2

The samples are glued with a Silver Paste onto a PCB board (Al_2O_3, 99.6%).

Detector produced by CNR

Matrix diamond neutron spectrometer for JET DT plasmas
VNS project (2012-today)

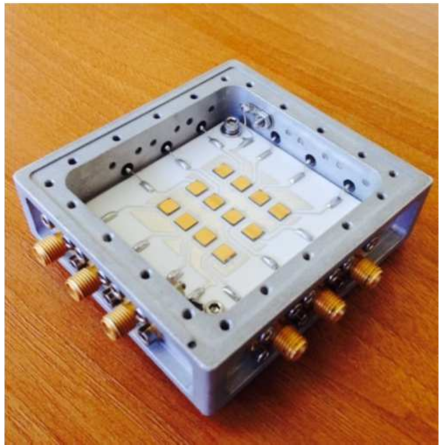

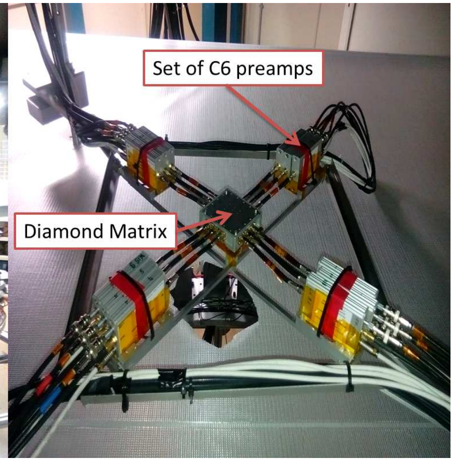

Collaboration with CNR-ISM, UNIMIB, ENEA, UPPSALA, JET

12 indipendent pixel, Detector produced by CNR

Single pixel dimension: 4.5x4.5x0.5 mm^3

Simultaneous measurement of **high energy resolution** (<1%@14 MeV) and **high count rate** capability (>1MHz) in a **compact**

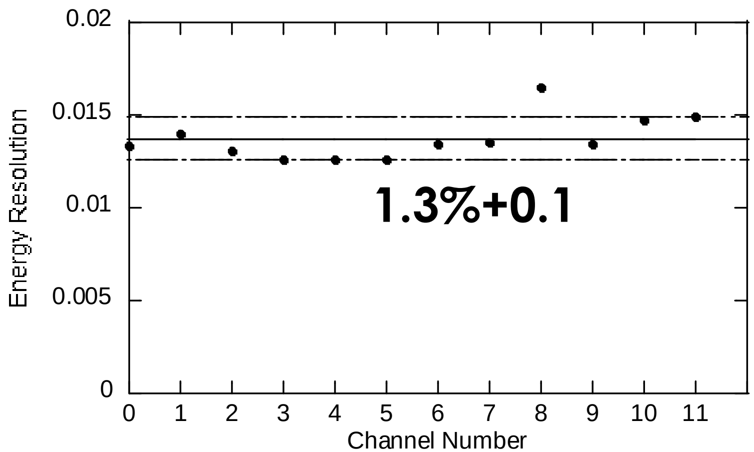

Energy resolution at 14 MeV

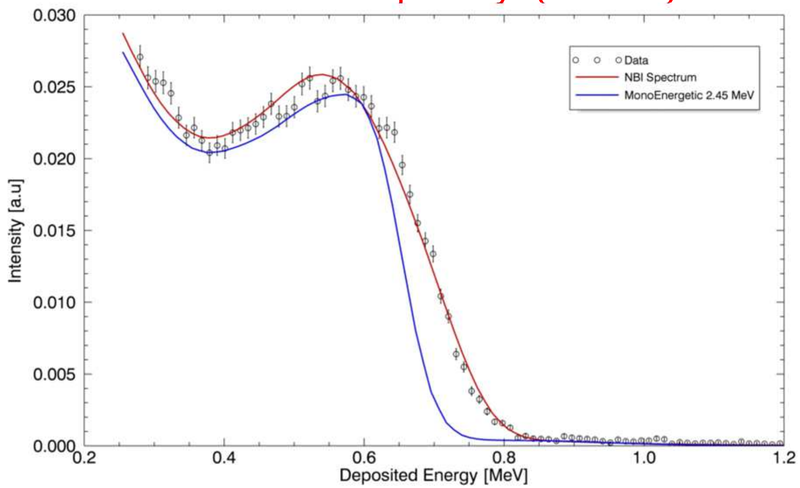

2.5 MeV neutron spectrum (with NBI) measured at JET compared to monoenergetic neutron repsonse

Example of 14 MeV neutron spectroscopy at very high energy resolution

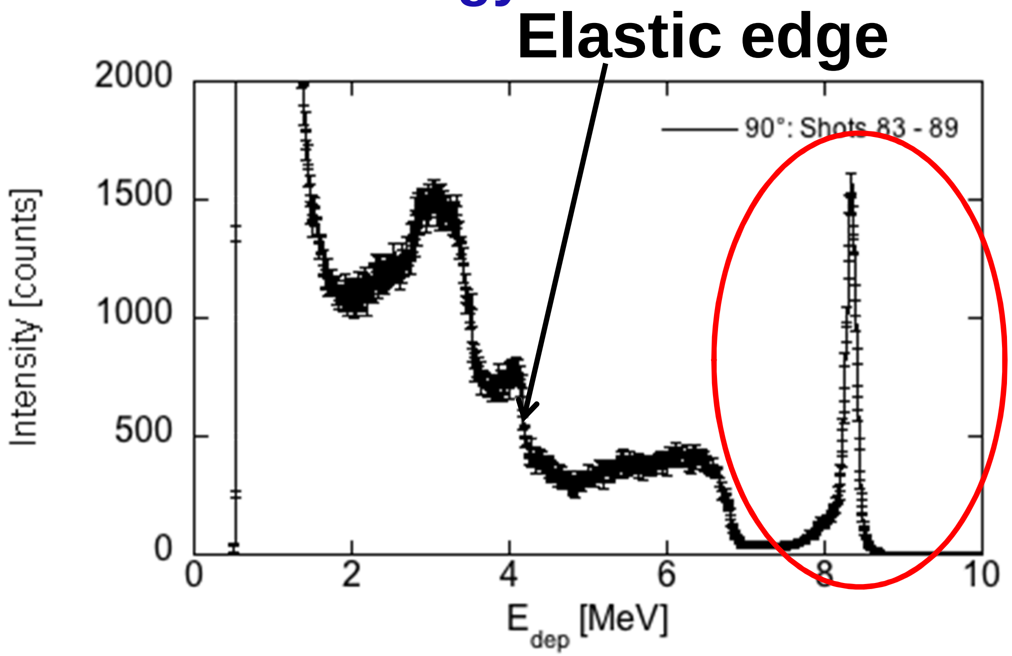

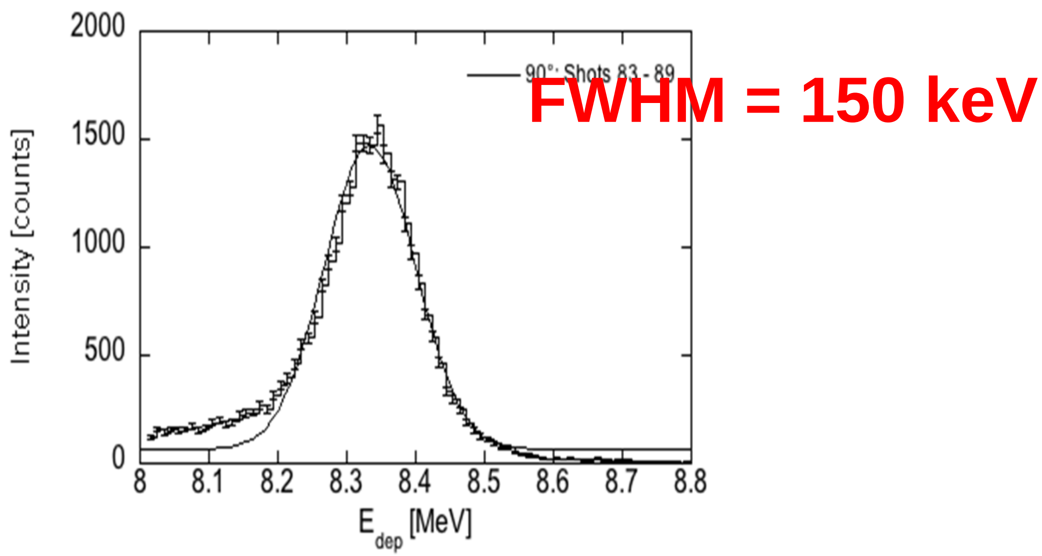

$n + {}^{12}C \rightarrow \alpha + {}^{9}Be$ -5.7 M

Spectra are broadened in the range of 150-300 keV

Need for <u>high resolution</u> measurements and <u>high precision calibration</u>

Istituto di Fisica del Plasma "Piero Caldirola"
Consiglio Nazionale delle Ricerche

Measurements at NPL- london

CNR diamond (90degree)

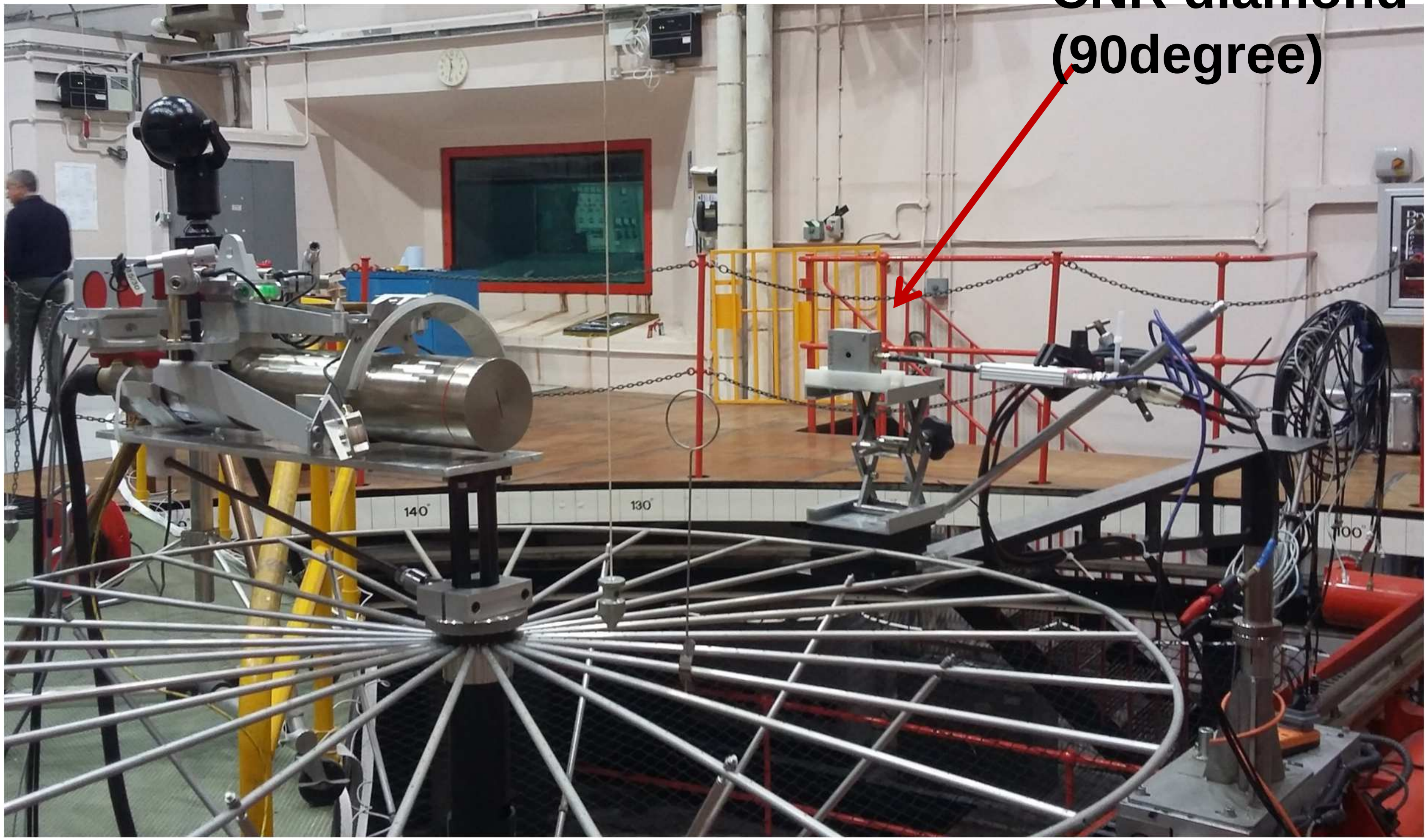

Istituto di Fisica del Plasma "Piero Caldirola"
Consiglio Nazionale delle Ricerche

Neutron spectroscopy of 14 MeV neutron generator with very high energy resolution

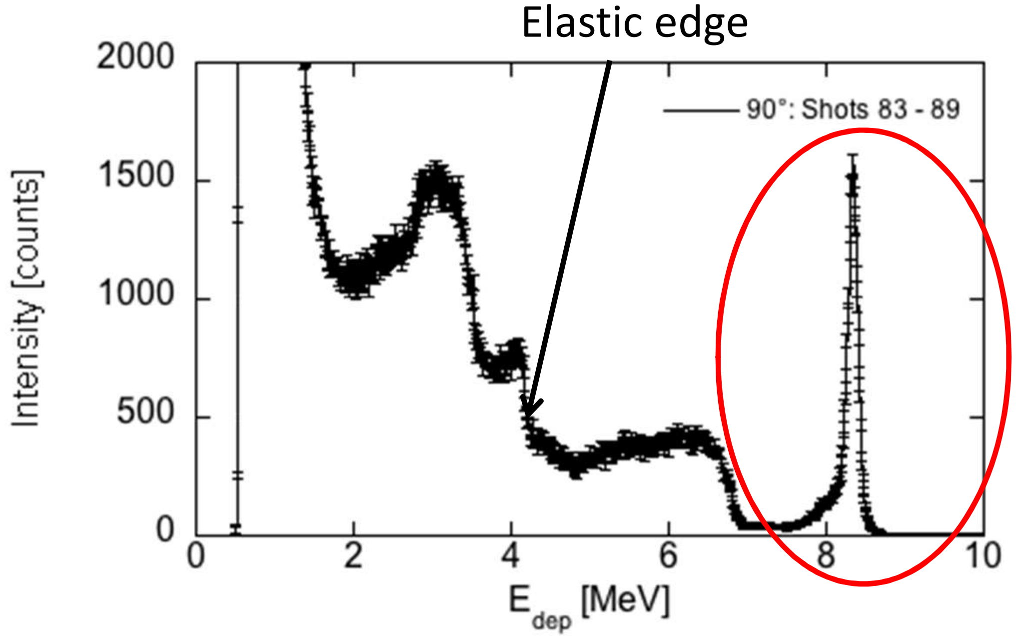

n +^{12}C→ α + ^{9}Be -5.7 MeV

Spectra are broadened in the range of 150-300 keV (depending on the angle)

Need for high resolution measurements and high precision calibration

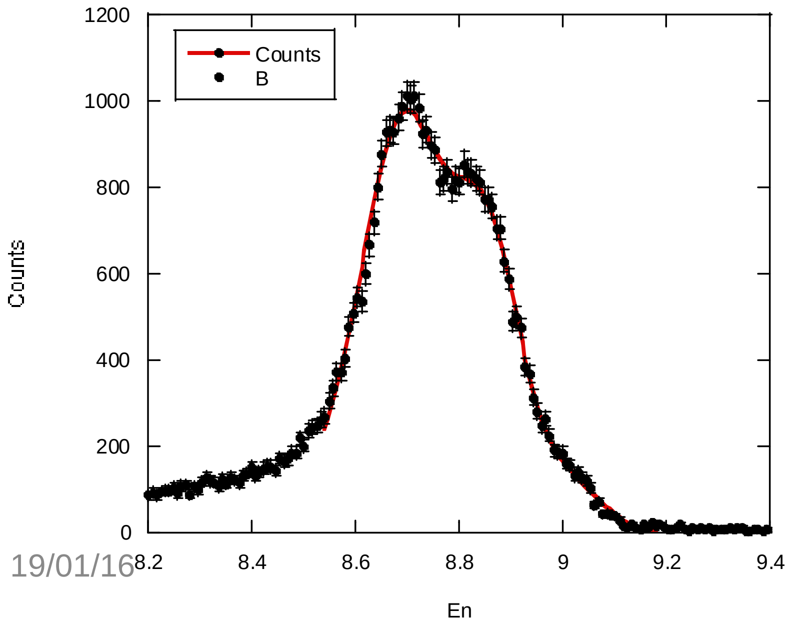

Fit with 5 components allows for determining incoming beam particle composition

D	**0.5**
D2	**8.0**
T	**2.6**
T2	**7.4**
DT	**81.5**

Incident particle beam composition:
DT was found the the dominant fraction

Istituto di Fisica del Plasma "Piero Caldirola"
Consiglio Nazionale delle Ricerche

Do we really need all the five free parameters to decribe the data?

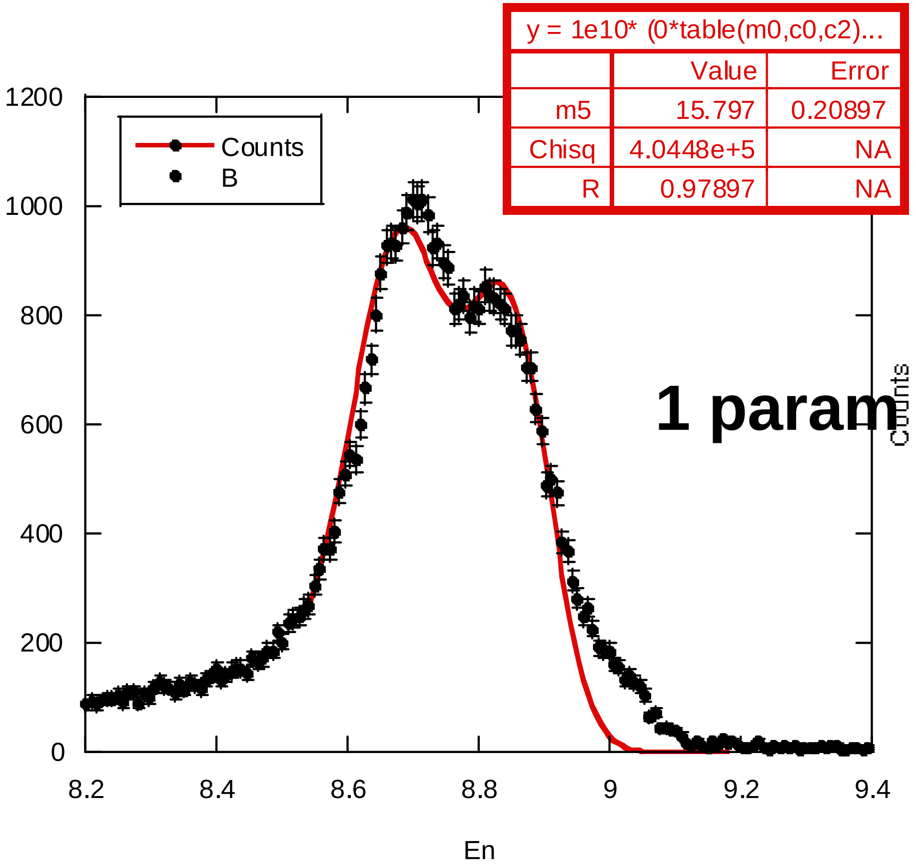

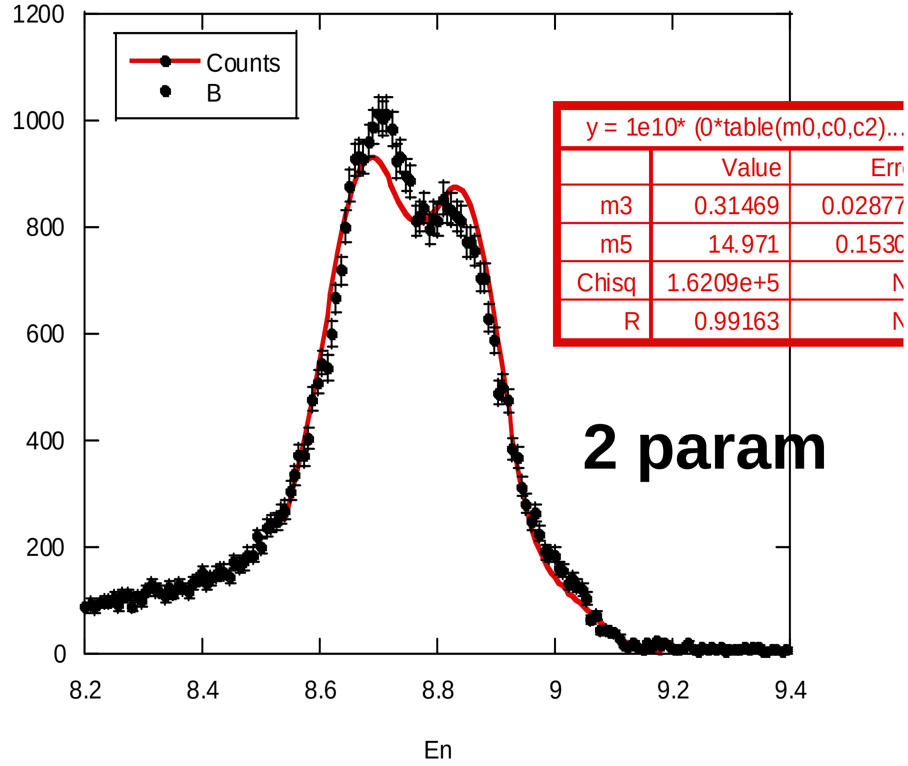

DT components provide main contribution

Tail due to a small fraction of T

Do we really need all the five free parameters to decribe the data?

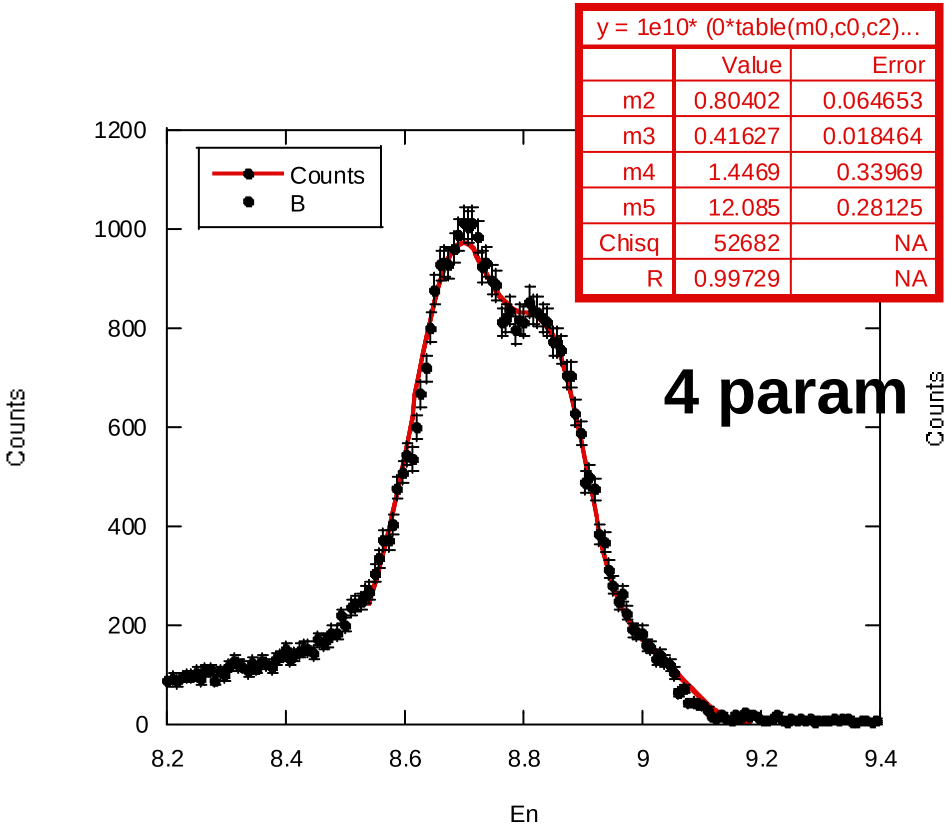

y = 1e10* (0*table(m0,c0,c2)...		
	Value	Error
m2	0.80402	0.064653
m3	0.41627	0.018464
m4	1.4469	0.33969
m5	12.085	0.28125
Chisq	52682	NA
R	0.99729	NA

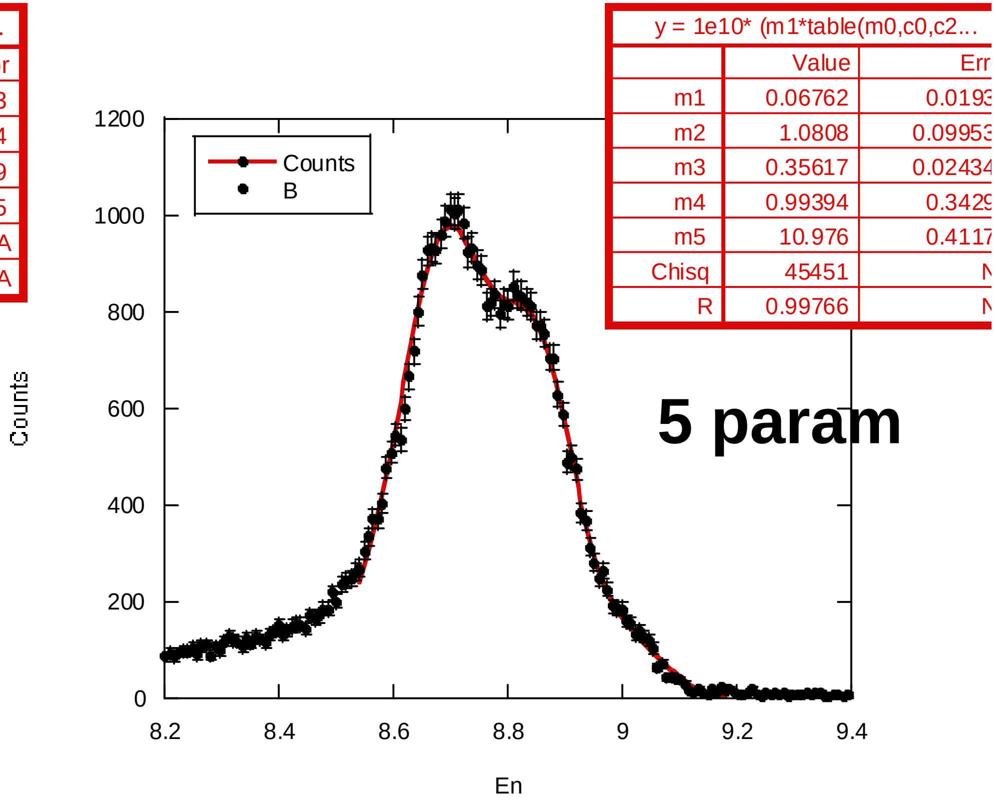

y = 1e10* (m1*table(m0,c0,c2...		
	Value	Err
m1	0.06762	0.0193
m2	1.0808	0.09953
m3	0.35617	0.02434
m4	0.99394	0.3429
m5	10.976	0.4117
Chisq	45451	N
R	0.99766	N

By adding D2 and T2 one get a good fit

By adding D negligible improvement is obtained

Istituto
di Fisica del Plasma
"Piero Caldirola"
Consiglio Nazionale delle Ricerche

Conclusions

Neutron measurements on fusion plama have been presented

Dedicated instruments (mainly spectrometers) have been developed to match the requirements of energy resolutions, efficiency and count rate capability of burning plasmas

The step being done now is to develop compact spectrometers to be used into neutron camera

If you are interested, write me!
tardocchi@ifp.cnr.it

END